Electronic Supplementary Material (ESI) for Inorganic Chemistry Frontiers.

Supporting Information

Unraveling the Transformative Pathways of Au-NHC and Au-Alkynyl Complexes and Bridging the Gap between Molecular and Nanoscale Gold Systems

Mariya V. Grudova, Alexey S. Galushko, Valentina V. Ilyushenkova, Mikhail E. Minyaev, Artem N. Fakhrutdinov, Darya O. Prima and Valentine P. Ananikov*

Zelinsky Institute of Organic Chemistry, Russian Academy of Sciences, Leninsky Pr. 47, Moscow, 119991, Russia; Email: val@ioc.ac.ru; https://AnanikovLab.ru

Table of contents

1. General experimental information

Chemicals and Solvents

Chemicals were obtained from P&M Invest, Sigma-Aldrich and Acros Organics and used as received without further purification. In the case of $HAuCl_4*3H_2O$, crystallization from a ethanol/pentane mixture was implemented. Solvents were purified using distillation: CH_2Cl_2 was distilled over CaH_2, hexane was distilled over 3 Å molecular sieves, and THF was distilled from sodium benzophenone ketyl. Ethanol and methanol were dried over 3 Å molecular sieves. Other solvents were purchased and used as received without further purification.

Physical Measurements and Instrumentation

ESI-HRMS study. The samples for the ESI-TOF-HRMS experiments were prepared in 1.8 mL glass vials with screwtop caps fitted with Teflon-lined septa (Agilent Technologies).
High-resolution mass spectra (HRMS) were recorded on a Bruker maXis q-TOF (tandem quadrupole/time-of-flight mass analyzer) mass spectrometer equipped with an electrospray ionization (ESI) source. The *m/z* scanning range was 50–3000. The measurements were carried out in positive ion mode (+) (grounded spray needle, –4500 V high-voltage capillary; 500 V HV End Plate) and in negative ion mode (–) (grounded spray needle, +4000 V high-voltage capillary; –500 V HV End Plate Offset). External calibration of the mass scale was carried out using a low-concentration calibration solution "Tuning mix" (Agilent Technologies). Samples were injected using a 500 μL Hamilton RN 1750 syringe (Switzerland). The flow rate during injection was controlled with a syringe pump (3 μL/min). Nitrogen was used as a nebulizer gas (1.0 bar) and dry gas (4.0 L/min, 200 °C). The data were processed using Bruker Data Analysis 4.0 software.

NMR study. NMR spectra were recorded using Bruker Avance-NEO 300, Bruker Fourier 300HD, Bruker Avance 400, Bruker Avance 500, Bruker Avance 600, spectrometers operating at 300.1, 400.16, 500.13, 600.13 MHz for ^{1}H; 61 MHz for ^{2}H; 76, 126, 151 MHz for ^{13}C and 282.4 MHz for ^{19}F. ^{1}H and ^{13}C NMR chemical shifts are reported relative to the solvent signals as internal standards: 2.50 ppm/39.5 ppm for DMSO-d_6, 7.26 ppm/77.2 ppm for $CDCl_3$, 5.32 ppm/54.0 ppm for CD_2Cl_2. ^{19}F NMR chemical shifts are reported relative to C_6F_6 ($\delta\ ^{19}F = -162.9$ ppm with respect to $CFCl_3$). All measurements were performed at room temperature.

SEM/DFSTEM analysis. The sample morphology was studied using a Hitachi SU8000 (Hitachi High-Technologies Corporation, Hitachinaka-shi, Japan) scanning electron microscope and

Regulus8230 (Hitachi High-Technologies Corporation, Hitachinaka-shi, Japan) scanning electron microscope at a 2-10 kV accelerating voltage. The DFSTEM images were acquired in annular dark-field mode at a 30 kV accelerating voltage using a Regulus8230 (Hitachi) scanning electron microscope. EDX (energy-dispersive X-ray spectroscopy) studies were carried out using an Oxford Instruments X-max EDX system (Oxford Instruments plc, Abingdon, UK).

X-ray crystallographic data and refinement details. Crystal structures of **3a**, **3b**•CH_2Cl_2, **3c**•0.92(CH_2Cl_2) and **4a** have been determined by the X-ray diffraction analysis. Crystals of **3a** exists as two polymorph modifications: **3a-I** and **3a-II**. Crystals of **3e** usually contained several domains and mimic a centrosymmetric monoclinic space group.

X-ray diffraction data for **3a-I** and **3e** were collected at 100K on a four-circle Rigaku Synergy S diffractometer equipped with a HyPix6000HE area-detector (kappa geometry, shutterless ω-scan technique), using monochromatized Mo K_α-radiation (**3a-I)** and Cu K_α-radiation (**3e**). The intensity data were integrated and corrected for absorption and decay by the CrysAlisPro program.[1]

X-ray diffraction data for **3a-II** and **3b**•CH_2Cl_2, **3c**•0.92(CH_2Cl_2) and **4a** were collected at 100K on a Bruker Quest D8 diffractometer equipped with a Photon-III area-detector (shutterless φ- and ω-scan technique), using graphite-monochromatized Mo K_α-radiation. The intensity data of collected reflections were integrated with the SAINT program[2] and semi-empirically corrected for absorption and decay from equivalent reflections by multi-scan methods with SADABS.[3] The structures were solved by direct methods using SHELXT[4] and refined by the full-matrix least-squares method on F^2 using SHELXL-2018[5] in the OLEX2 program[6] (**3a-I** and **3e**) or in the SHELXTL program suite[7] (**3a-II**, **3b**•CH_2Cl_2, **3c**•0.92(CH_2Cl_2) and **4a**). All non-hydrogen atoms were refined with anisotropic displacement parameters. Hydrogen atoms were placed in ideal calculated positions (C-H distance = 0.950 Å for aromatic, 0.980 Å for methyl, 0.990 Å for methylene and 1.000 Å for tertiary hydrogen atoms) and refined as riding atoms with relative isotropic displacement parameters taken as $U_{iso}(H)=1.5U_{eq}(C)$ for methyl groups and $U_{iso}(H)=1.2U_{eq}(C)$ otherwise. A rotating group model was applied for methyl groups. The SHELXTL program suite[7] and Mercury program[8] were used for molecular graphics.

Crystal data, data collection and structure refinement details for **3a-I**, **3a-II, 3b**•CH_2Cl_2, **3c**•0.92(CH_2Cl_2), **3e** and **4a** are summarized in Table S6 below. The structures have been deposited at the Cambridge Crystallographic Data Center with the reference CCDC numbers 2282626-2282629, 2321627 and 2282630; they also contain the supplementary crystallographic data. These data can be obtained free of charge from the CCDC *via* https://www.ccdc.cam.ac.uk/structures/

Computation details. The calculations were performed using the Gaussian 16 program[9] within the framework of density functional theory (DFT). A hybrid PBE1PBE functional[10] with the empirical Grimme correction[11] and Def2TZVP triple zeta valence basis set[12] were employed in this study. The polarizable continuum model (PCM)[13] was used to consider the solvent effect on the process under consideration. Stationary points were characterized as minima by evaluating the elements of the Hessian matrix.

2. Experimental procedures

2.1. Synthesis of THT-AuCl

THT-AuCl was obtained from $HAuCl_4 \cdot 3H_2O$ and tetrahydrotiophene (THT) in EtOH-H_2O medium as a white solid with 90% yield by the previously described procedure.[14]

2.2. Synthesis of IPrAuCl 1

THT-AuCl was directly used for the synthesis of IPrAuCl **1** by following the procedure reported by L. Belpassi and coworkers.[15] It should be noted that the reaction vessel should be covered from sun lights and should not be airtight. The formation of metallic gold particles with different shapes, from pieces to balls, were observed whenever the reaction vessel was airtight and uncovered.

2.3. General procedure for the synthesis of NHC-alkynyl gold(I) complexes 3a-e

NHC-AuCl **1** (1 eq, 0.03 mmol, 0. 020 g) and the appropriate alkyne (1 eq, 0.03 mmol) were placed in a 5 mL vial. Then, the residue was dissolved in a 2 mL mixture of CH_2Cl_2:EtOH=2:1 (v/v). Then, AcONa (3 eq, 0.09 mmol) was added at once. The reaction mixture was stirred at r.t. for 18 h. Then, the reaction mixture was filtered through a filter paper, and the solvent was evaporated under reduced pressure. After that, the crude gold(I) complex was purified by flash-chromatography (Al_2O_3, eluent CH_2Cl_2:hexane = 1:4 → 1:2). Target NHC-Au-alkynyl complexes were obtained as white or off-white powders with good yields.

Gold complexes **3f**[16], **3g**[17], and **3h**[13] were synthesized in accordance with previously described procedures.

2.4. General procedure for synthesis gold complex 2

To a solution of 1,3-bis-(2,4,6-tribenzhydrylphenyl)-1H-imidazol-3-ium chloride (IPr*HCl) (1 eq, 0.12 mmol, 0.050 g) in 3.3 mL of CH_2Cl_2 chloro(tetrahydrothiophene)gold(I) (THT-AuCl) (1 eq, 0.12 mmol, 0.038 g) was added. The reaction mixture was sonicated in ultrasound bath for 1 min and then stirred for 15 min at room temperature. After 15 min, large part of solvent was evaporated from the resulting turbid solution under reduced pressure to 0.5

mL. Then 10 mL of Et_2O was added. The resulting precipitate was filtered through a 3-pore Schott filter, washed with Et_2O (3x2 mL) and dried under reduced pressure. The yield of the target product **2** was 0.062 g, 80%.

2.5. General procedure for synthesis gold complex 4a

1-Ethynyl-4-(trifluoromethyl)benzene (2 eq, 0.03 mmol, 0.010 g, 10 μL) and AcONa (2.1 eq, 0.062 mmol, 0.005 g) were placed in a 5 mL vial. Then, 2 mL of CH_2Cl_2 were added to the vial. After that, $NHC^+[AuCl_2]^-$ **2** (1 eq, 0.03 mmol, 0. 020 g) was added. The reaction mixture was stirred at room temperature for 18 h. Then, the mixture was filtered through a filter paper, and the solvent was evaporated under reduced pressure. Then, Et_2O (5 mL) was added, and the reaction mixture was sonicated in ultrasound bath for 1 minute. Then, the residue was filtered through a Schott filter (3 porous) and dried with under reduced pressure. Target bis-alkynyl complex **4a** was obtained as an off-white (or yellowish) solid. Yield 42%.

References

1. CrysAlisPro. Version 1.171.42. *Rigaku Oxford Diffraction*, 2023.
2. Bruker. APEX-III. *Bruker AXS Inc.*, Madison, Wisconsin, USA, 2020.
3. Krause, L.; Herbst-Irmer, R.; Sheldrick, G. M.; Stalke, D. Comparison of silver and molybdenum microfocus X-ray sources for single-crystal structure determination. *J. Appl. Cryst.* 2015, **48**, 3.
4. Sheldrick, G. M. SHELXT - Integrated space-group and crystal-structure determination. *Acta Cryst.* 2015, **A71**, 3.
5. Sheldrick, G. M. Crystal structure refinement with SHELXL. *Acta Cryst.* 2015, **C71**, 3.
6. Dolomanov O.V.; Bourhis L.J.; Gildea R.J.; Howard J.A.K.; Puschmann H. OLEX2: a complete structure solution, refinement and analysis program. *J. Appl. Cryst.* 2009, **42**, 339.
7. Sheldrick, G.M. A short history of SHELX. *Acta Cryst.*, *Sect. A* 2008, **A64**, 112.
8. Macrae, C. F.; Sovago, I.; Cottrell, S. J.; Galek, P. T. A.; McCabe, P.; Pidcock, E.; Platings, M.; Shields, G. P.; Stevens, J. S.; Towler, M.; Wood, P. A. Mercury 4.0: from visualization to analysis, design and prediction. *J. Appl. Cryst.* 2020, **53**, 226.
9. M. J. Frisch, G. W. Trucks, H. B. Schlegel, G. E. Scuseria, M. A. Robb, J. R. Cheeseman, G. Scalmani, V. Barone, G. A. Petersson, H. Nakatsuji, X. Li, M. Caricato, A. V. Marenich, J. Bloino, B. G. Janesko, R. Gomperts, B. Mennucci, H. P. Hratchian, J. V. Ortiz, A. F. Izmaylov, J. L. Sonnenberg, D. Williams-Young, F. Ding, F. Lipparini, F. Egidi, J. Goings, B. Peng, A. Petrone, T. Henderson, D. Ranasinghe, V. G. Zakrzewski, J. Gao, N. Rega, G. Zheng, W. Liang,

M. Hada, M. Ehara, K. Toyota, R. Fukuda, J. Hasegawa, M. Ishida, T. Nakajima, Y. Honda, O. Kitao, H. Nakai, T. Vreven, K. Throssell Jr., J. A. Montgomery, J. E. Peralta, F. Ogliaro, M. J. Bearpark, J. J. Heyd, E. N. Brothers, K. N. Kudin, V. N. Staroverov, T. A. Keith, R. Kobayashi, J. Normand, K. Raghavachari, A. P. Rendell, J. C. Burant, S. S. Iyengar, J. Tomasi, M. Cossi, J. M. Millam, M. Klene, C. Adamo, R. Cammi, J. W. Ochterski, R. L. Martin, K. Morokuma, O. Farkas, J. B. Foresman and D. J. Fox, Gaussian 16, Revision C.01, Gaussian, Inc., Wallingford CT, 2016

10. C. Adamo and V. Barone, Toward reliable density functional methods without adjustable parameters: The PBE0 model, *J. Chem. Phys.*, 1999, **110**, 6158.

11. S. Grimme, S. Ehrlich and L. Goerigk, Effect of the damping function in dispersion corrected density functional theory, *J. Comput. Chem.,* 2011, **32**, 1456.

12. F. Weigend and R. Ahlrichs, Balanced basis sets of split valence, triple zeta valence and quadruple zeta valence quality for H to Rn: Design and assessment of accuracy, *Phys. Chem. Chem. Phys.*, 2005, **7**, 3297.

13. Scalmani G. and Frisch M. J. Continuous surface charge polarizable continuum models of solvation. I. General formalism, *J. Chem. Phys.*, 2010, **132**, 114110.

14. Rezsnyak C. E., Autschbach J., Atwood J. D. and Moncho S., Reactions of gold (III) complexes with alkenes in aqueous media: generation of bis-(β-hydroxyalkyl) gold (III) complexes, *J. Coord. Chem.*, 2013, **66**, 1153.

15. Ciancaleoni G., Biasiolo L., Bistoni G., Macchioni A., Tarantelli F., Zuccaccia D. and Belpassi L., NHC-gold-alkyne complexes: Influence of the carbene backbone on the ion pair structure, *Organometallics*, 2013, **32**, 4444.

16. Scattolin T., Tzouras N. V., Falivene L., Cavallo L. and Nolan S. P., Using sodium acetate for the synthesis of [Au(NHC)X] complexes, *Dalton Trans.*, 2020, **49**, 9694.

17. Oberkofler J., Aikman B., Bonsignore R., Pöthig A., Platts J., Casini A. and Kühn F. E., Exploring the Reactivity and Biological Effects of Heteroleptic *N*-Heterocyclic Carbene Gold (I)-Alkynyl Complexes. *Eur. J. Inorg. Chem.*, 2020, **2020**, 1040.

3. Optimization conditions of 3a complex synthesis

First of all, the formation of *N*-heterocyclic gold(I) alkynyl complex **3a** was studied. The influence of external parameters on the yield of target complex **3a** was investigated. To obtain IPr-Au-alkynyl complex **3a** the strong base route (KOH, *t*-BuOK, Entries 1-2 in Table S1) and the weak base route (Et_3N, AcONa, Entries 3-4 in Table S1) were performed.

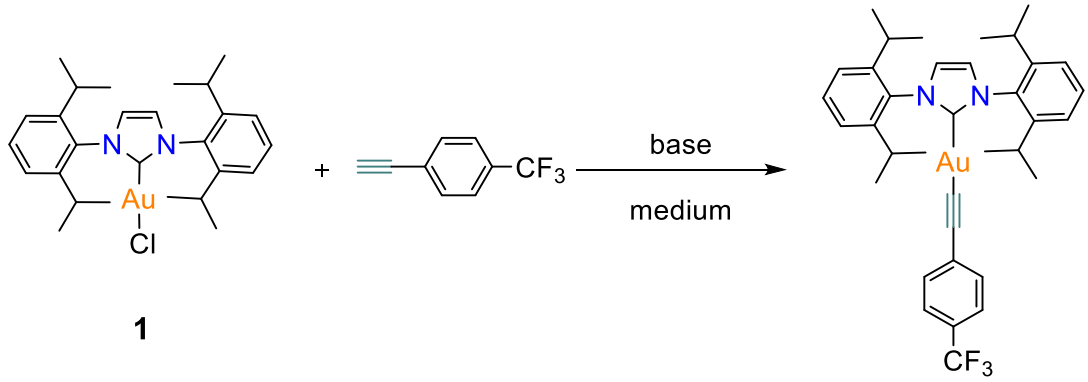

1 **3a**

Table S1. Optimization of the model reaction conditions for the synthesis of the NHC-alkynyl gold(I) complex. Reaction conditions: 18 h, r.t., **1** (0.03 mmol), alkyne (0.03 mmol), base (0.1 mmol). Isolated yields reported.

Entry	Base	Medium	Yield of 3a, %
1	KOH	EtOH: CH_2Cl_2 = 1:1	19
2	*t*-BuOK	EtOH: CH_2Cl_2 = 1:1	44
3	Et_3N	EtOH: CH_2Cl_2 = 1:1	59
4	**AcONa**	**EtOH: CH_2Cl_2 = 1:1**	**75**
5	Without base	CH_2Cl_2	–
6	AcONa	EtOH	35
7	AcONa	MeOH: CH_2Cl_2 = 1:1	57
8	AcONa	MeOH	55
9	**AcONa**	**CH_2Cl_2**	**74**
10	AcONa	THF	15
11	AcONa	Benzene	27

The formation of gold NPs and Au black in the case of the strong base route (Entries 1-2, Table S1) were discovered. At the same time, the yield of the target complex **3a** was not high. Therefore, the largest part of the gold(I) complexes was consumed into gold NPs and Au black formation. After that the influence of weak base route was investigated. Replacing *O*-containing base with an *N*-containing base did not result in an increase in conversion (Entry 3, Table S1). The formation

of two gold(I) complexes was established by NMR, ESI-HRMS and X-ray diffraction study (Entries 6-8, Table S1) when AcONa was used as a base. The reaction between equimolar amounts of IPrAuCl **1** and appropriate alkyne without any base did not occur by ^{1}H NMR monitoring (Entry 5, Table S1).

After that the solvents effect was investigated (Entries 6-11, Table S1). Replacing the solvent with a less polar solvent did not increase the conversion and the yield of target complex **3a** (Entries 6-8, 10-11, Table S1). The yield of the complex **3a** increased by up to 74% when the solvent was switched out for the less polar solvent CH_2Cl_2 (Entry 9, Table S1). Following that, complex **3a** was synthesized in a CH_2Cl_2 medium using AcONa as a base. However, IPrAuCl **1** was not fully converted. After that the ^{1}H NMR spectra of reaction mixtures were compared with ^{1}H NMR spectrum started alkyne. It was stand that when reaction was carried out in DCM only did not full conversion were observed. The 3.20 ppm NMR shift (in $CDCl_3$ as a solvent) which corresponds to initial alkyne was fixed in ^{1}H NMR spectrum of DCM reaction mixture. At the same time, in DCM:EtOH mixture almost none 3.20 ppm NMR shift was established. The full conversion in DCM was not observed, probably, due to the poor solubility of AcONa in dichloromethane. In the case of DCM:EtOH mixture the partial solubility of AcONa was stand. Therefore, AcONa as the base and CH_2Cl_2/EtOH as the medium have been chosen for the synthesis of Au(I) complexes **3a-f**.

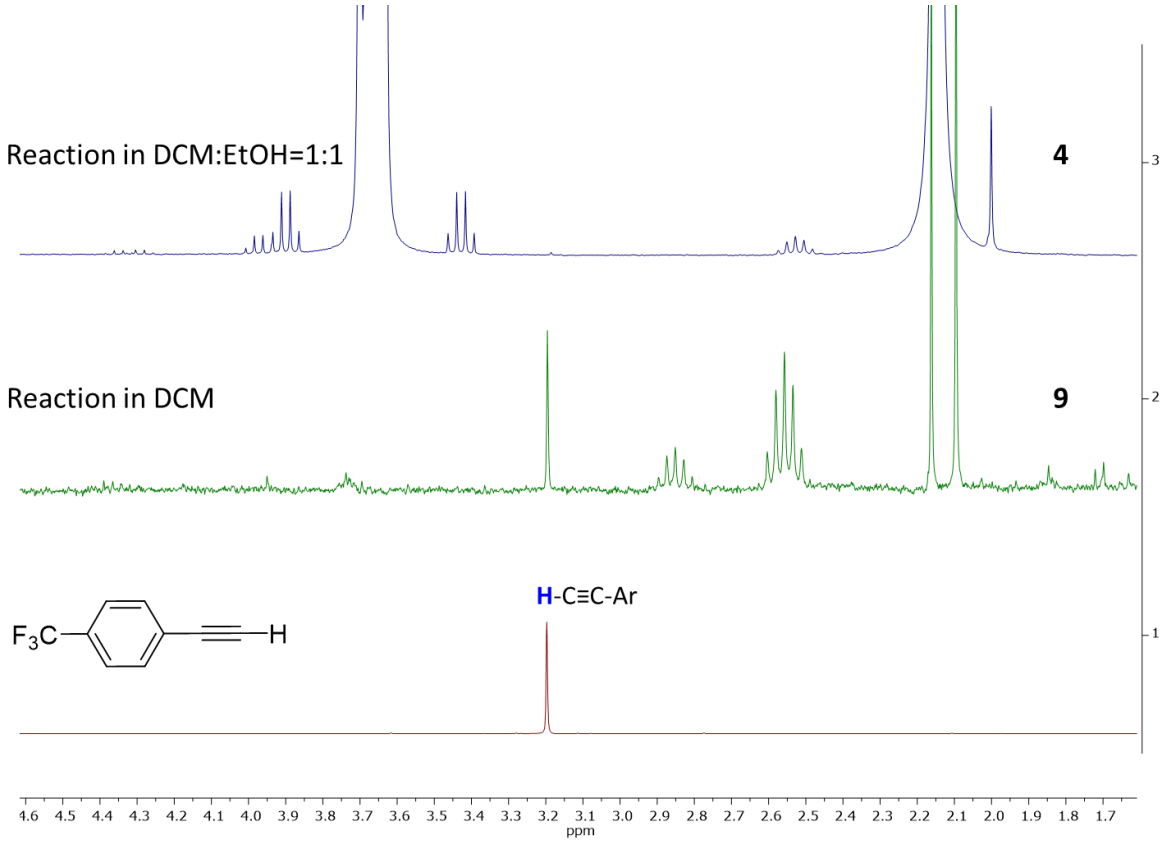

Scheme S1. ^{1}H NMR spectra of investigated reactions, solvent $CDCl_3$, 300 MHz of initialalkyne.and studied reaction in: **4**) DCM:EtOH=1:1 (v/v); **9**) DCM.

4. Product characterization

(1,3-bis(2,6-diisopropylphenyl)-2,3-dihy(1,3-bis(2,6-diisopropylphenyl)-2,3-dihydro-1H-imidazol-2-yl)((4-(trifluoromethyl)phenyl)ethynyl)gold (3a). Yield 70% (Yield 55% when base=*t*-BuOK), white powder.

^{1}H NMR ($CDCl_3$, 300 MHz): δ 7.55 – 7.47 (t, J = 7.8 Hz, 2H), 7.39 – 7.32 (m, 4H), 7.30 (d, J = 7.8 Hz, 4H), 7.13 (s, 2H), 2.60 (sept, J = 6.9 Hz, 4H), 1.38 (d, J = 6.9 Hz, 12H), 1.22 (d, J = 6.9 Hz, 12H).

^{13}C{^{1}H} NMR (CD_2Cl_2, 126 MHz): δ 190.7, 146.4, 134.8, 134.3, 132.5, 131.1, 130.80 (d, $J_{C\text{-}F}$ = 1.4 Hz), 127.60 (q, $J_{C\text{-}F}$ = 32.2 Hz), 125.21 (q, $J_{C\text{-}F}$ = 3.8 Hz), 125.0 (CF_3, q, $J_{C\text{-}F}$ = 271.5 Hz), 124.8, 124.1, 102.5, 29.4, 24.9, 24.2.

^{19}F{^{1}H} NMR ($CDCl_3$, 282 MHz): δ -65.60.

ESI-(+)HRMS, *m/z*: 755.2890, calcd for $C_{36}H_{40}AuF_3N_2$: 755.2882 $[M+H]^+$, (Δ = 1.06 ppm).

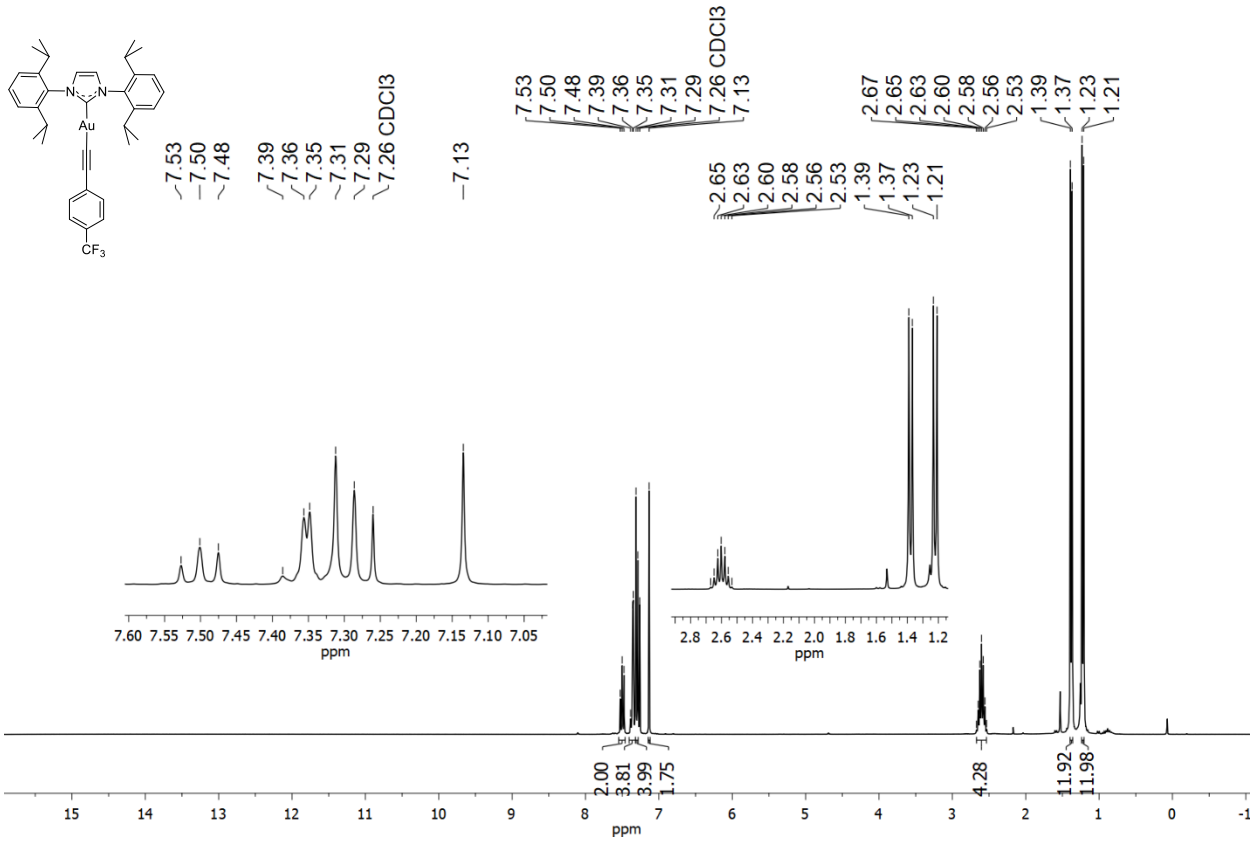

Figure S1. ^{1}H NMR spectrum of compound **3a** ($CDCl_3$, 300 MHz).

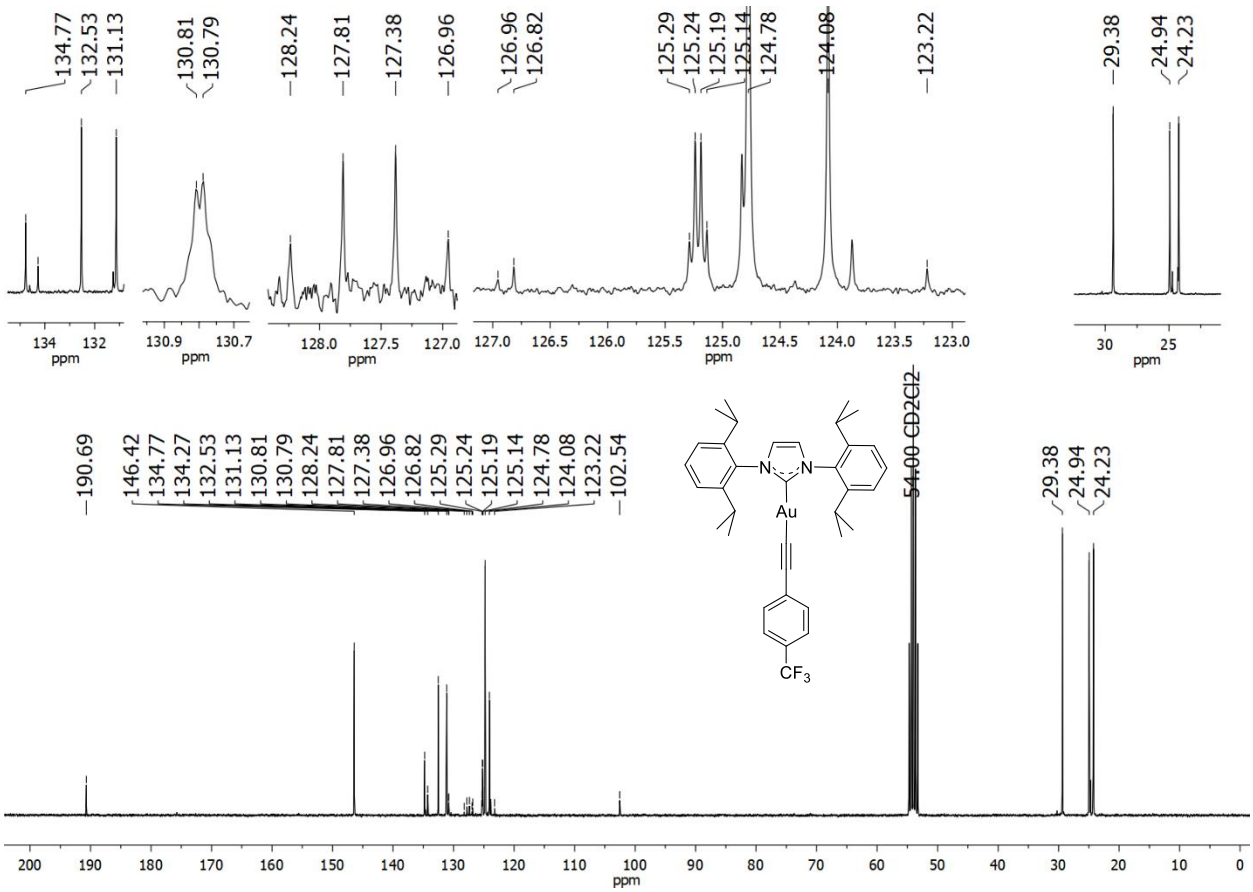

Figure S2. $^{13}C\{^{1}H\}$ NMR spectrum of compound **3a** (CD_2Cl_2, 126 MHz).

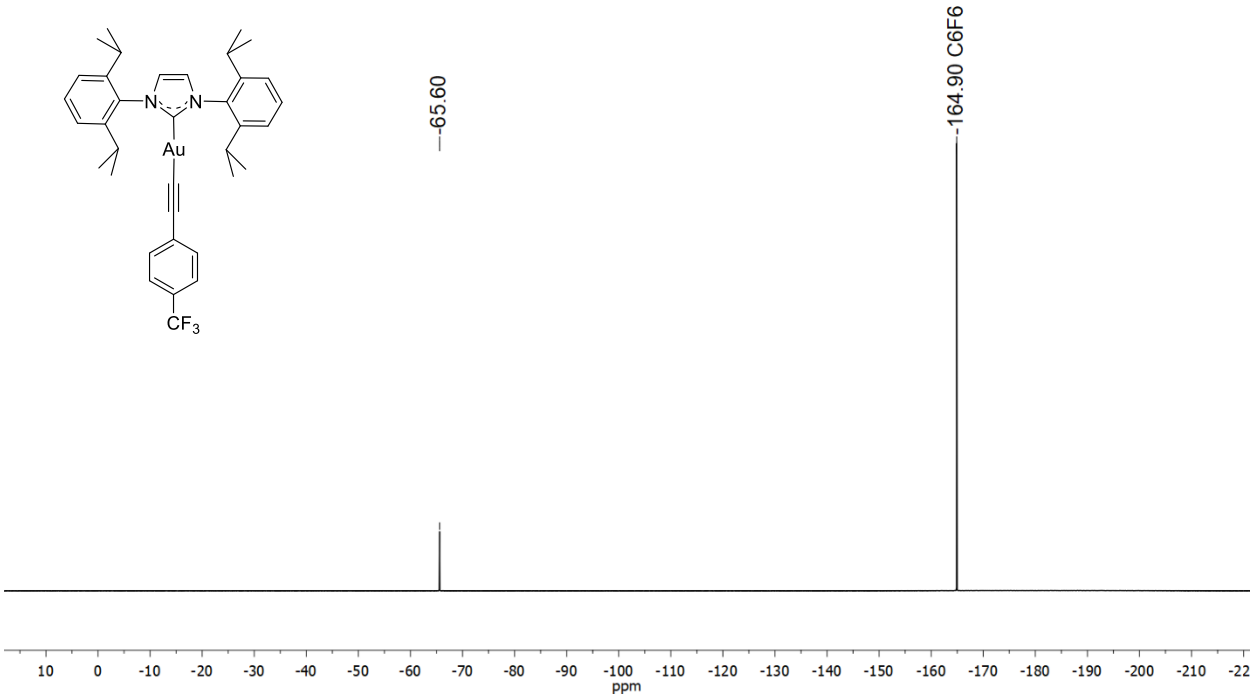

Figure S3. $^{19}F\{^{1}H\}$ NMR spectrum of compound **3a** ($CDCl_3$, 282 MHz). Standard: C_6F_6 with respect to $CFCl_3$).

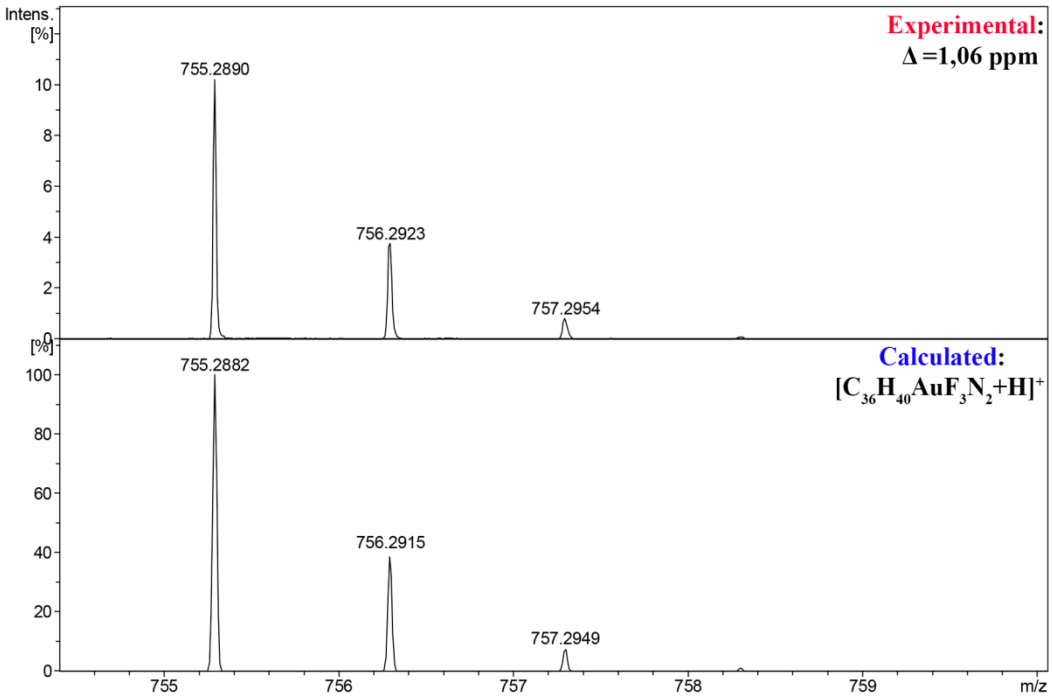

Figure S4. Experimental and theoretical ESI-(+)HRMS spectrum of **3a** in CH_3CN solution: experimental peak $[M+H]^+$ = 755.2890 Da, calculated for $C_{36}H_{40}AuF_3N_2$ = 755.2882, Δ = 1.06 ppm.

(1,3-bis(2,6-diisopropylphenyl)-2,3-dihy(1,3-bis(2,6-diisopropylphenyl)-2,3-dihydro-1H-imidazol-2-yl)((4-(dimethylamino)phenyl)ethynyl)gold (3b). Yield 78% (Yield 57% when base = *t*-BuOK), white powder.

^{1}H NMR ($CDCl_3$, 300 MHz): δ 7.48 (t, J = 7.7 Hz, 2H), 7.28 (d, J = 7.8 Hz, 4H), 7.19 (d, J = 8.7 Hz, 2H), 7.10 (s, 2H), 6.48 (d, J = 8.7 Hz, 2H), 2.86 (s, 2H), 2.60 (sept, J = 6.6 Hz, 4H), 1.38 (d, J = 6.8 Hz, 12H), 1.20 (d, J = 6.9 Hz, 12H).

^{13}C{^{1}H} NMR ($CDCl_3$, 76 MHz): δ 191.6, 148.8, 145.8, 134.6, 133.3, 130.6, 124.4, 124.3, 123.3, 114.0, 111.9, 104.4, 40.6, 29.0, 24.8, 24.2.

ESI-(+)HRMS, *m/z*: 730.3447, calcd for $C_{37}H_{46}AuN_3$: 730.3430 $[M+H]^+$, (Δ = 2,32 ppm).

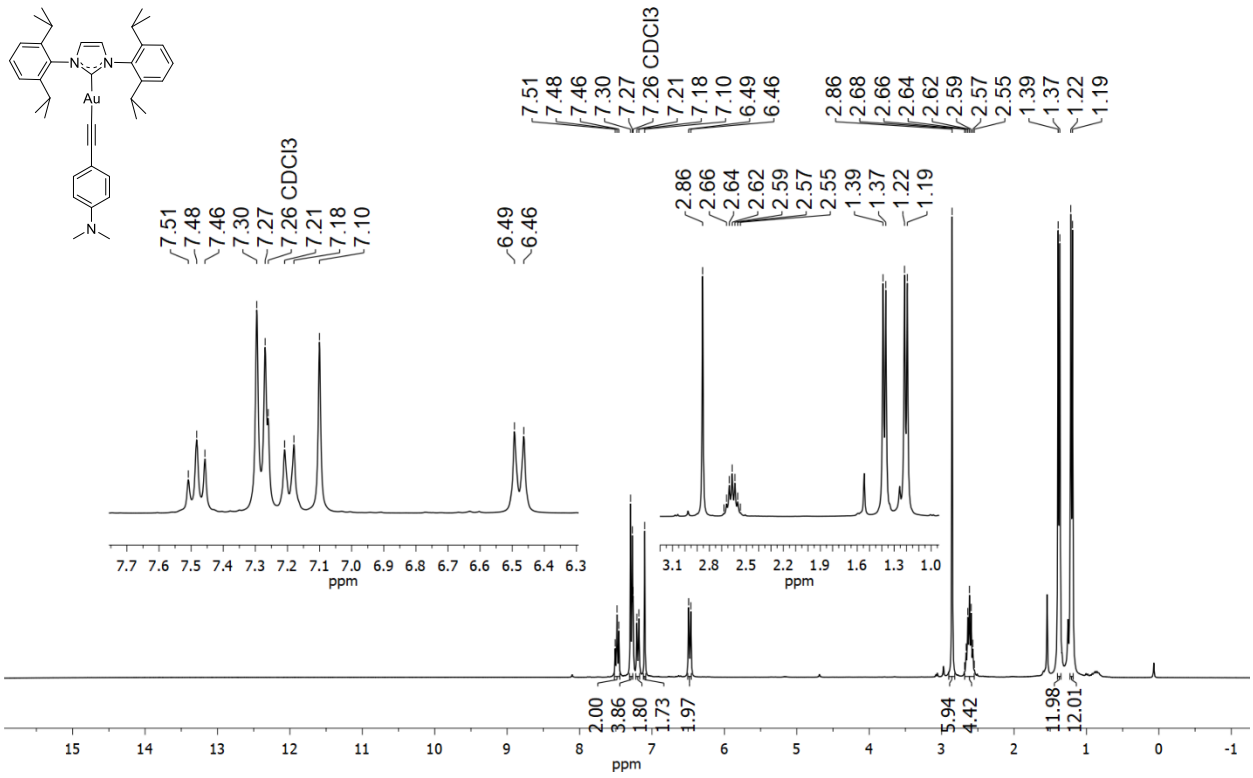

Figure S5. ^{1}H NMR spectrum of compound **3b** ($CDCl_3$, 300 MHz).

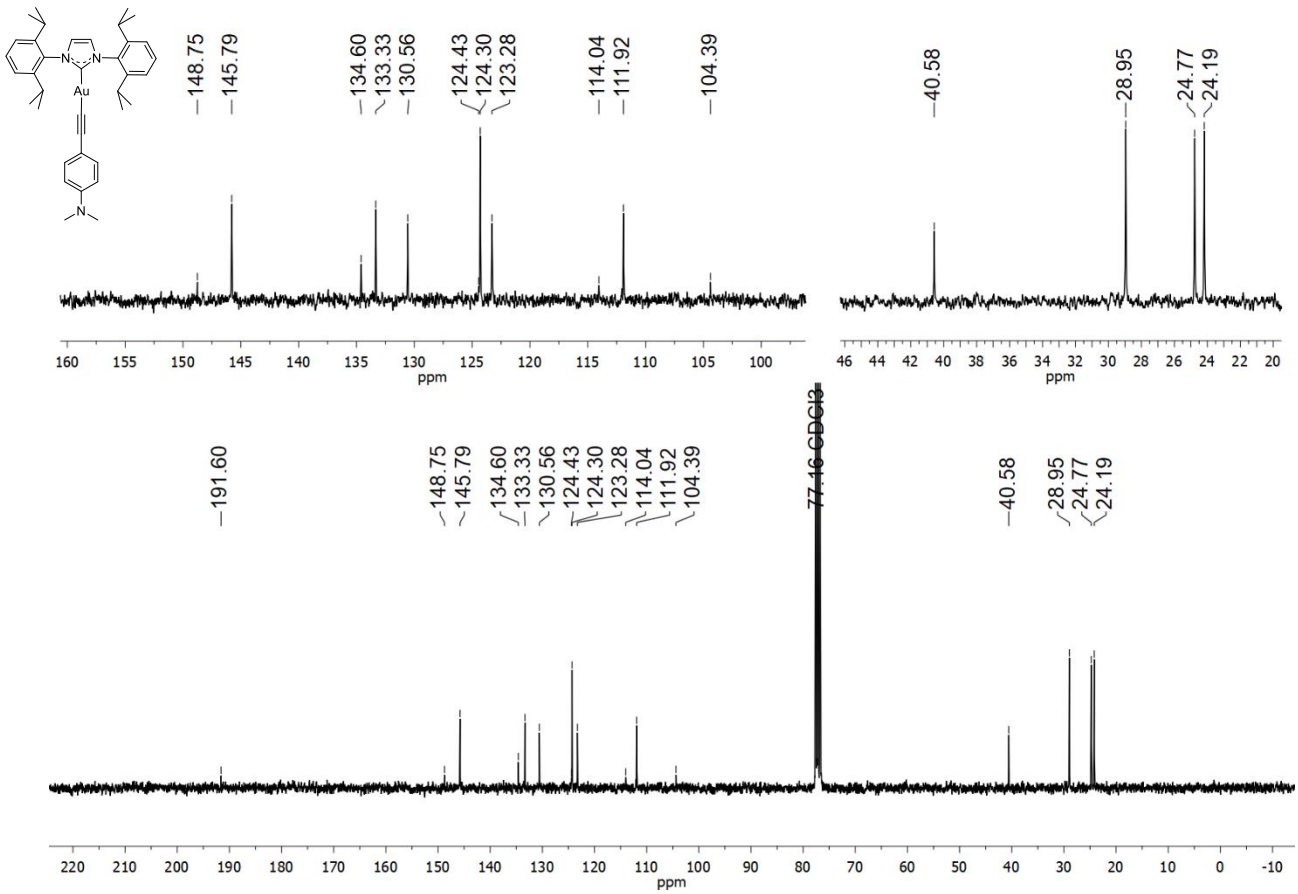

Figure S6. $^{13}C\{^{1}H\}$ NMR spectrum of compound **3b** ($CDCl_3$, 76 MHz).

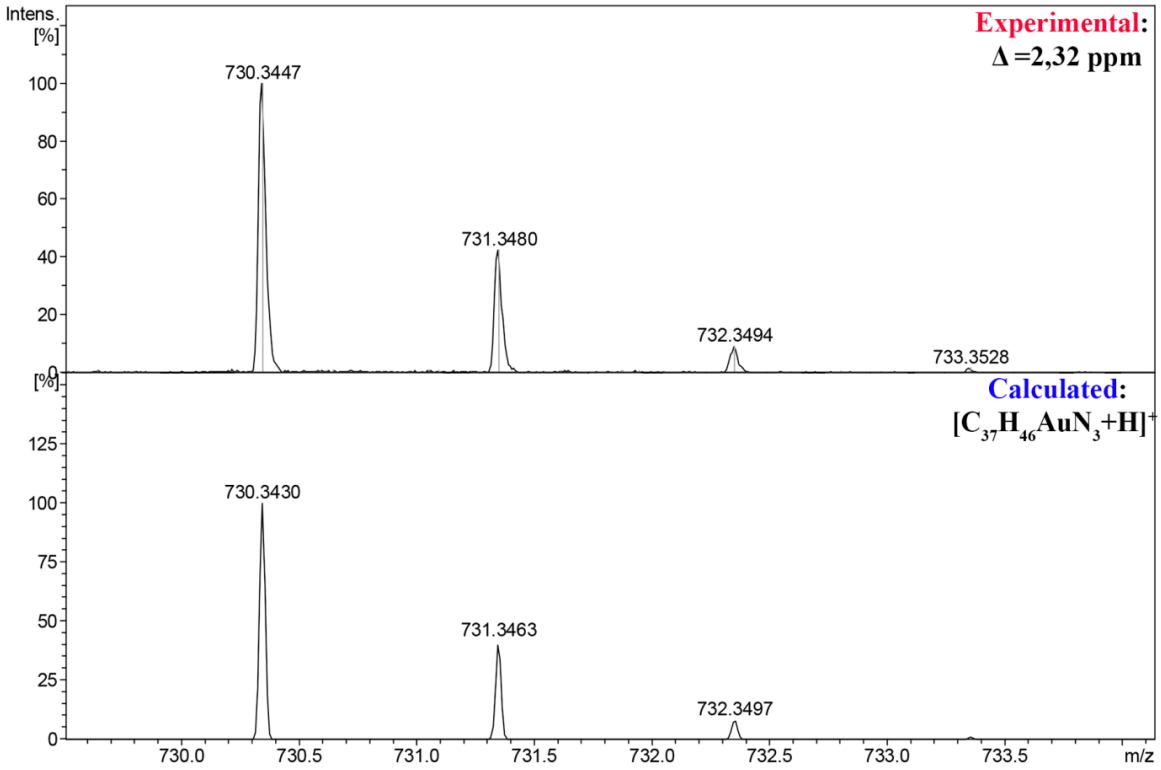

Figure S7. Experimental and theoretical ESI-(+)HRMS spectrum of **3b** in CH_3CN solution: experimental peak $[M+H]^+$ = 730.3447 Da, calculated for $C_{37}H_{46}AuN_3$ = 730.3430, Δ = 2,32 ppm.

(1,3-bis(2,6-diisopropylphenyl)-2,3-dihydro-1H-imidazol-2-yl)((4-ethoxyphenyl)ethynyl)gold (3c). Yield 77% (Yield 57% when base = *t*-BuOK), white powder.

^{1}H NMR ($CDCl_3$, 300 MHz): δ 7.49 (t, J = 7.8 Hz, 2H), 7.28 (d, J = 7.8 Hz, 4H), 7.25 – 7.19 (m, 2H), 7.11 (s, 2H), 6.66 – 6.60 (m, 2H), 3.93 (q, J = 7.0 Hz, 2H), 2.61 (sept, J = 6.9 Hz, 4H), 1.38 (d, J = 6.9 Hz, 12H), 1.33 (t, J = 7.1 Hz, 3H), 1.21 (d, J = 6.9 Hz, 12H).

^{13}C{^{1}H} NMR ($CDCl_3$, 76 MHz): δ 191.3, 157.2, 145.8, 134.5, 133.6, 130.6, 127.0, 124.3, 123.3, 118.4, 113.8, 103.5, 63.3, 28.9, 24.8, 24.2, 14.9.

ESI-(+)HRMS, *m/z*: 731.3280, calcd for $C_{37}H_{45}N_2AuO$: 731.3270 $[M+H]^+$, (Δ = 1,37 ppm).

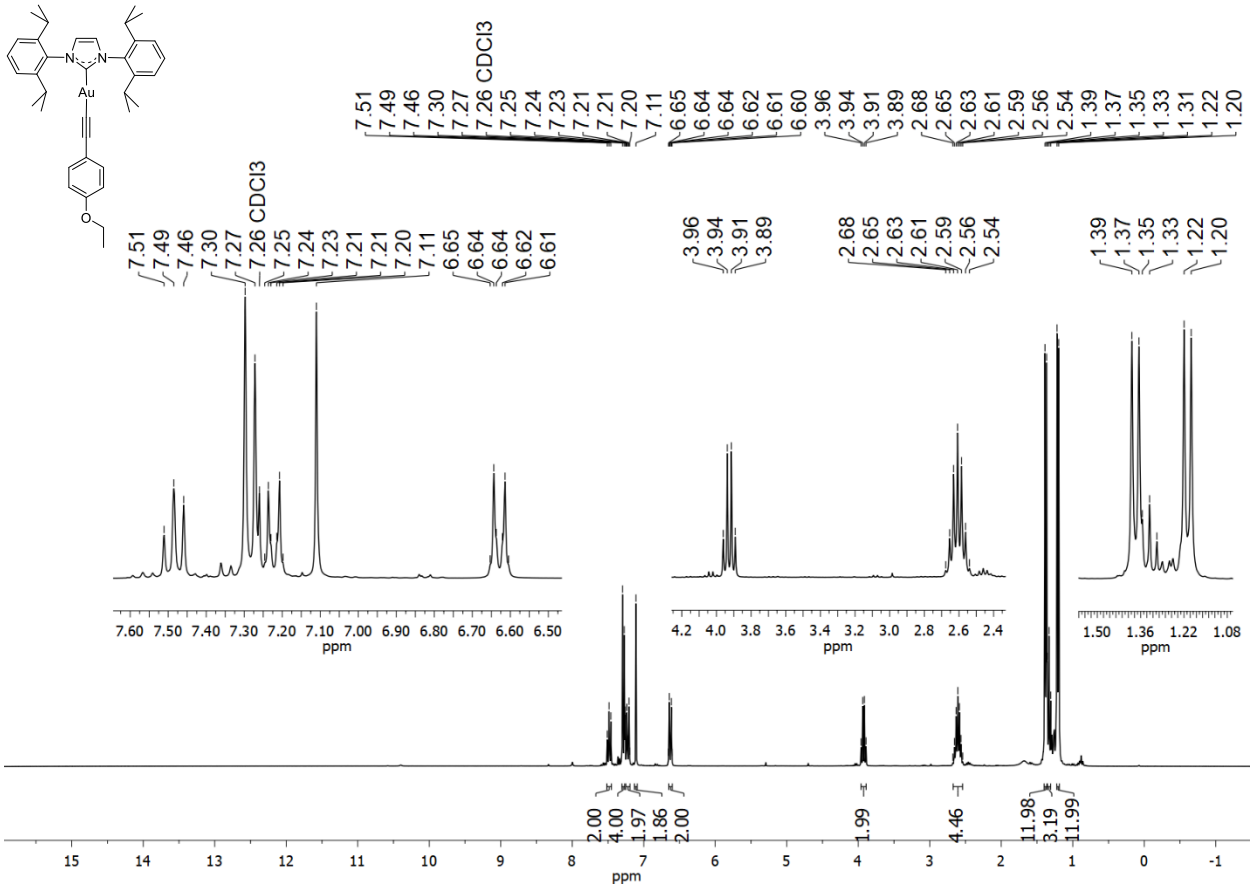

Figure S8. ^{1}H NMR spectrum of compound **3c** ($CDCl_3$, 300 MHz).

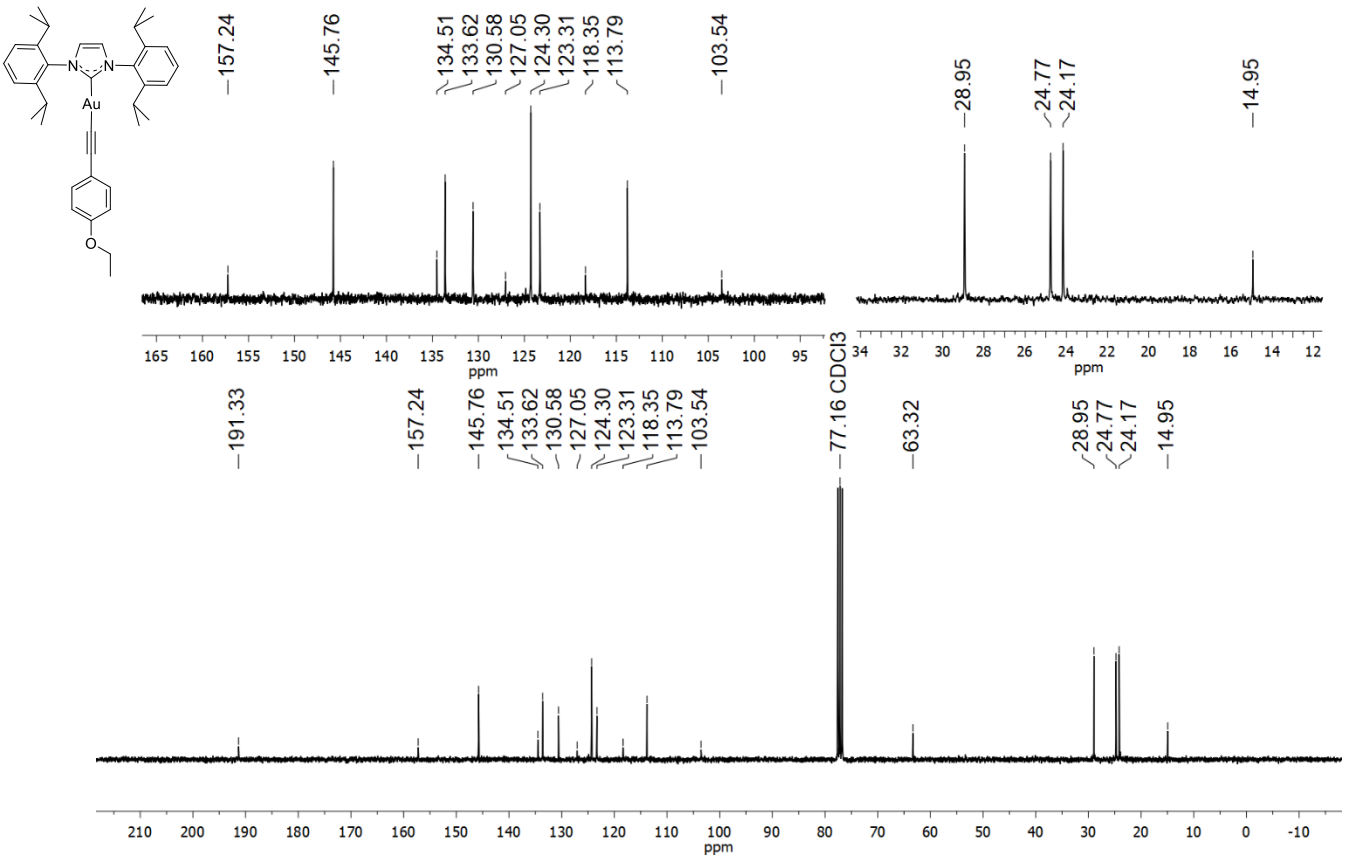

Figure S9. $^{13}C\{^{1}H\}$ NMR spectrum of compound **3c** ($CDCl_3$, 76 MHz).

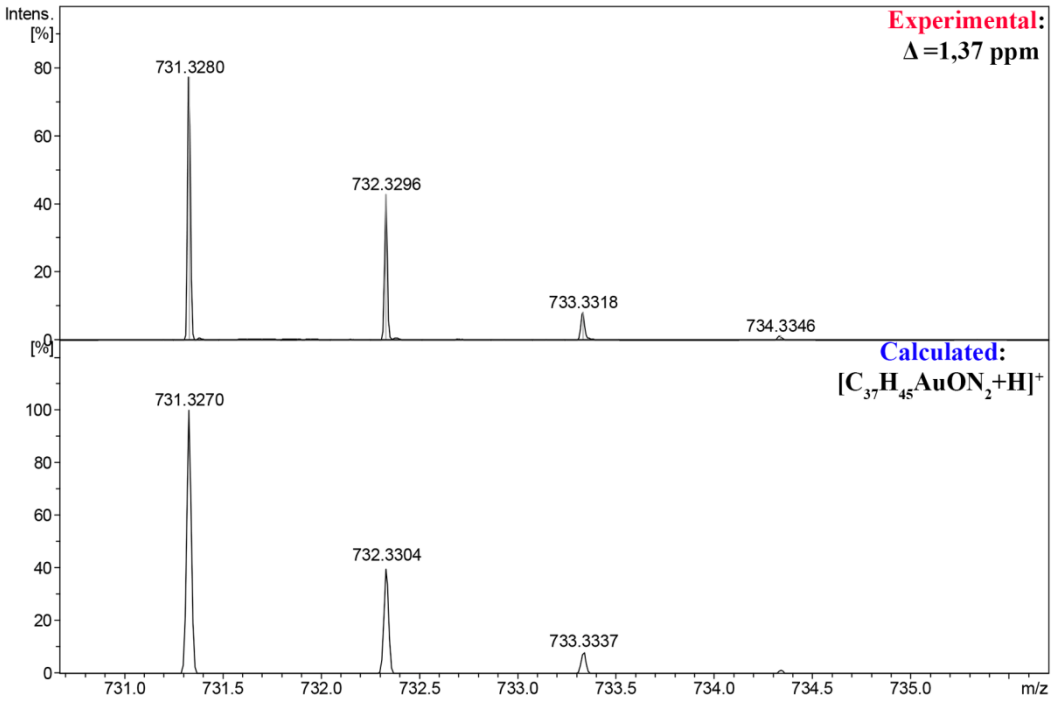

Figure S10. Experimental and theoretical ESI-(+)HRMS spectrum of **3c** in CH_3CN solution: experimental peak $[M+H]^+$ = 731.3280 Da, calculated for $C_{37}H_{45}N_2AuO$ = 731.3270, Δ = 1,37 ppm.

(1,3-bis(2,6-diisopropylphenyl)-2,3-dihydro-1H-imidazol-2-yl)(pent-1-yn-1-yl)gold (3d). Yield 54%, white powder.

^{1}H NMR ($CDCl_3$, 300 MHz): δ 7.47 (t, J = 7.8 Hz, 2H), 7.26 (d, J = 7.8 Hz, 4H), 7.07 (s, 2H), 2.59 (sept, J = 6.9 Hz, 4H), 2.16 (t, J = 7.4 Hz, 2H), 1.48 – 1.38 (m, 2H), 1.35 (d, J = 6.9 Hz, 12H), 1.19 (d, J = 6.9 Hz, 12H), 0.83 (t, J = 7.3 Hz, 3H).

^{13}C{^{1}H} NMR ($CDCl_3$, 76 MHz): δ 191.7, 145.7, 134.6, 130.5, 124.3, 123.2, 115.8, 104.5, 28.9, 24.7, 24.1, 23.7, 22.5, 13.9.

ESI-(+)HRMS, *m/z*: 653.3179, calcd for $C_{32}H_{43}AuN_2$: 653.3165 $[M+H]^+$, (Δ = 2.14 ppm).

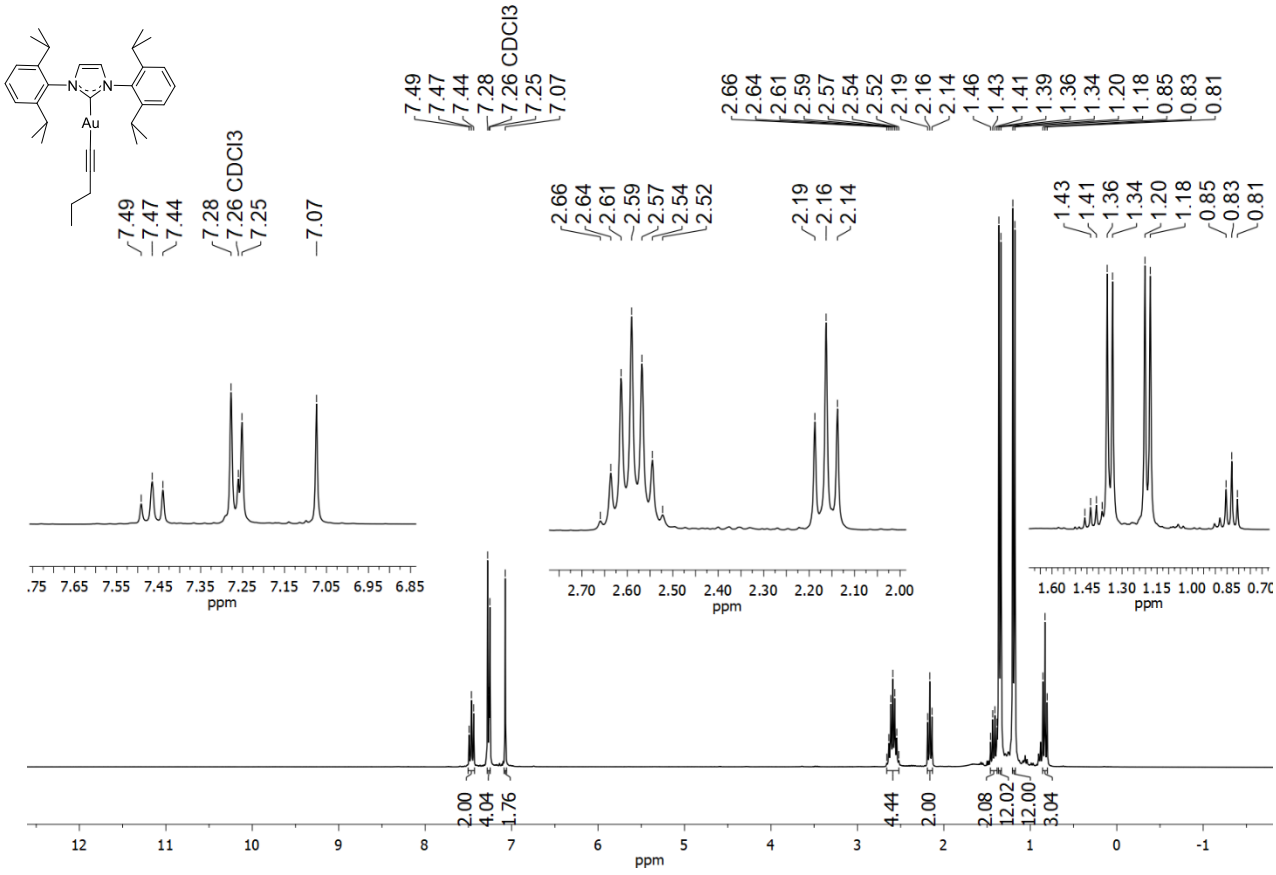

Figure S11. ^{1}H NMR spectrum of compound **3d** ($CDCl_3$, 300 MHz).

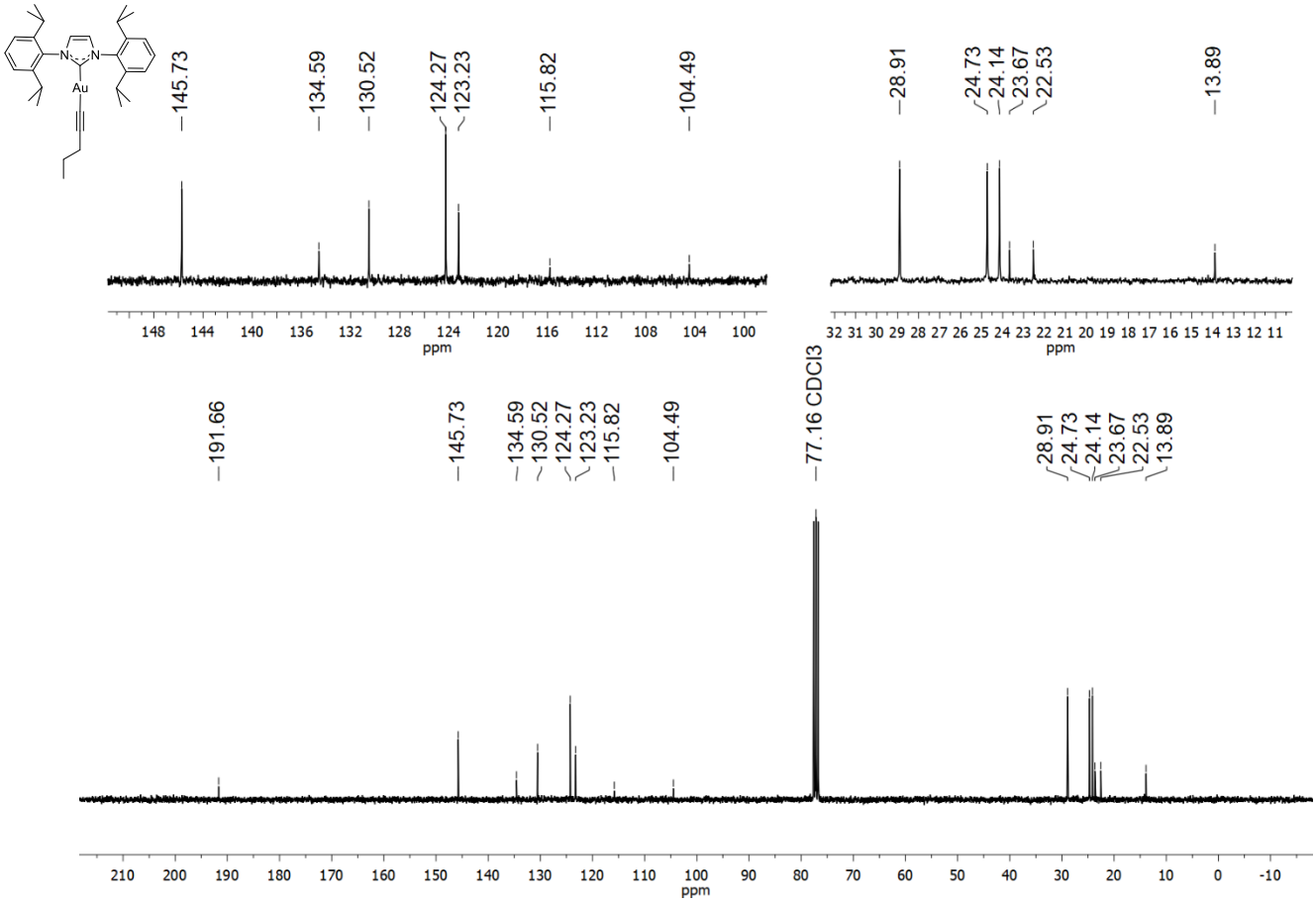

Figure S12. $^{13}C\{^{1}H\}$ NMR spectrum of compound **3d** ($CDCl_3$, 76 MHz).

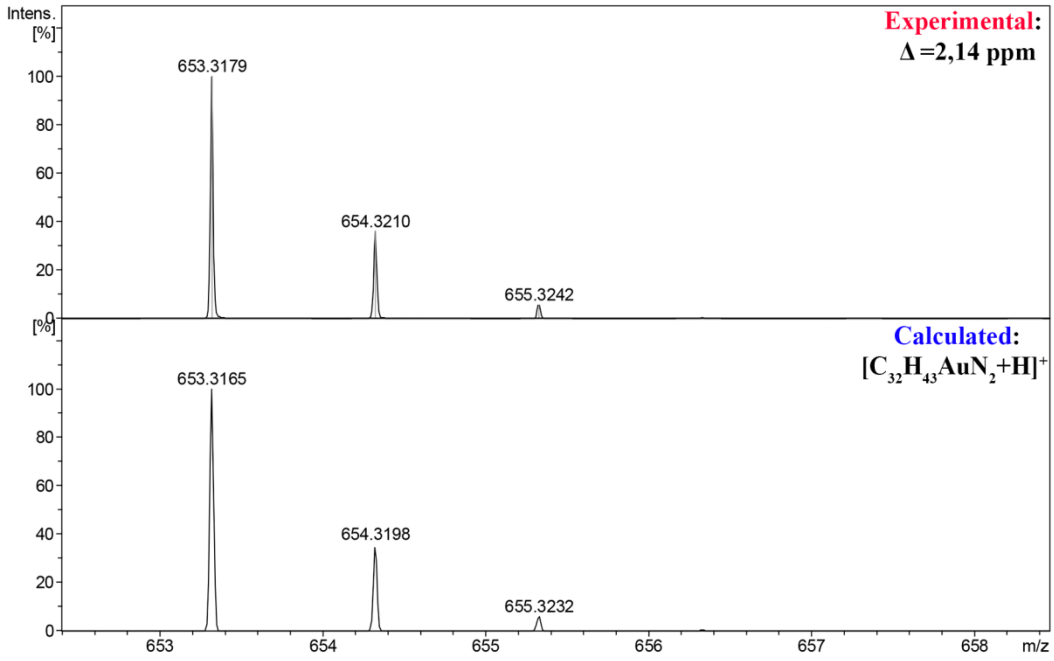

Figure S13. Experimental and theoretical ESI-(+)HRMS spectrum of **3d** in CH_3CN solution: experimental peak $[M+H]^+$ = 653.3179 Da, calculated for $C_{32}H_{43}AuN_2$ = 653.3165, Δ = 2.14 ppm.

(1,3-bis(2,6-diisopropylphenyl)-2,3-dihydro-1H-imidazol-2-yl)(pyridin-2-ylethynyl)gold (3e). Yield 22%, off-white powder.

^{1}H NMR (CD_2Cl_2, 300 MHz): δ 8.33 (d, J = 4.1 Hz, 1H), 7.58 (t, J = 7.7 Hz, 2H), 7.44 (t, J = 7.6 Hz, 1H), 7.37 (d, J = 7.7 Hz, 4H), 7.22 (s, 2H), 7.13 (d, J = 7.8 Hz, 1H), 7.01 – 6.91 (m, 1H), 2.58 (sept, J = 6.6 Hz, 4H), 1.38 (d, J = 6.8 Hz, 12H), 1.24 (d, J = 6.8 Hz, 12H).

^{13}C{^{1}H} NMR (CD_2Cl_2, 151 MHz): δ 190.8, 149.8, 146.4, 145.8, 135.8, 134.7, 131.9, 131.1, 127.2, 124.7, 124.0, 121.1, 103.4, 29.4, 24.9, 24.3.

ESI-(+)HRMS, *m/z*: 688.2961, calcd for $C_{34}H_{40}AuN_3$: 688.2961 $[M+H]^+$, (Δ = 0 ppm).

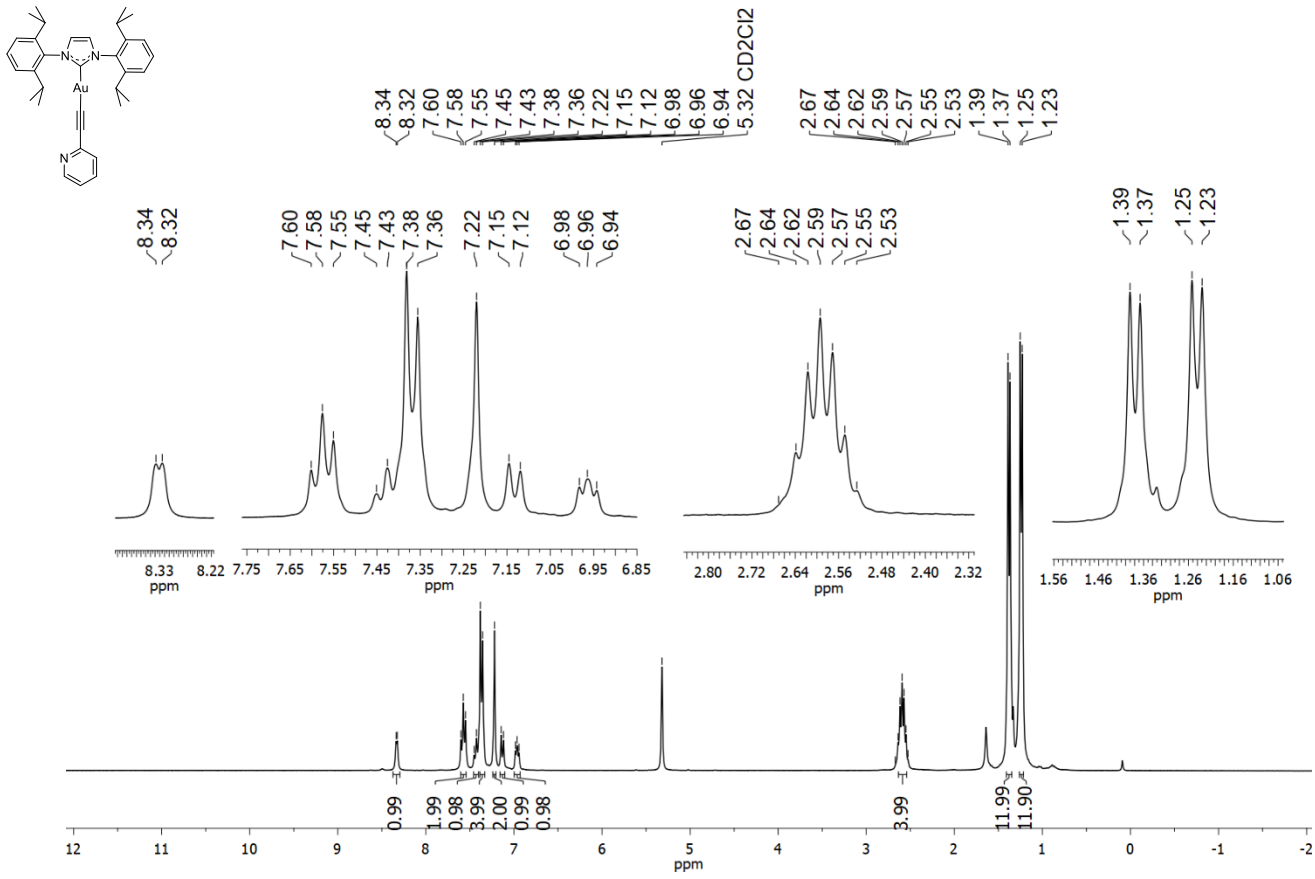

Figure S14. ^{1}H NMR spectrum of compound **3e** (CD_2Cl_2, 300 MHz).

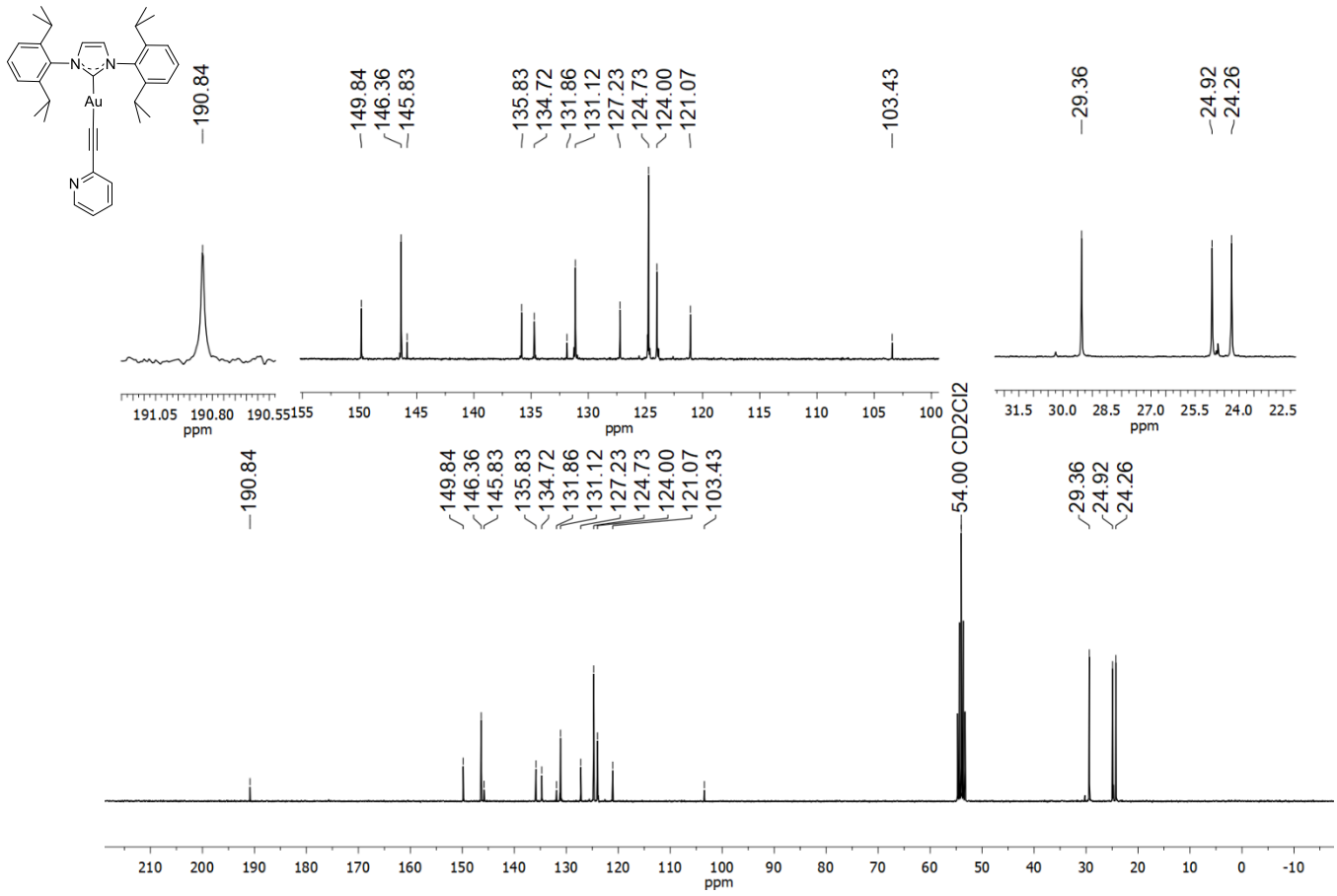

Figure S15. $^{13}C\{^{1}H\}$ NMR spectrum of compound **3e** (CD_2Cl_2, 151 MHz).

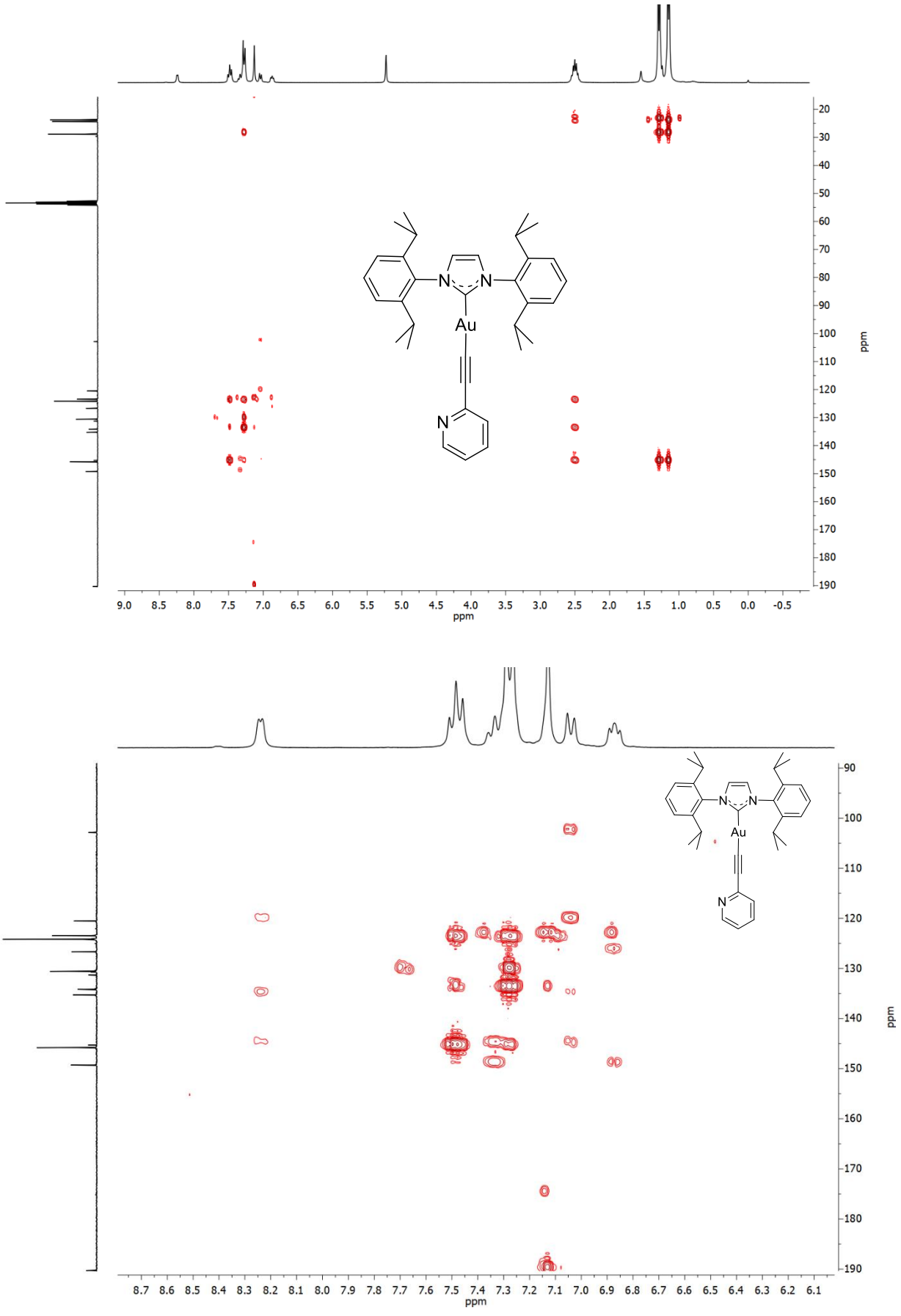

Figure S16. ^{1}H-^{13}C HMBC spectra of compound **3e** (400 MHz, CD_2Cl_2).

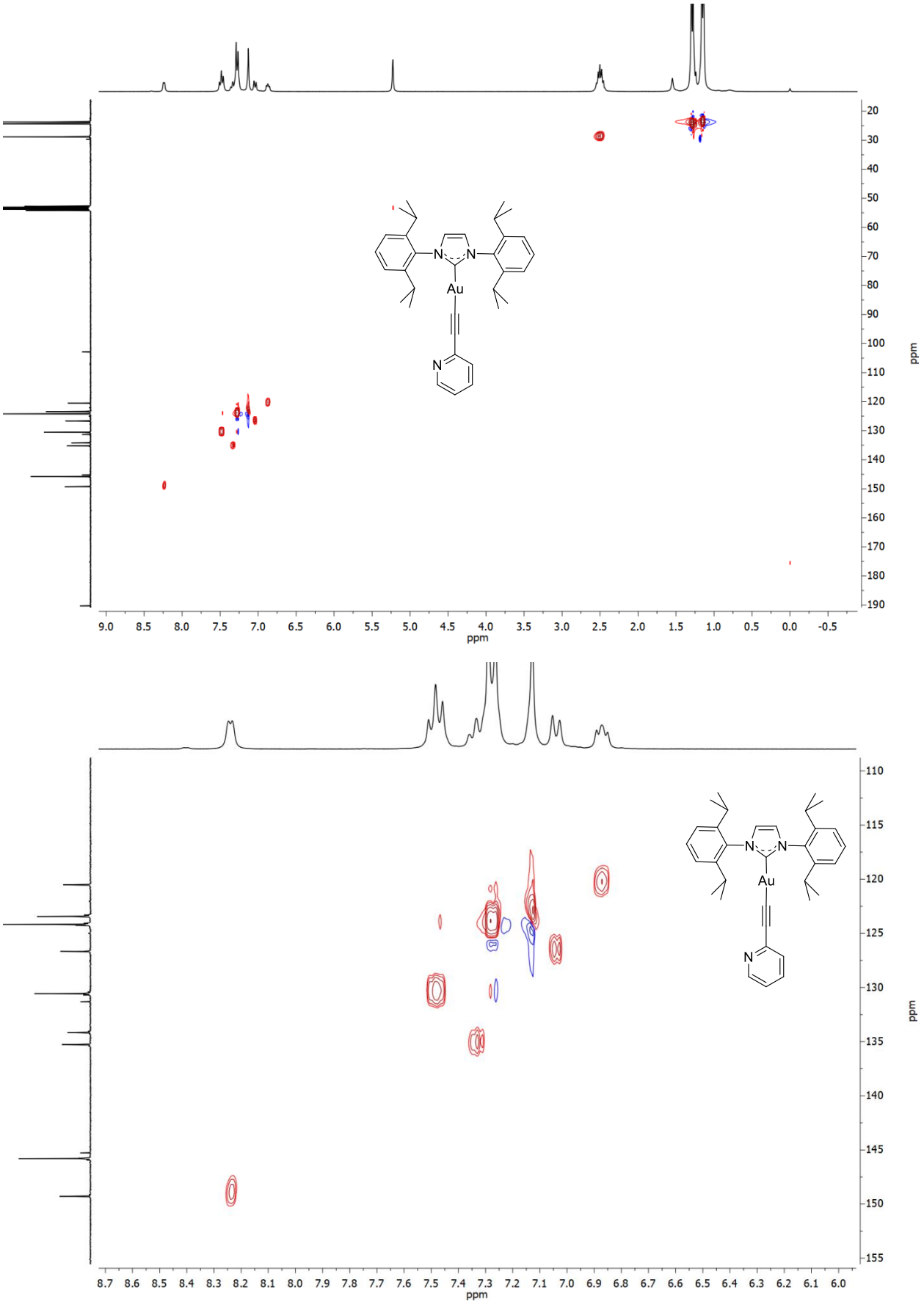

Figure S17. ^{1}H-^{13}C HSQC spectra of compound **3e** (400 MHz, CD_2Cl_2).

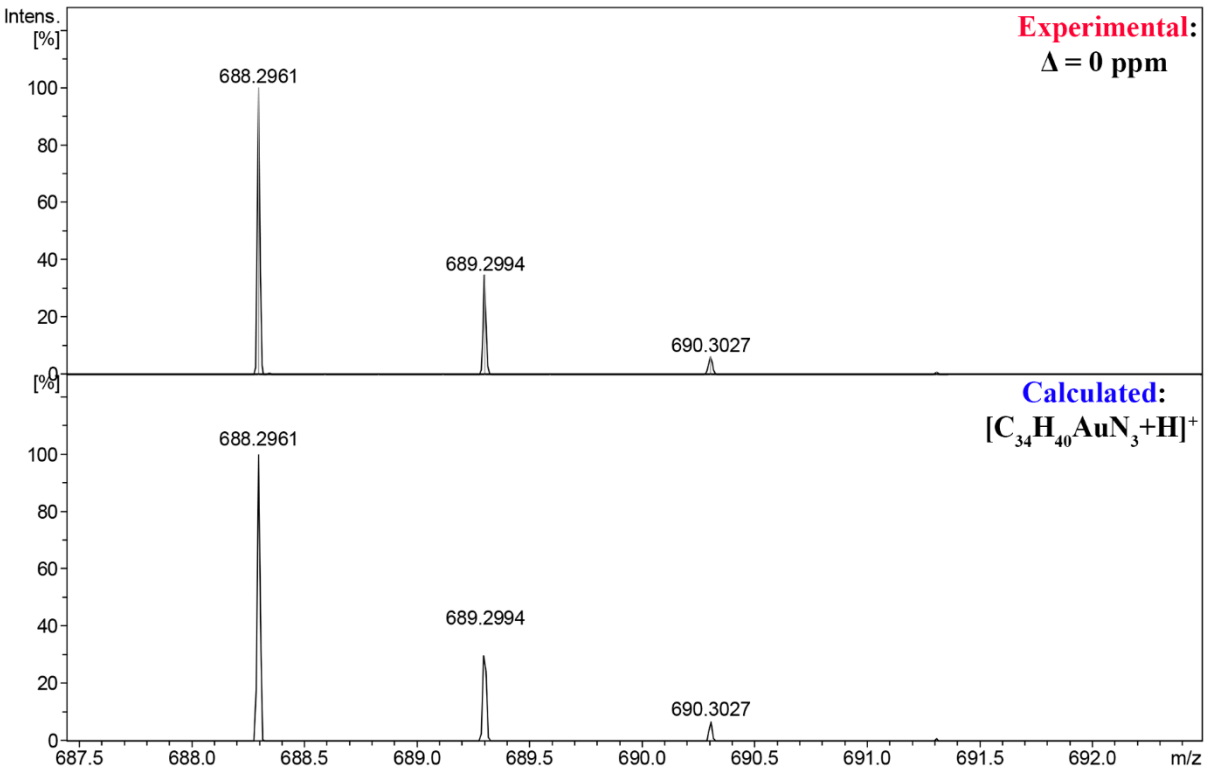

Figure S18. Experimental and theoretical ESI-(+)HRMS spectrum of **3e** in CH_3CN solution: experimental peak $[M+H]^+$ = 688.2961 Da, calculated for $C_{34}H_{40}AuN_3$ = 688.2961, Δ = 0 ppm.

1,3-bis(2,6-diisopropylphenyl)-1H-imidazol-3-ium bis((4-(trifluoromethyl)phenyl)ethynyl)aurate(I) (4a).
Yield 42%, yellowish or white powder.

^{1}H NMR (CD_2Cl_2, 300 MHz): δ 8.67 (s, 1H), 7.95 (s, 2H), 7.63 (t, J = 7.8 Hz, 2H), 7.40 (d, J = 7.6 Hz, 4H), 7.36 (d, J = 8.1 Hz, 4H), 7.30 (d, J = 8.1 Hz, 4H), 2.41 (sept, J = 6.4 Hz, 4H), 1.28 (d, J = 6.7 Hz, 12H), 1.21 (d, J = 6.8 Hz, 12H).

^{13}C{^{1}H} NMR (CD_2Cl_2, 126 MHz): δ 145.5, 139.9, 137.1, 133.2, 132.4, 131.8 (d, $J_{C\text{-}F}$ = 1.4 Hz), 129.9, 127.0 (q, $J_{C\text{-}F}$ = 32.7 Hz), 126.9, 125.7, 125.21 (q, $J_{C\text{-}F}$ = 3.8 Hz), 125.15 (q, $J_{C\text{-}F}$ = 271.4 Hz), 102.1, 29.8, 24.9, 24.1.

^{19}F{^{1}H} NMR ($CDCl_3$, 282 MHz): δ -65.54 (CF_3).

ESI-(-)HRMS, *m/z*: 535.0201, calcd for $C_{18}H_8AuF_6$: 535.0190 $[M]^-$, (Δ = 2.06 ppm).

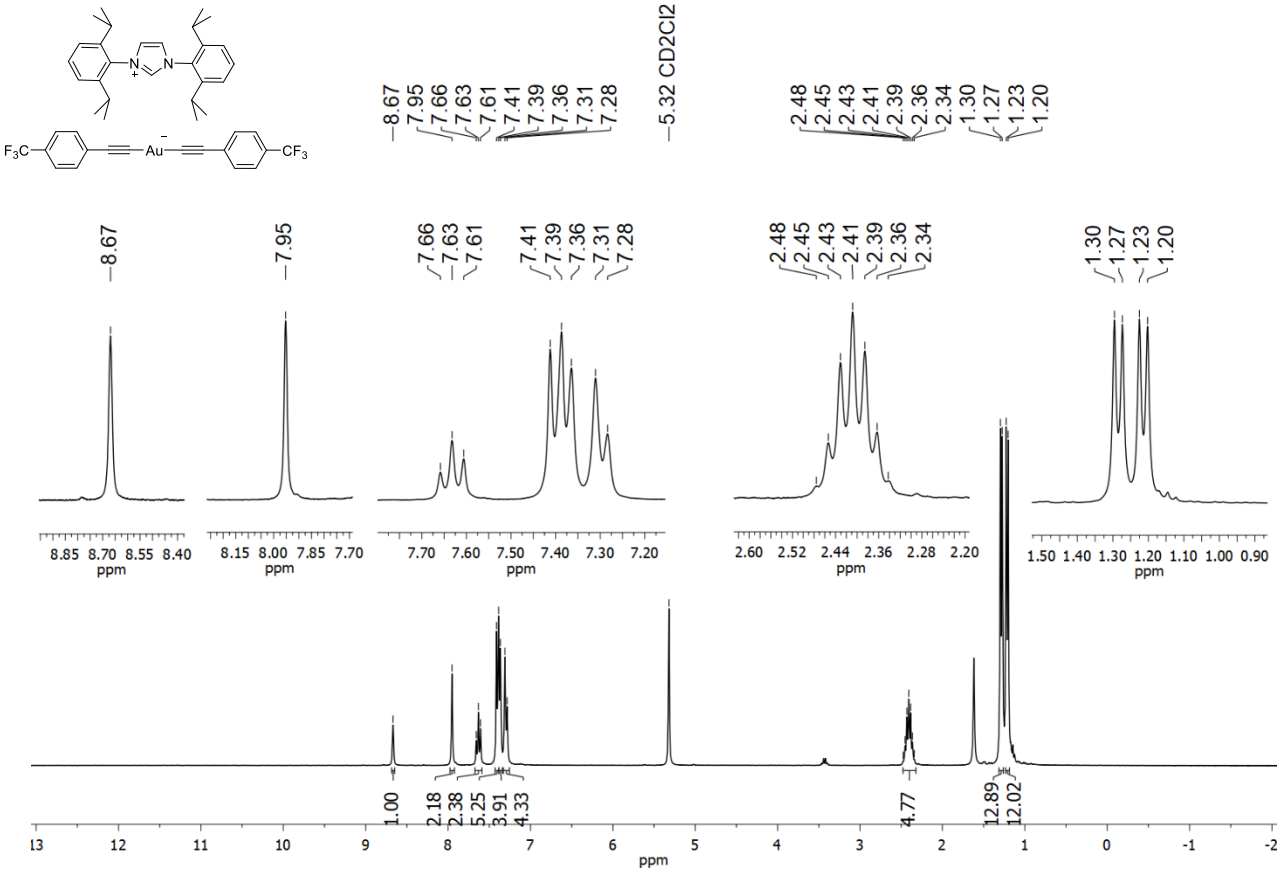

Figure S19. ^{1}H NMR spectrum of compound **4a** (CD_2Cl_2, 300 MHz).

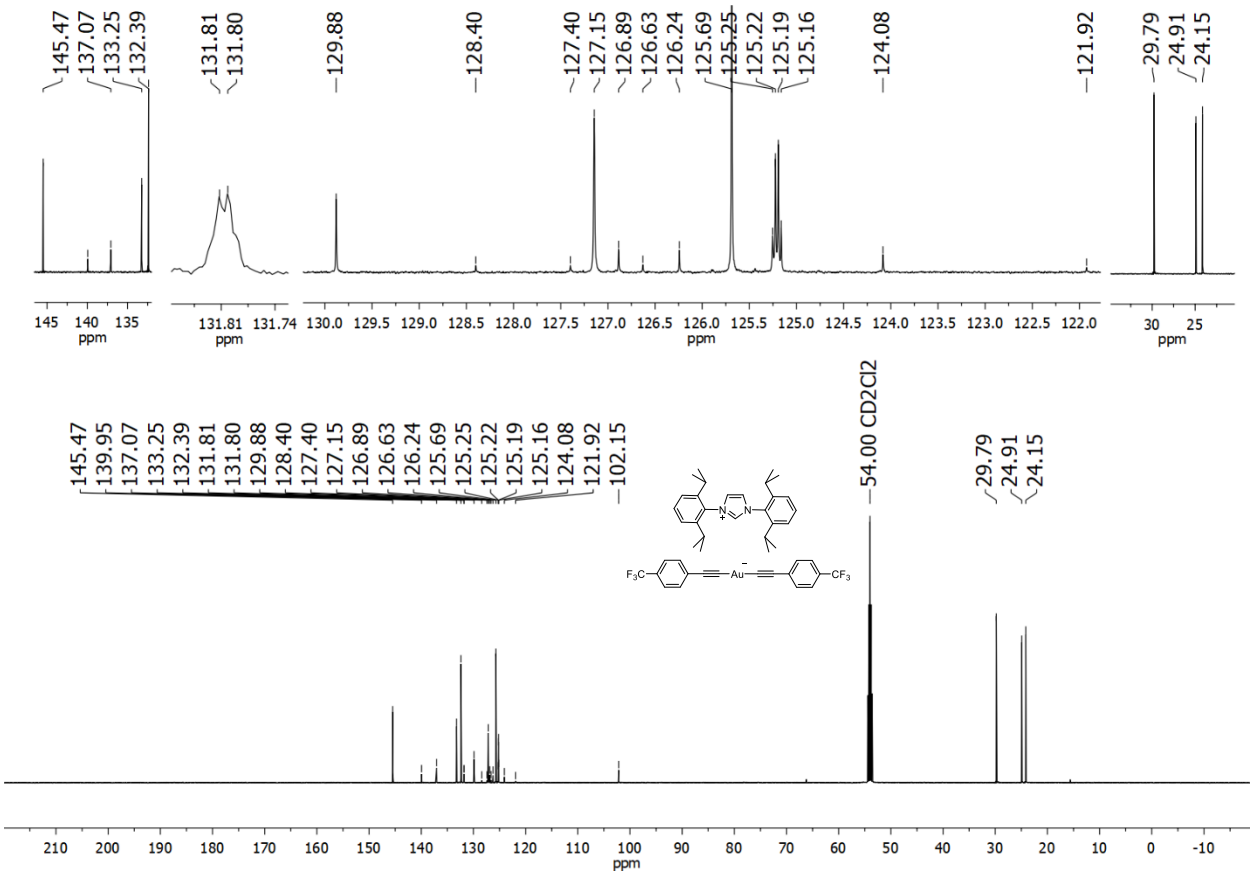

Figure S20. $^{13}C\{^{1}H\}$ NMR spectrum of compound **4a** (CD_2Cl_2, 126 MHz).

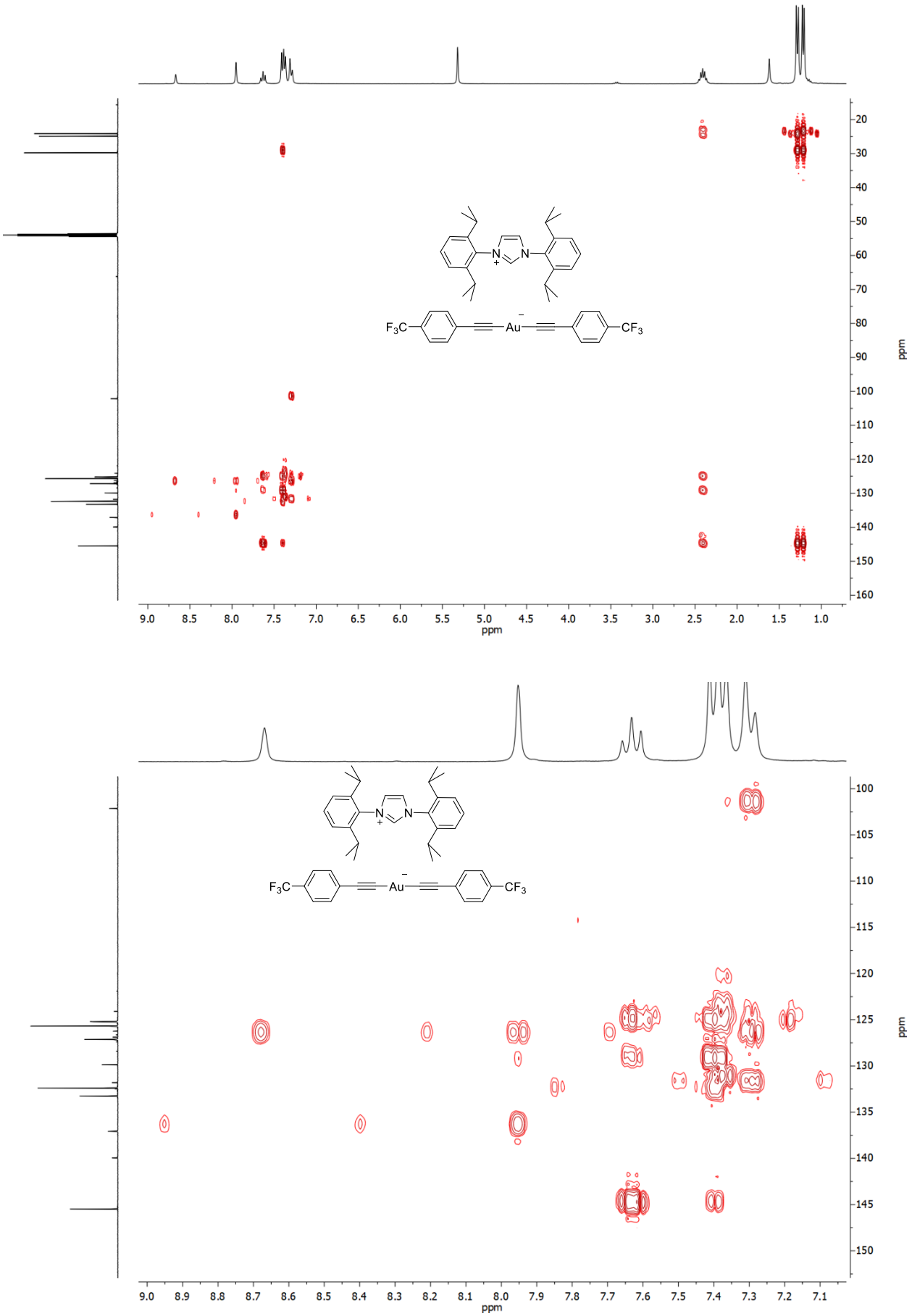

Figure S21. ^{1}H-^{13}C HMBC spectra of compound **4a** (400 MHz, CD_2Cl_2).

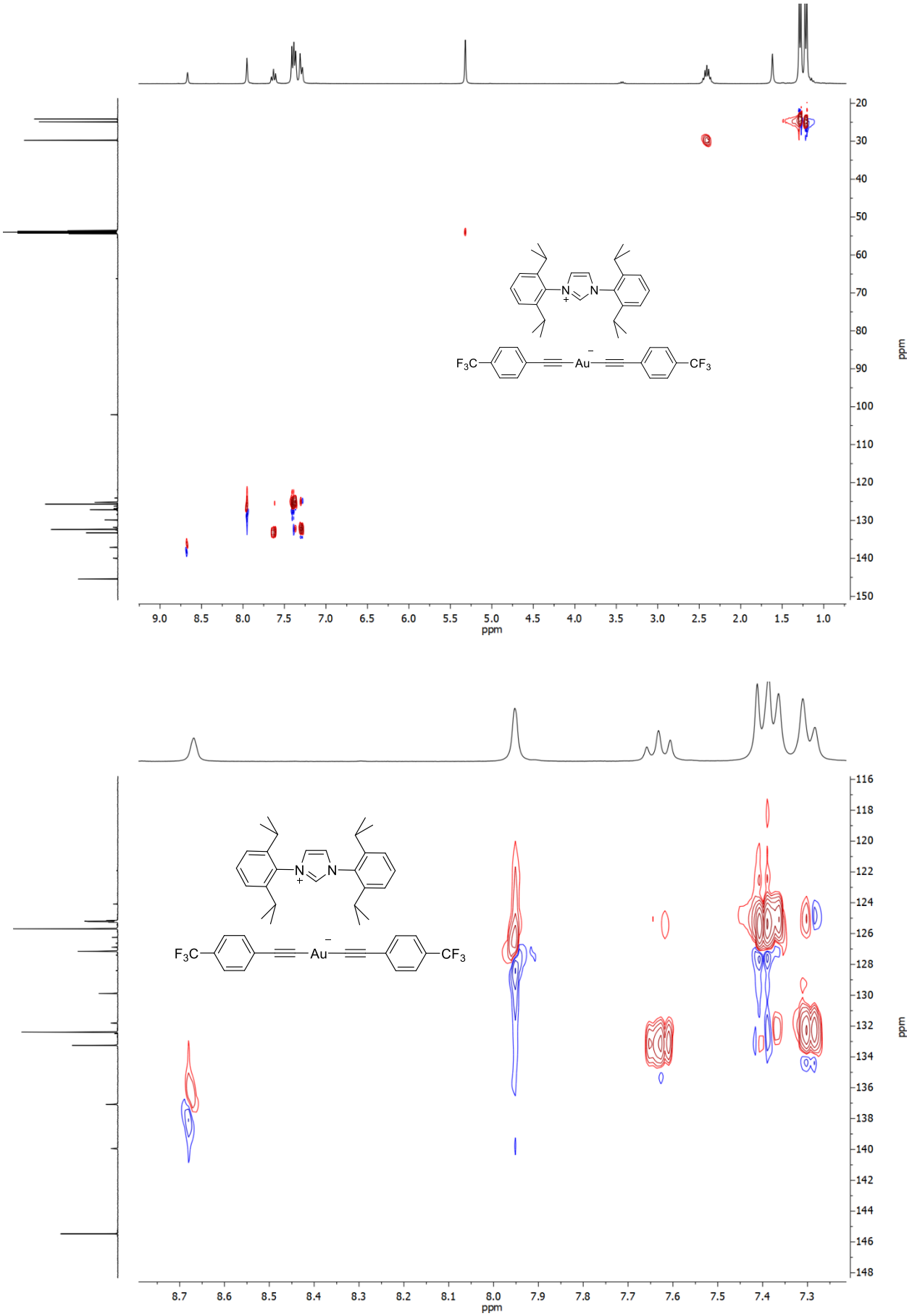

Figure S22. ^{1}H-^{13}C HSQC spectra of compound **4a** (400 MHz, CD_2Cl_2).

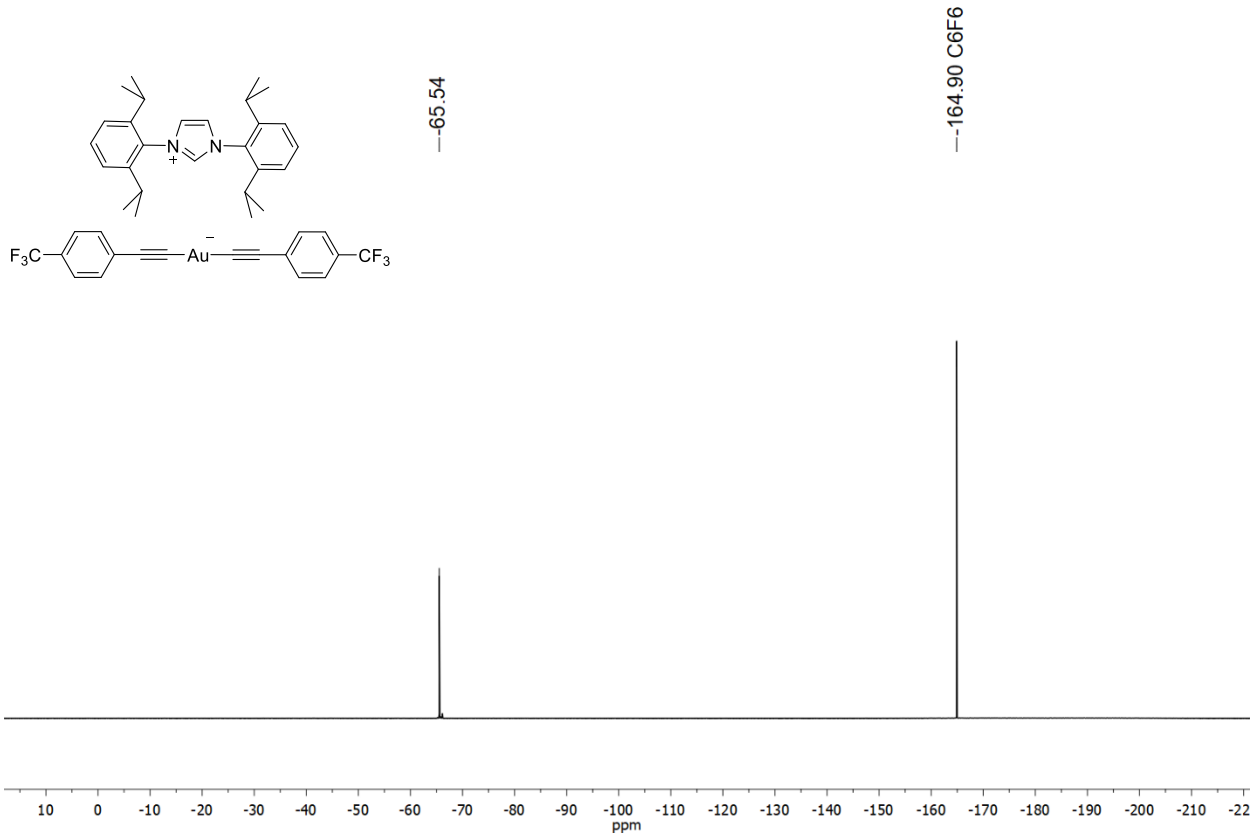

Figure S23. $^{19}F\{^{1}H\}$ NMR spectrum of compound **4a** ($CDCl_3$, 282 MHz). Standard: C_6F_6 with respect to $CFCl_3$.

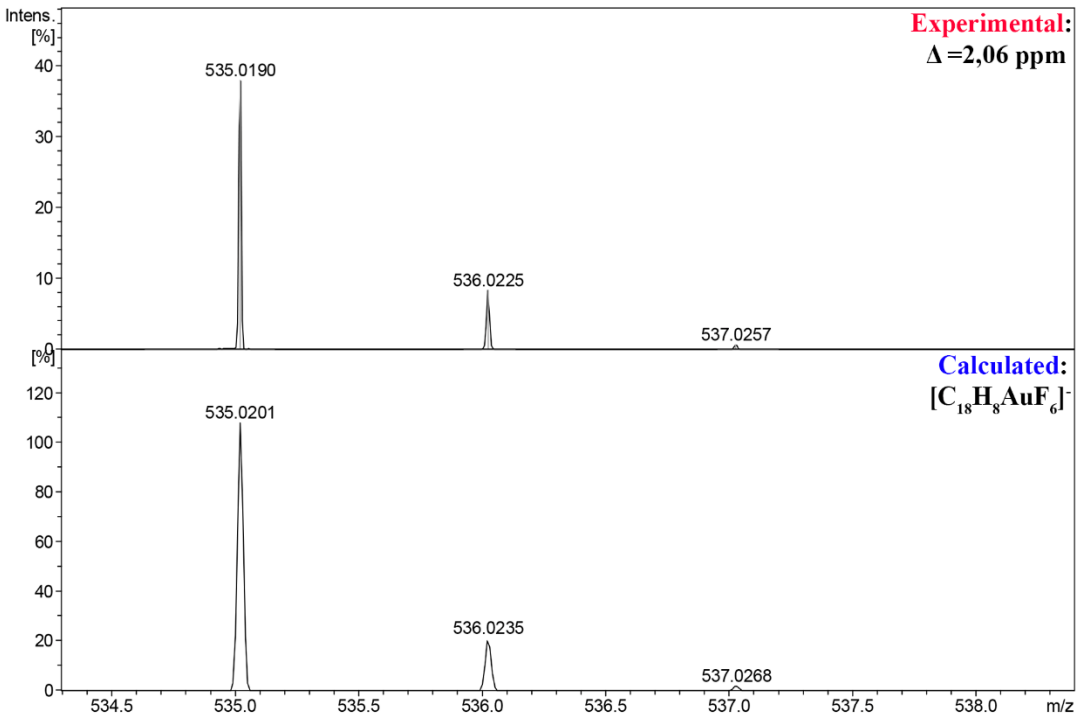

Figure S24. Experimental and theoretical ESI-(-)HRMS spectrum of **4a** in CH_3CN solution: experimental peak $[M]^-$ = 535.0201 Da, calculated for $C_{18}H_8AuF_6$ = 535.0190, Δ = 2.06 ppm.

5. Study of contaminated commercial reagents

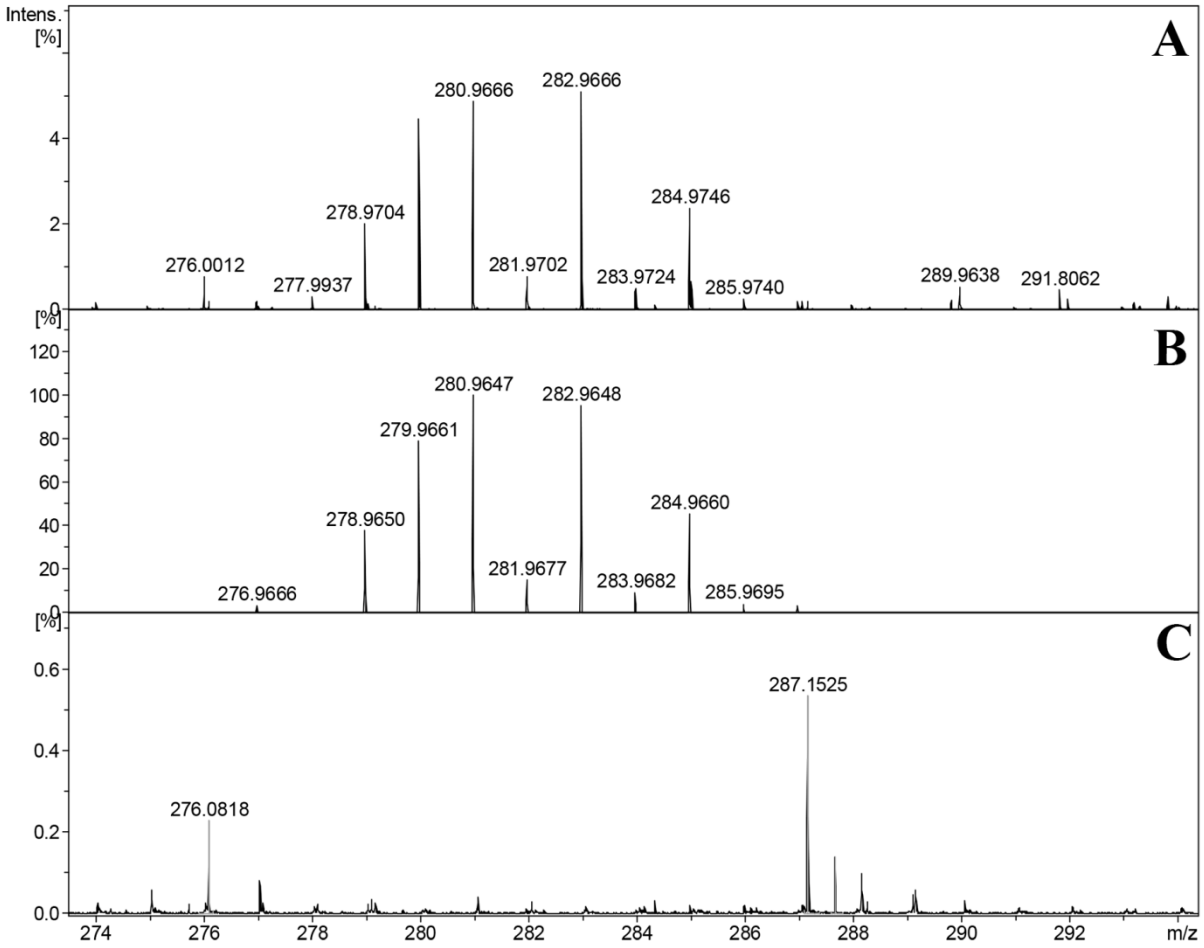

Figure S25. Experimental (A) and theoretical (B) ESI-(+)HRMS spectrum of THT-AuCl from commercial source contaminated with Pd for the $[(C_4H_7S)_2PdH]^+$ ion; and experimental ESI-(+)HRMS spectrum (C) of the THT-AuCl prepared by ourselves, the same region.

6. SEM/DFSTEM and EDX investigation of Au particles and nanoparticles

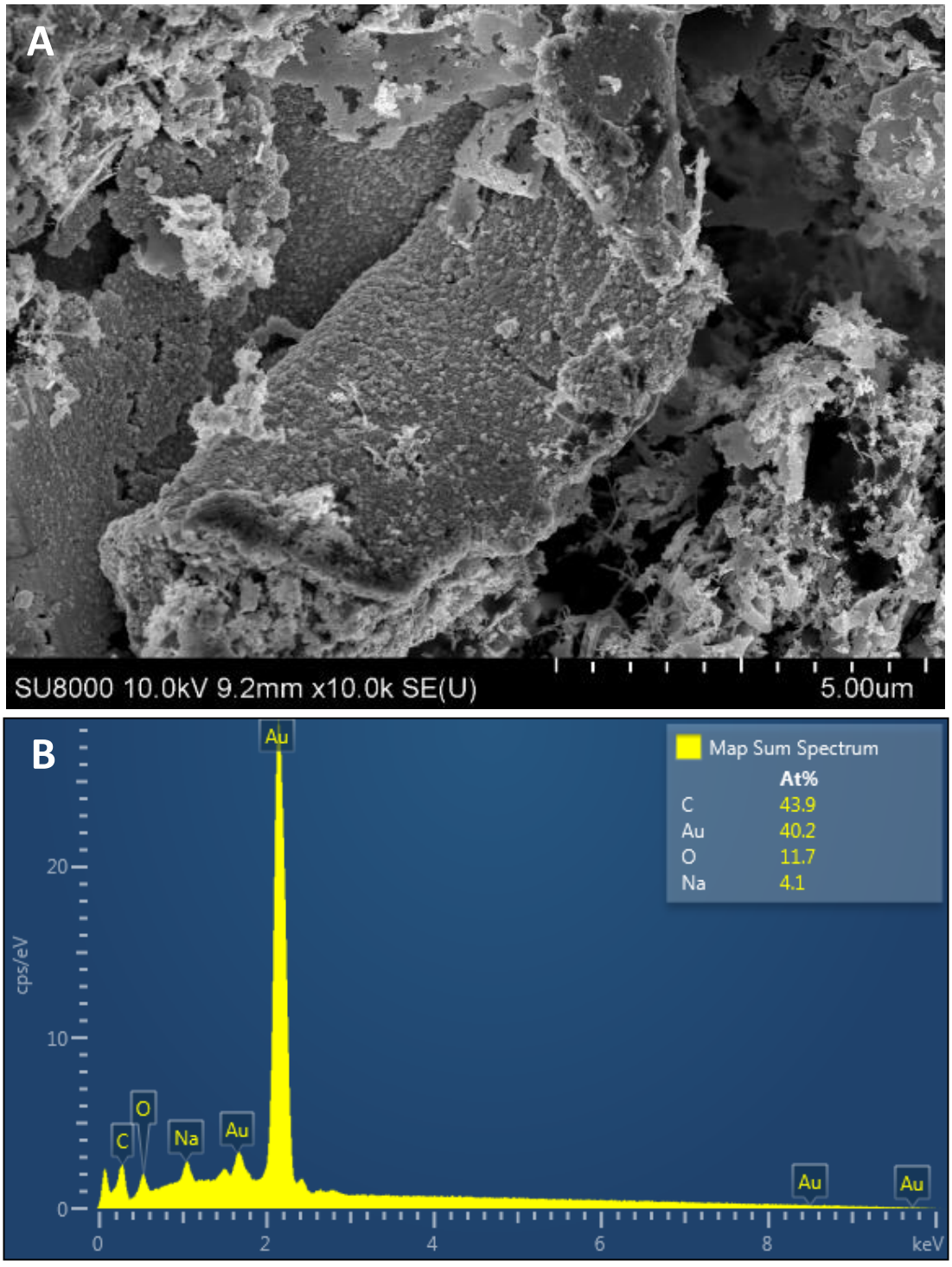

Figure S26. A) SEM image of the gold plaque under magnetic stirrer anchor obtained from reaction between IPrAuCl **1** and AcONa after 1 week at r.t.; B) EDX spectrum of the gold plaque obtained from reaction between IPrAuCl **1** and AcONa after 1 week at r.t.

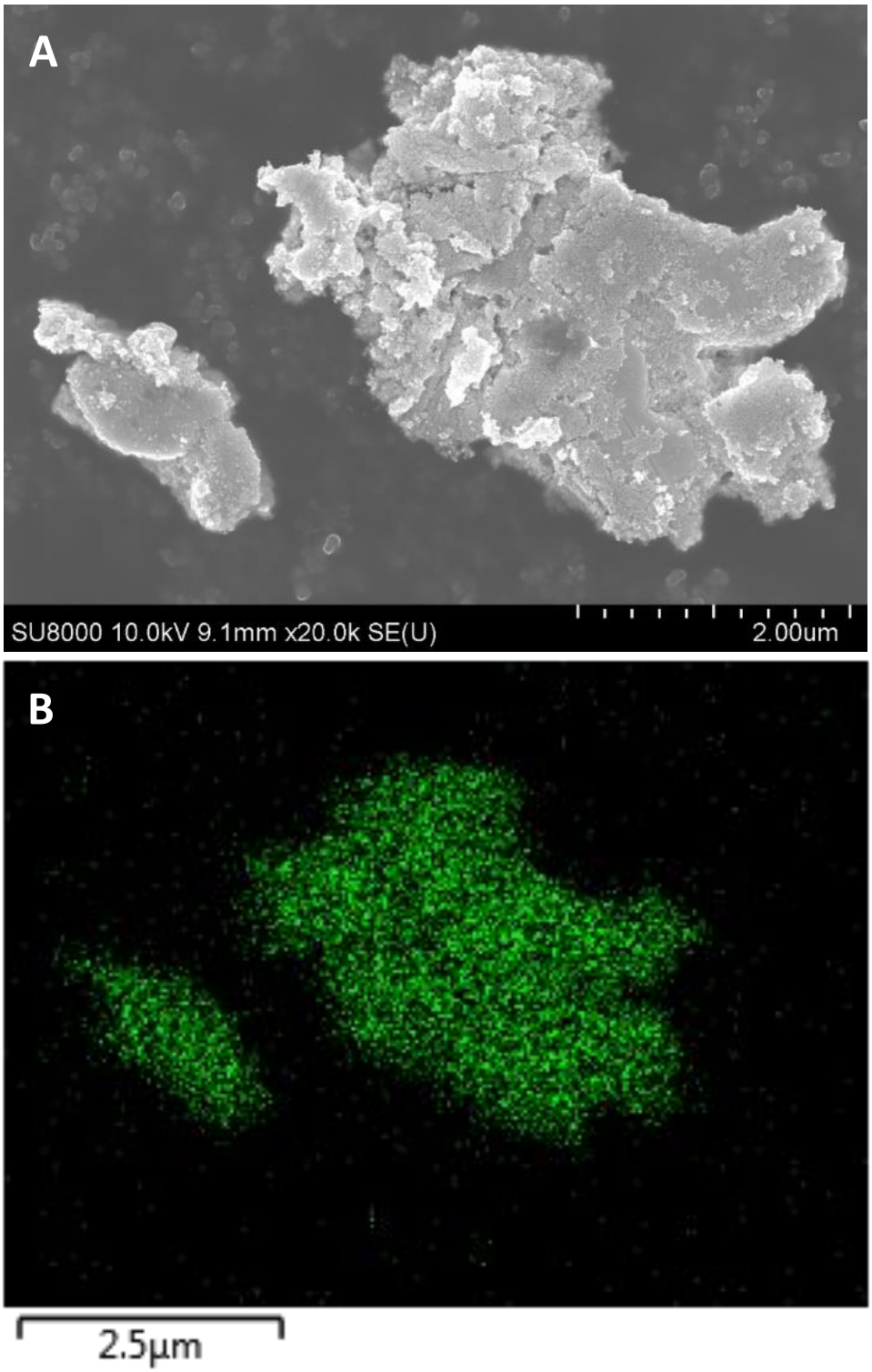

Figure S27. A) SEM image of gold plaque under glass vial obtained from synthesis of complex **3b** at r.t. B) EDX element mapping of gold plaque under glass vial obtained from synthesis of complex **3b** at r.t.

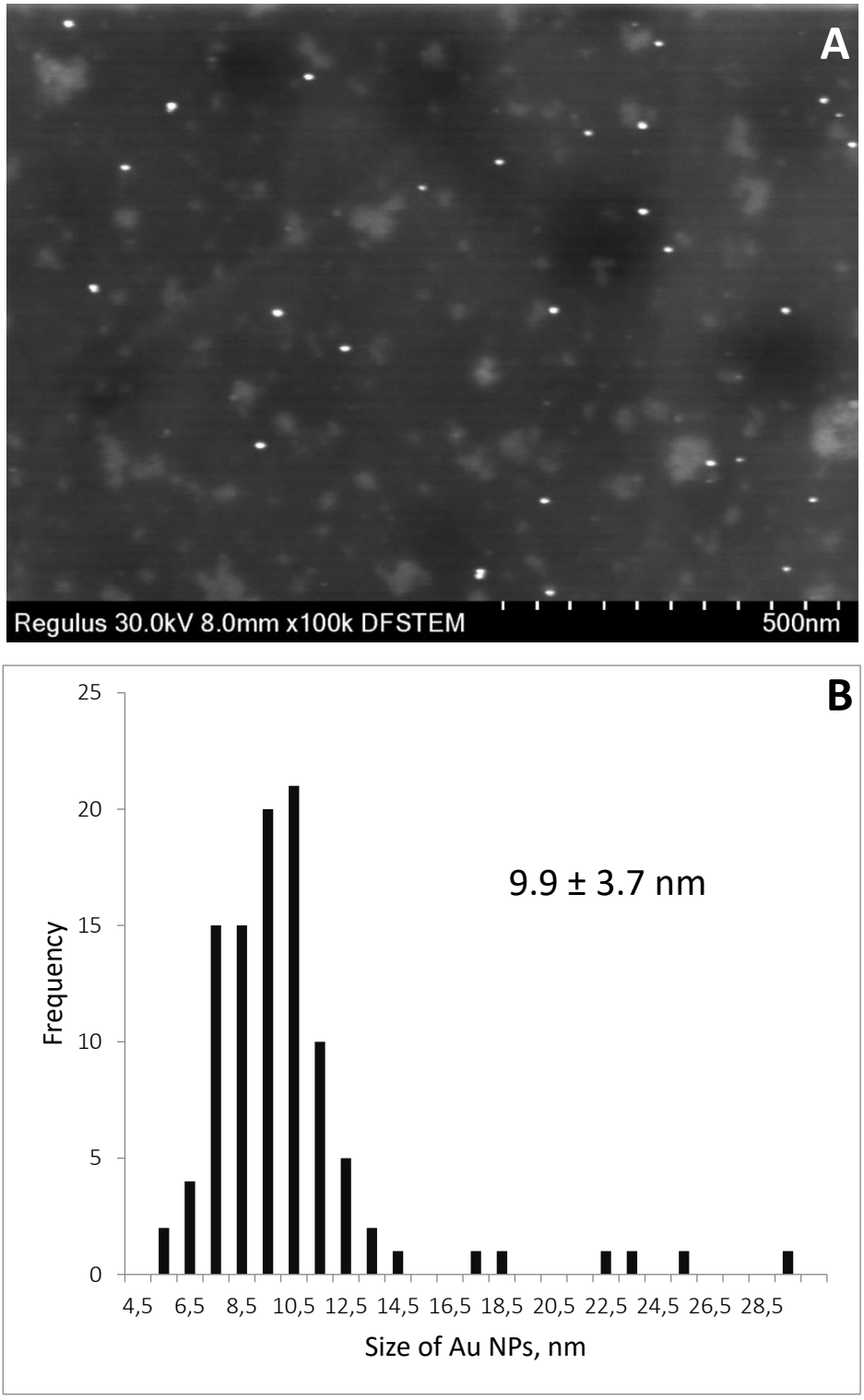

Figure S28. A) DFSTEM image of Au NPs obtained after heating of complex **3g** at 120°C in DMF-d_7 for 30 min; B) Au NPs size distribution histogram obtained from DFSTEM micrographs after heating complex **3g** at 120°C in DMF-d_7 for 30 min.

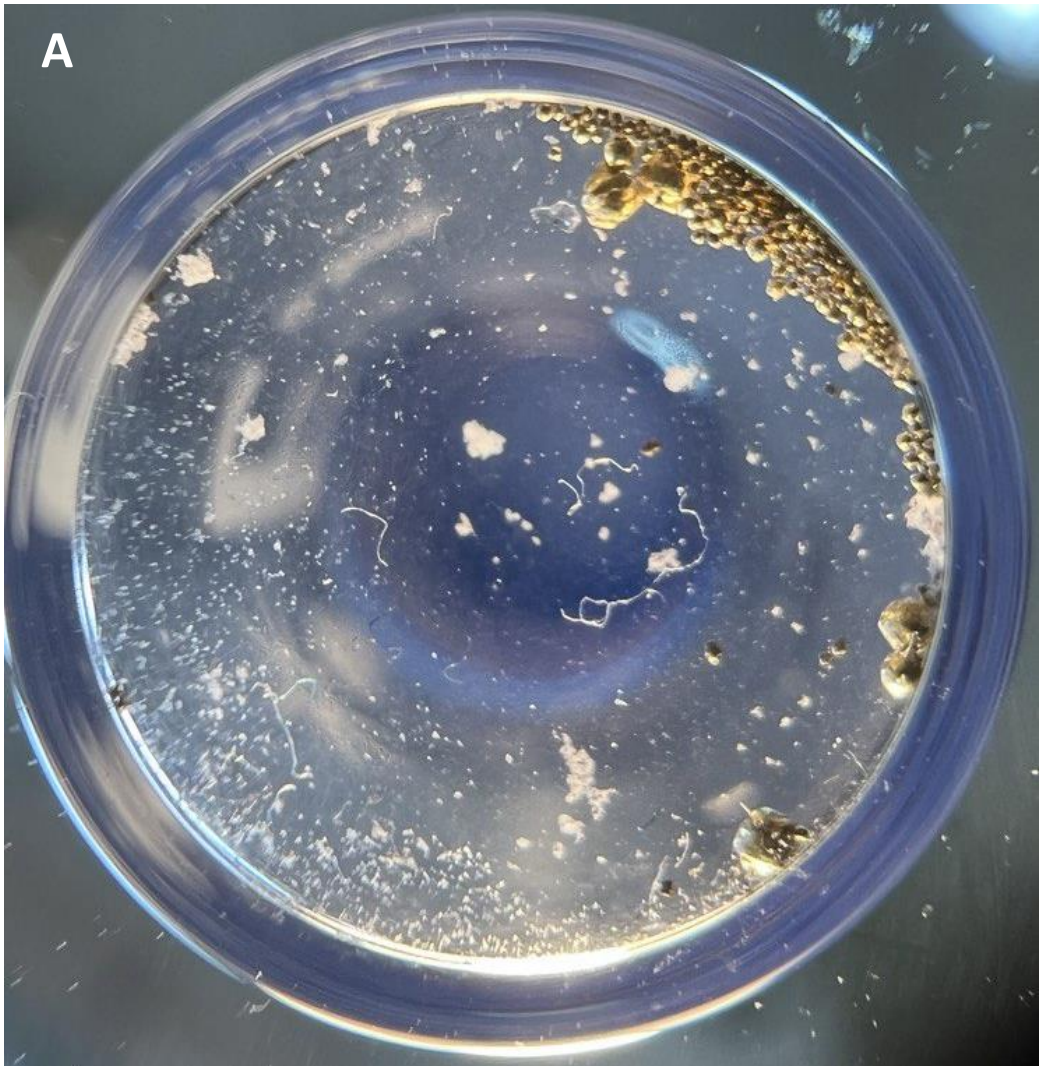
A

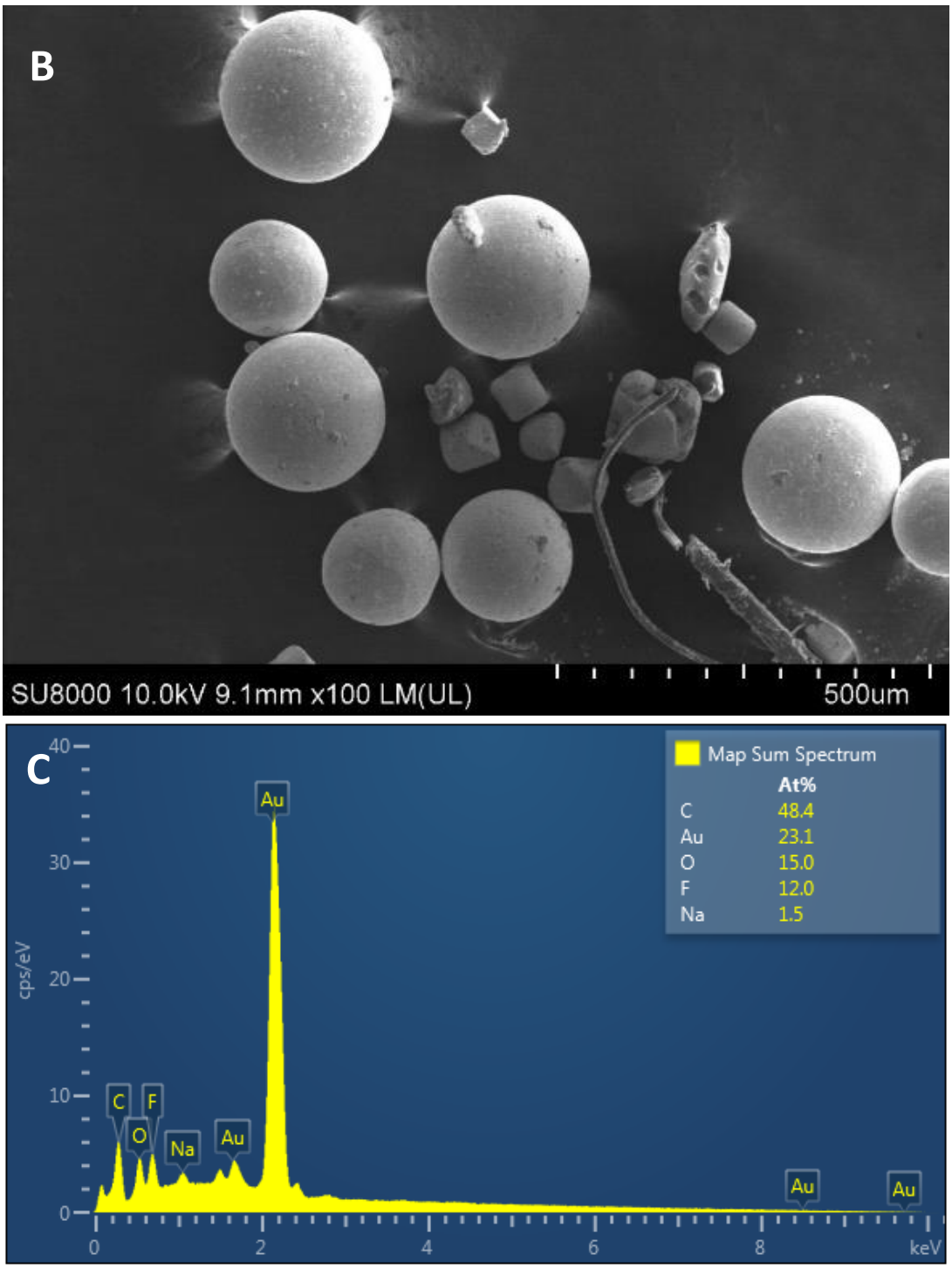

Figure S29. A) Picture of gold microspheres; B) SEM image of gold microspheres obtained from synthesis IPrAuCl **1** at r.t.; C) EDX spectrum of the gold microspheres obtained from synthesis of complex **1**.

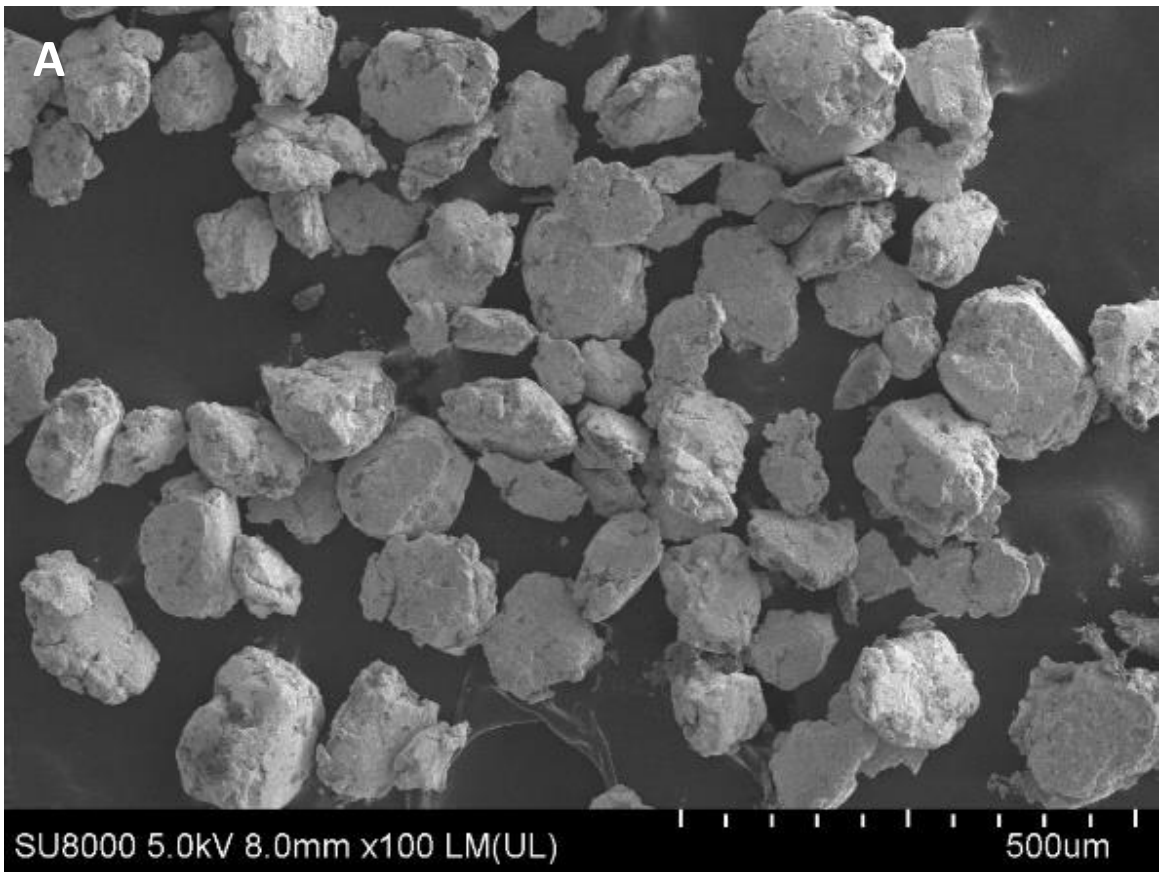

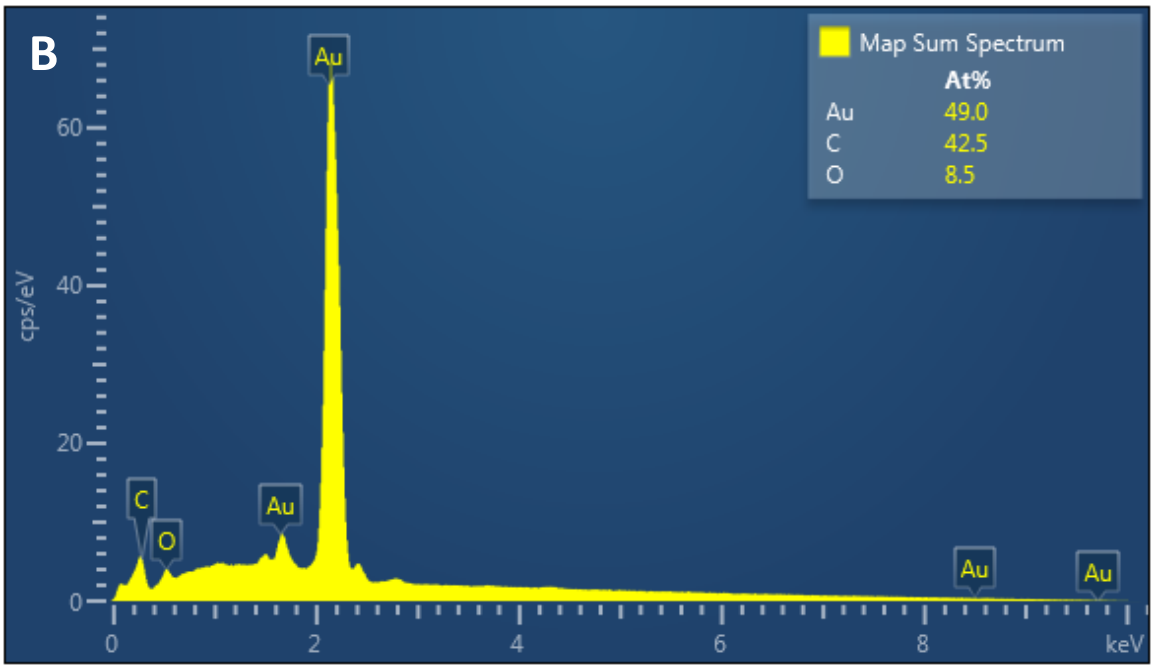

Figure S30. A) SEM image of gold microparticles obtained from synthesis IPrAuCl **1** at r.t.; B) EDX spectrum of the gold paticles obtained from synthesis of complex **1.**

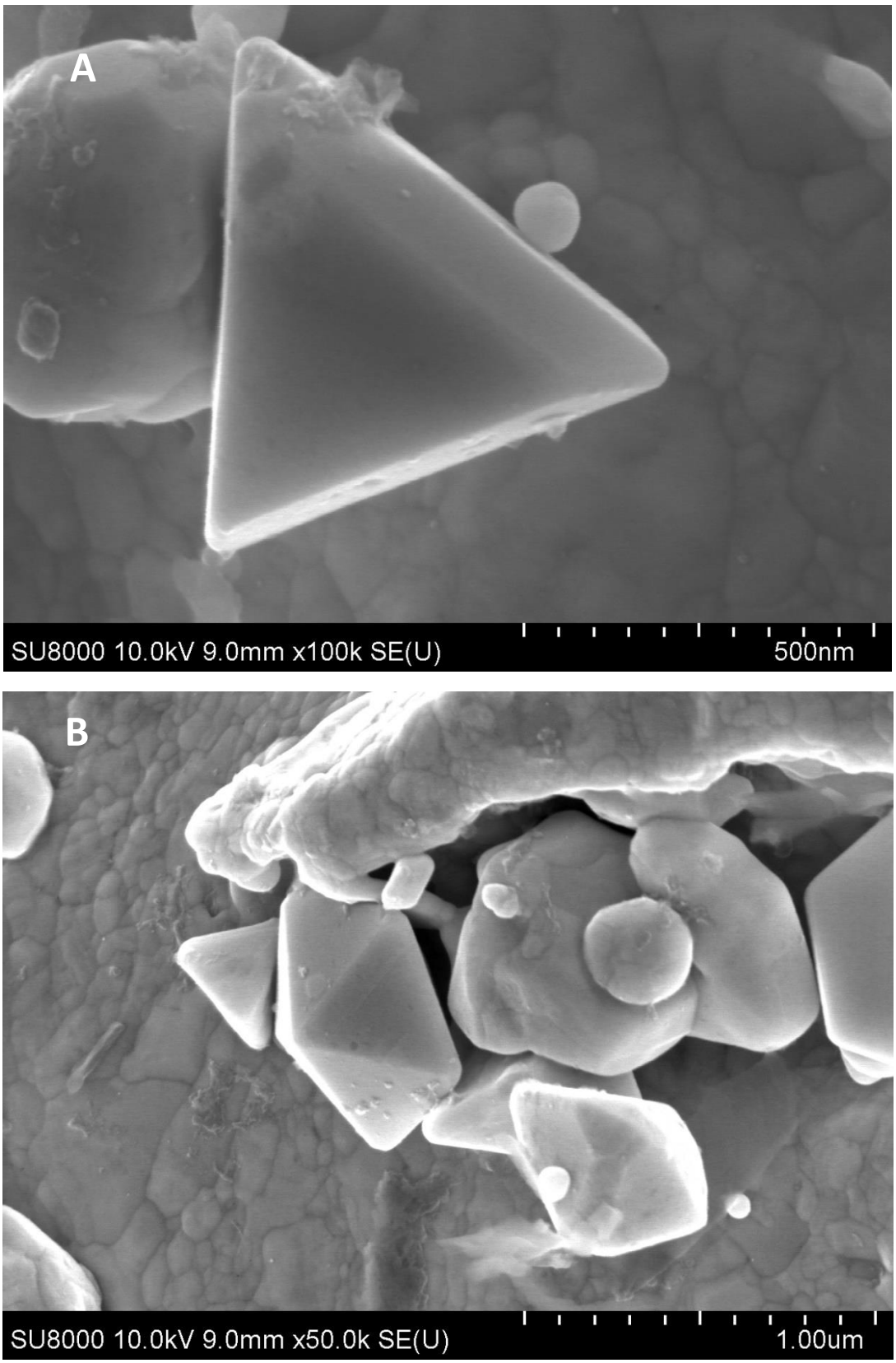

Figure S31. SEM images of gold triangle shape crystals obtained from synthesis IPrAuCl **1** at r.t.

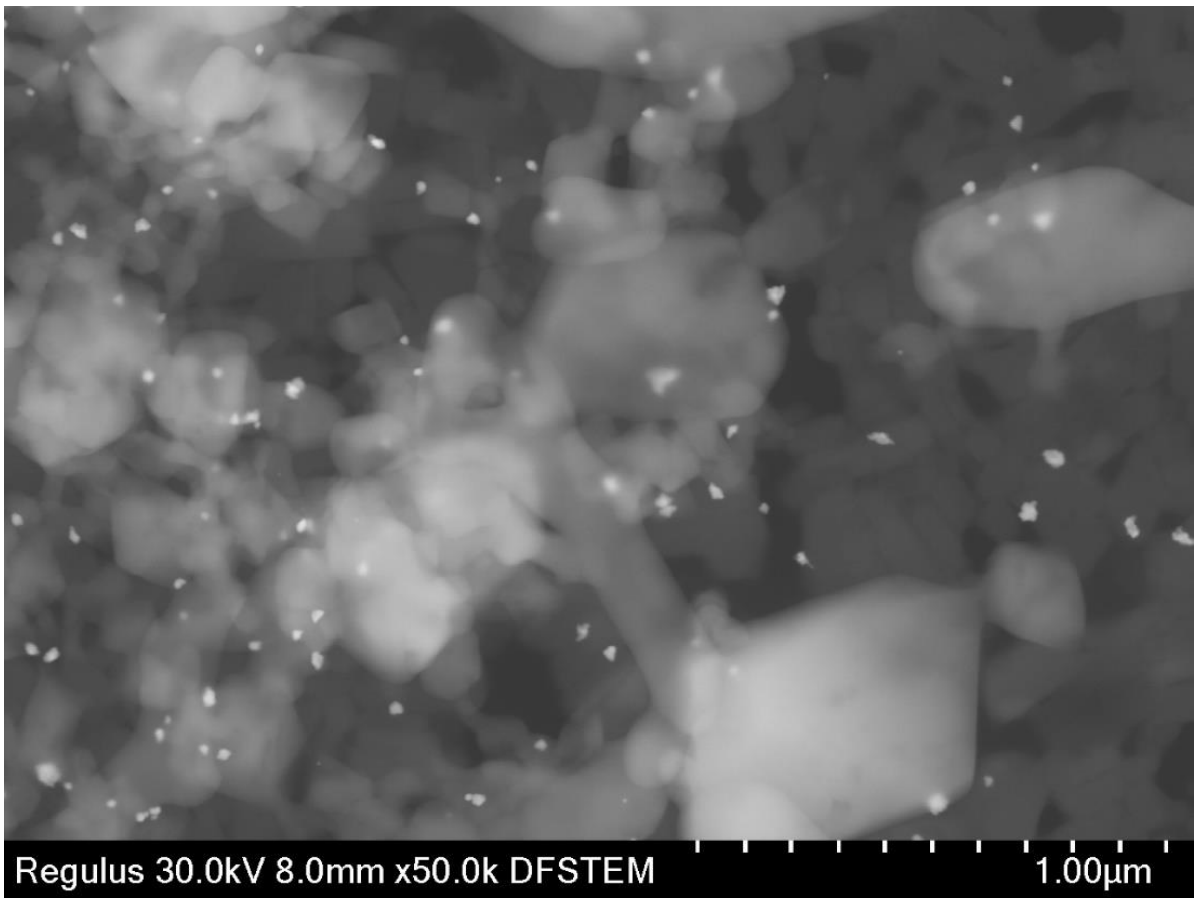

Figure S32. DFSTEM image of Au NPs obtained from tranformation complex **2** to complex **1** in acetone-d_6 at 60°C for 15 minutes.

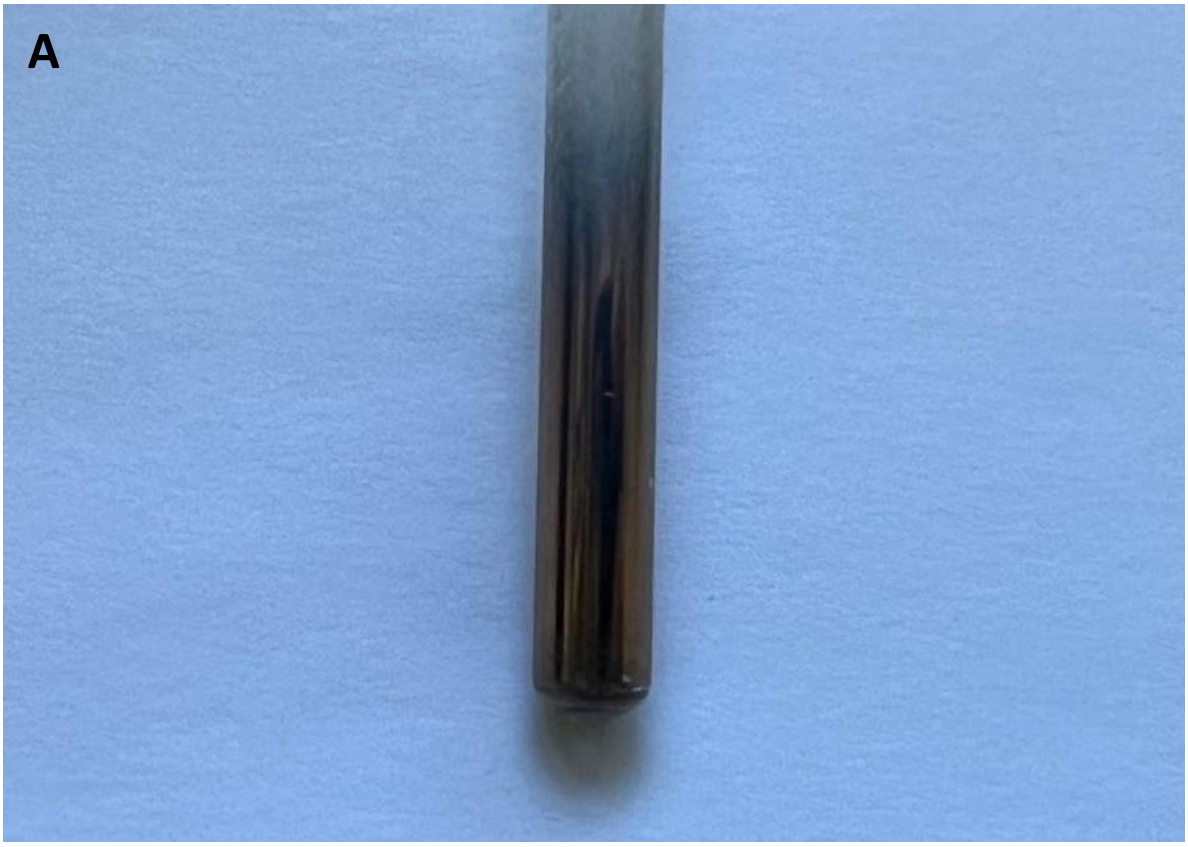

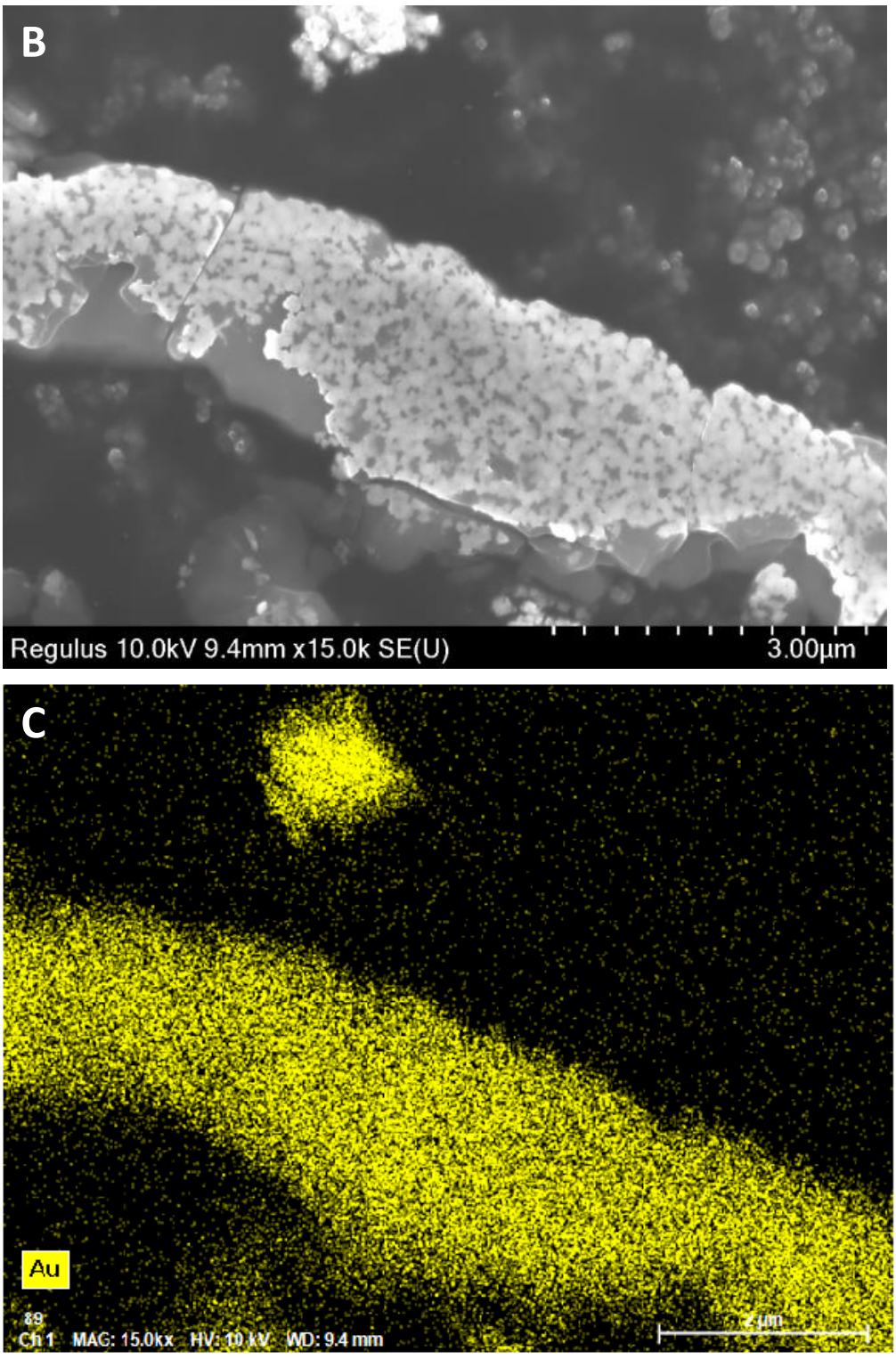

Figure S33. A) Picture of the gold plaque under NMR tube surface after reaction between complex **3g** and 1 eq. SO_2Cl_2 at r.t.; B) SEM image of gold plaque under NMR tube obtained from reaction of complex **3g** with 1 eq. SO_2Cl_2 at r.t.; C) EDX element mapping of Au NPs obtained from gold plaque on the NMR tube surface after reaction of complex **3g** with 1 eq. SO_2Cl_2 at r.t.

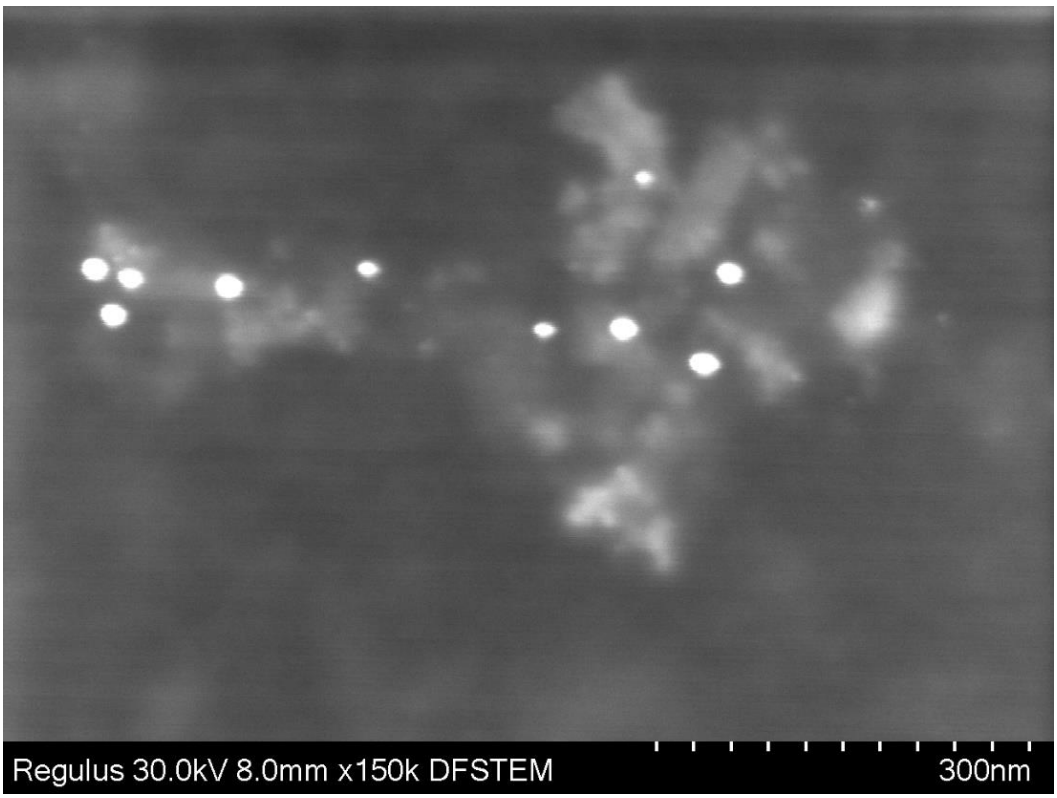

Figure S34. DFSTEM image of Au NPs obtained after heating of complex **4a** at 100 °C in DMSO-d_6 for 15 mins.

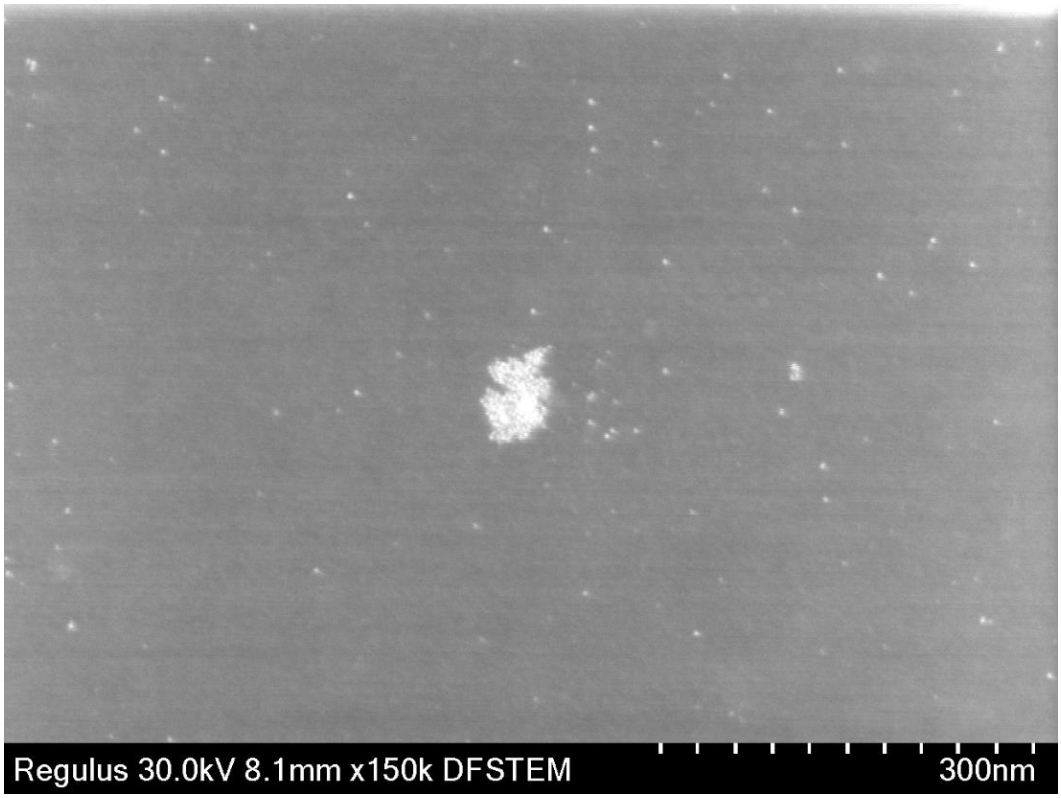

Figure S35. DFSTEM image of Au NPs obtained after degradation of complex **4a** in the presence of $NaBH_4$/EtOH.

Table S2. The connection between molecular and ionic gold complexes and Au nano- and microparticles. [a] Detected via ESI-HRMS study; [b] Detected by NMR study; [c] Rationalized size of Au NPs obtained with size distribution histogram from SEM micrographs.

Starting reagents	**Products**		**Medium**	**Temperature/ time**
	Au complexes	**[Au] particles**		
IPrAuCl **1** (1 eq) + alkyne (1.1 eq) + AcONa (3 eq)	Complex **3b** [a,b]	Au nano- and microparticles from 20 nm to 2 μm Gold plaque on the glass vial	CH_2Cl_2:EtOH = 1:1	r.t. 12 h
THT-Au-Cl (1 eq) + IPr*HCl (1 eq) + $NaHCO_3$ (4.1 eq)	IPrAuCl **1** [a,b]	Au microparticles 100-200 μm	CH_2Cl_2:MeOH=5:1	r.t. 3 days
THT-Au-Cl (1 eq) + IPr*HCl (1 eq) + $NaHCO_3$ (4.1 eq)	IPrAuCl **1** [a,b]	Au microparticles 50-100 μm	CH_2Cl_2:MeOH=5:1	r.t. 3 days
IPr[$AuCl_2$] **2**	IPrAuCl **1** [a,b]	Au NPs 50 nm and smaller	acetone-d_6	60°C 15 min
Complex **3g** (1 eq.) + SO_2Cl_2 (2 eq.)	$[IMes_2Au]^+$ [a] +NHC-C (NHC-ethynyl) [a] +NHC-H [a,b]	Au NPs 100 nm Gold plaque on the glass vial	$CDCl_3$	r.t. 2 week
Complex **4a** (1 eq.) + $NaBH_4$ (1 eq.)	Diyne [a, b] +NHC-C (NHC-Me) [a] +NHC=O [a]	Au NPs ~1 nm	EtOH	r.t. 15 min
Complex **3g**	Complex **3g** [a]	Au NPs (9.9±3.7) nm [c]	DMF-d_7	140 °C 30 min
Complex **4a**	Complex **3a** [a]	Au NPs 10 nm	DMSO-d_6	100 °C 15 min
Complex **4a** + $PhI(OAc)_2$ (2 eq.)	Complex **3a** [a]	Au NPs (7.5±1.2) nm [c]	DMSO-d_6	120 °C 15 min
IPrAuCl **1** (1 eq.) + AcONa (1 eq.)	IPrAuCl **1** [a,b]	Au nano- and microparticles from 50 nm to 50 μm Au plaque on the anchor	CH_2Cl_2:EtOH = 1:1	r.t. 3 week
Complex **3f** (1 eq.) + 2 eq. SO_2Cl_2	NHC-H [a] (IPr-H)	–	$CDCl_3$	r.t. 1 h
Complex **3f** (1 eq.) + 1 eq. KOH	NHC-H [a] (IPr-H)	–	DMSO-d_6	r.t. 1 h
Complex **3a** (1 eq.)	+NHC=O [a]	–	1,4-dioxane	120°C 1 h
Au NPs + IMes*HCl (1 eq.) + *t*-BuOK (1 eq.)	$[IMes_2Au]^+$ [a] +NHC=O [a]	–	THF	90°C 1 h

7. ESI-HRMS and NMR study of the deuteration pathway of gold complexes

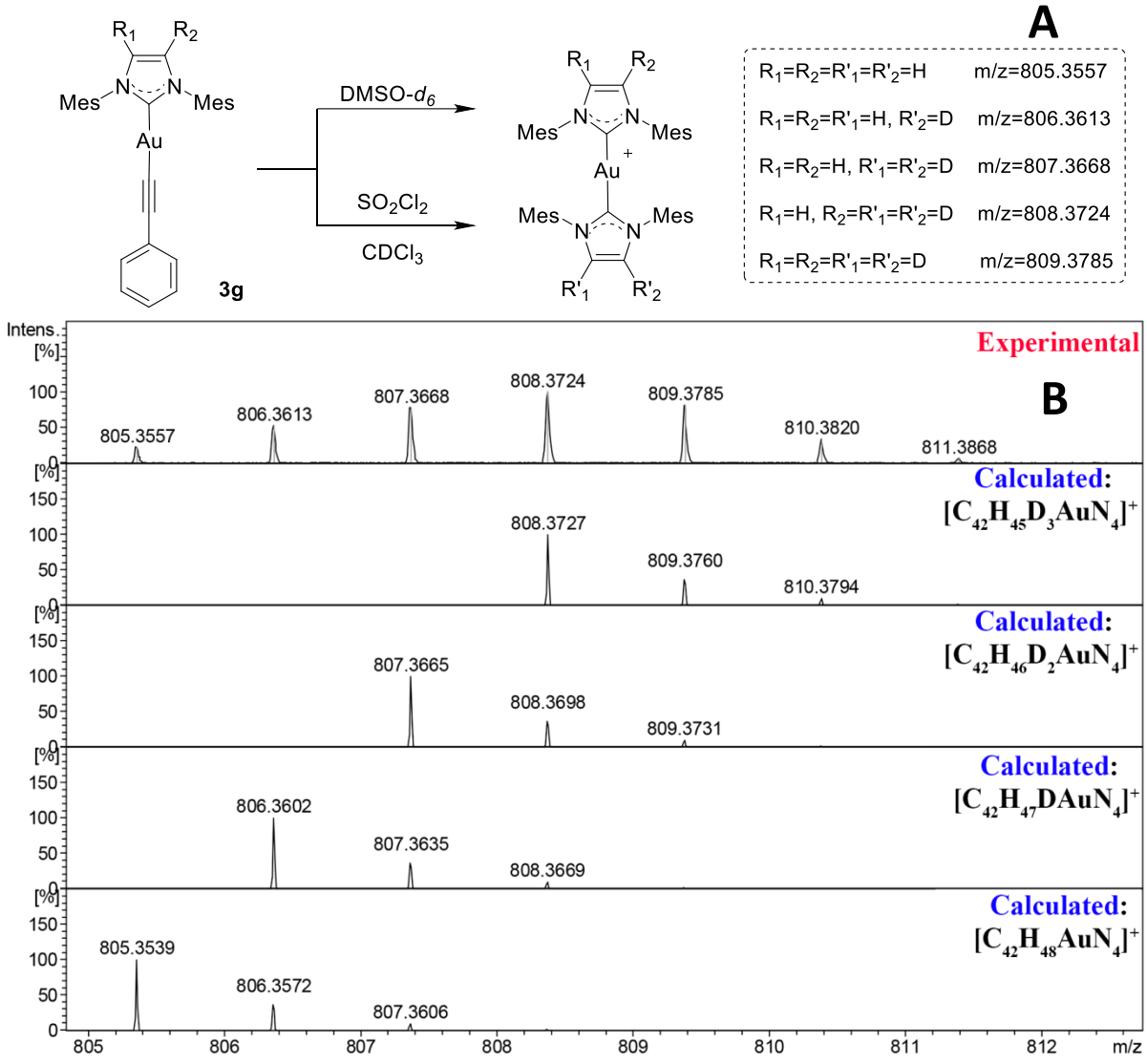

Figure S36. A) Scheme of the deuteration process of complex **3g**; B) Experimental and theoretical ESI-(+)HRMS spectrum of the reaction mixture after 1 h of the deuteration process of complex **3g** in DMSO-*d*6, expanded to the homoleptic bis-NHC gold(I) complex $[IMes_2Au+H]^+$ region. Sample diluted in CH_3CN.

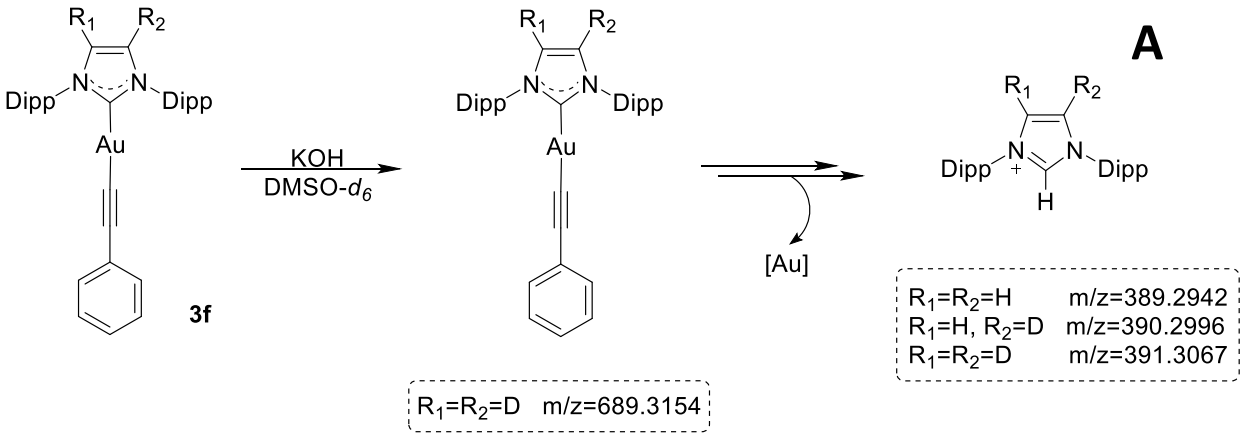
A
Dipp
Au
3f
KOH
DMSO-d_6
[Au]
R_1=R_2=H m/z=389.2942
R_1=H, R_2=D m/z=390.2996
R_1=R_2=D m/z=391.3067
R_1=R_2=D m/z=689.3154

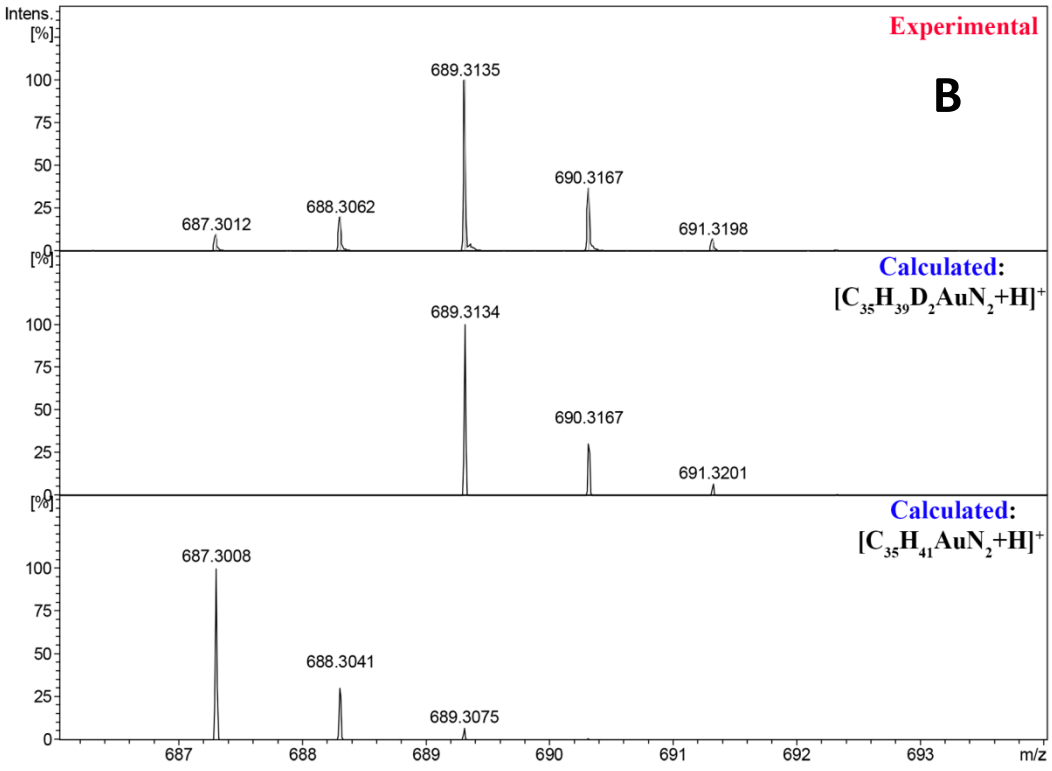
B
Experimental
689.3135
690.3167
687.3012
688.3062
691.3198
Calculated:
$[C_{35}H_{39}D_2AuN_2+H]^+$
689.3134
690.3167
691.3201
Calculated:
$[C_{35}H_{41}AuN_2+H]^+$
687.3008
688.3041
689.3075
Intens.
[%]
m/z

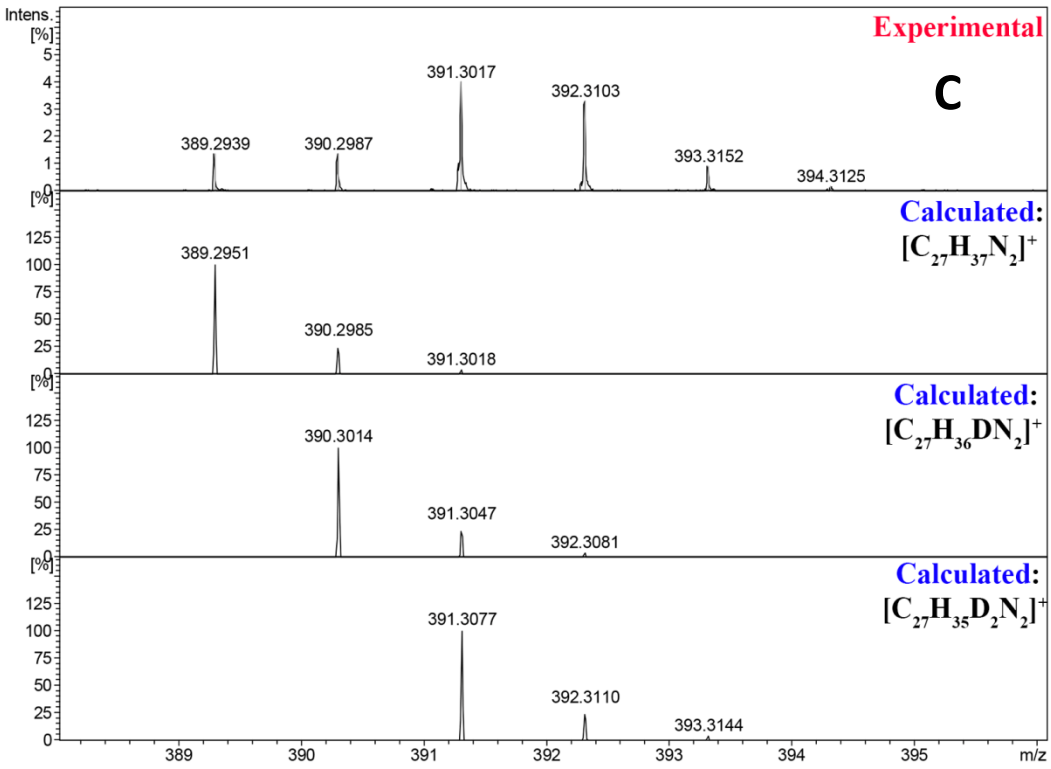

Figure S37. A) Scheme of the deuteration process of complex **3f**; B) Experimental and theoretical ESI-(+)HRMS spectrum of the reaction mixture after 1 h of the deuteration process of complex **3f** in DMSO-d_6 catalyzed by KOH, expanded to the heteroleptic Au(I) complex [NHC-Au(I)-alkynyl+H]$^+$ region. Sample diluted in CH_3CN; C) Experimental and theoretical ESI-(+)HRMS spectrum of the reaction mixture after 1 h of the deuteration process of complex **3f** in DMSO-d_6 catalyzed by KOH, expanded to the [NHC+H]$^+$ region. Sample diluted in CH_3CN.

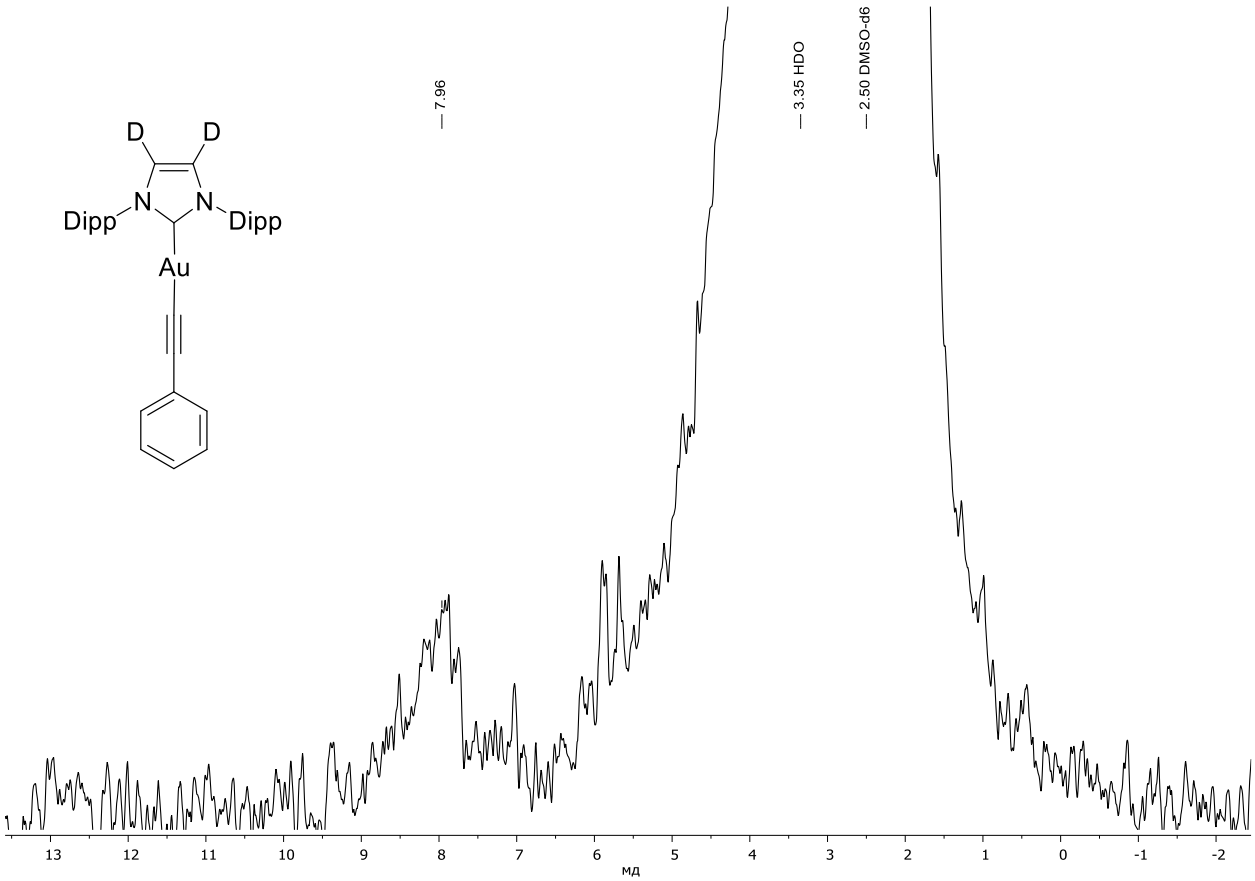

Figure S38. ^{2}H-NMR spectra of deuterated imidazolium fragment of NHC-Au(I) complex **3f** in DMSO-d_6 (61 MHz).

8. ESI-HRMS study of the dynamic behavior of gold complexes

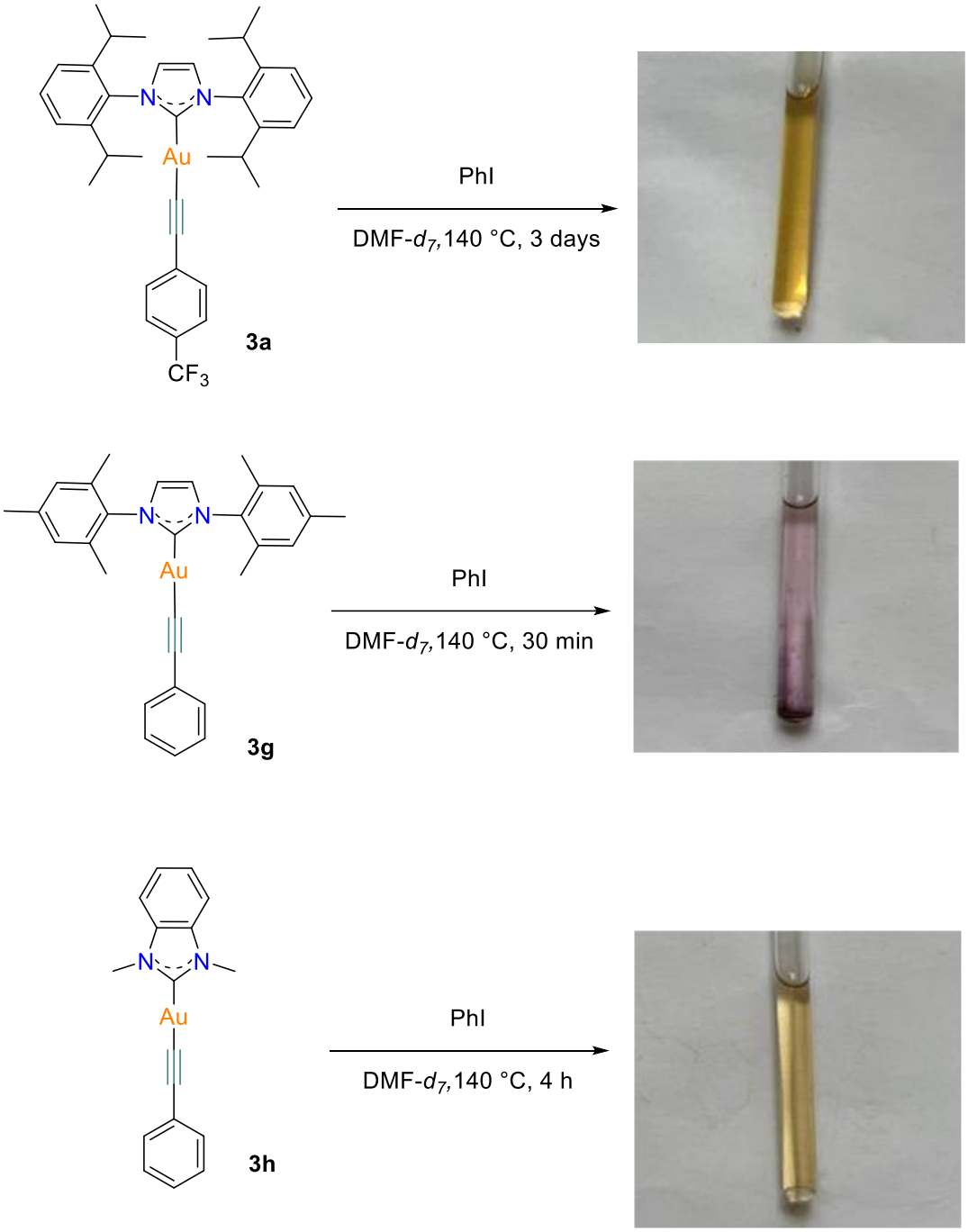

Figure S39. Study of the physical properties of NHC gold(I) alkynyl complexes with various NHC ligands by heating of appropriate NHC-Au(I) complexes with 1 eq. of PhI at 140 °C.

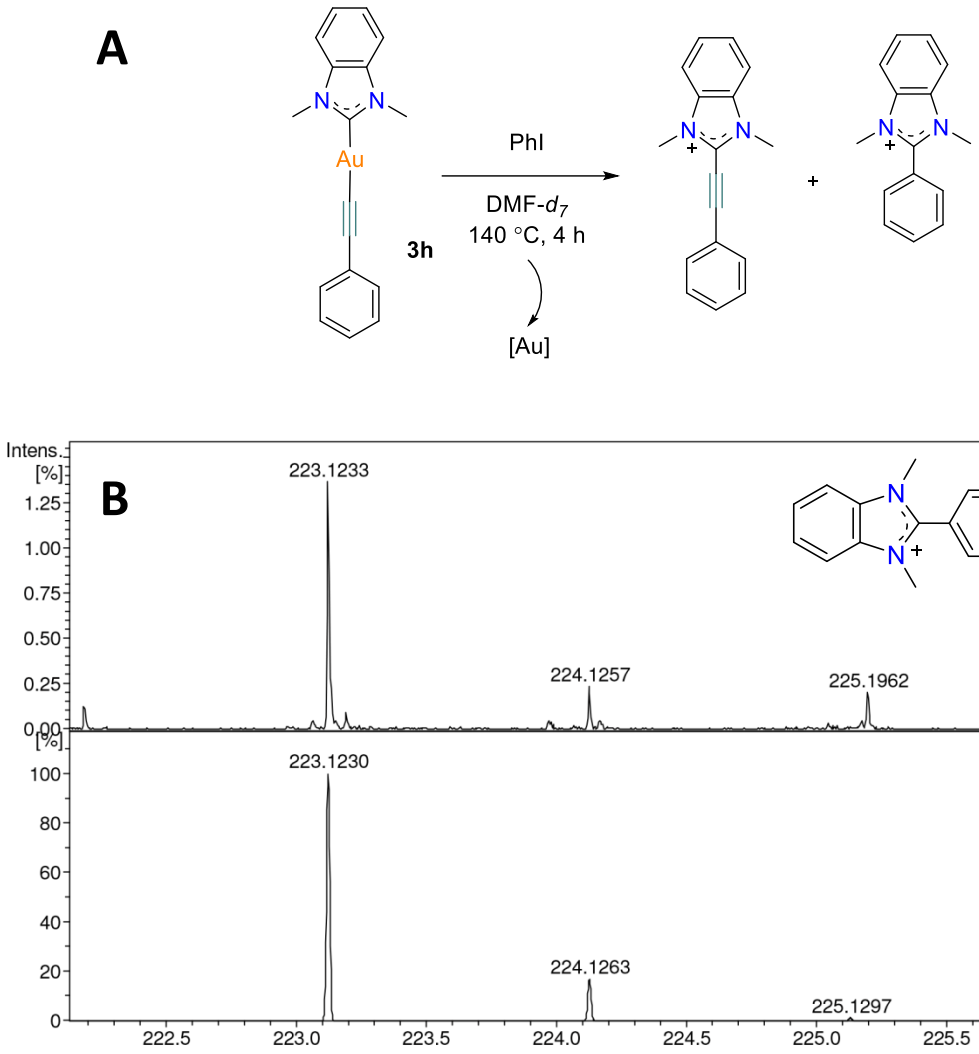
A
Au
3h
PhI
DMF-d_7
140 °C, 4 h
[Au]
B
Intens.
[%]
223.1233
224.1257
225.1962
Experimental:
Δ =1,34 ppm
223.1230
224.1263
225.1297
Calculated:
$[C_{15}H_{15}N_2]^+$
m/z

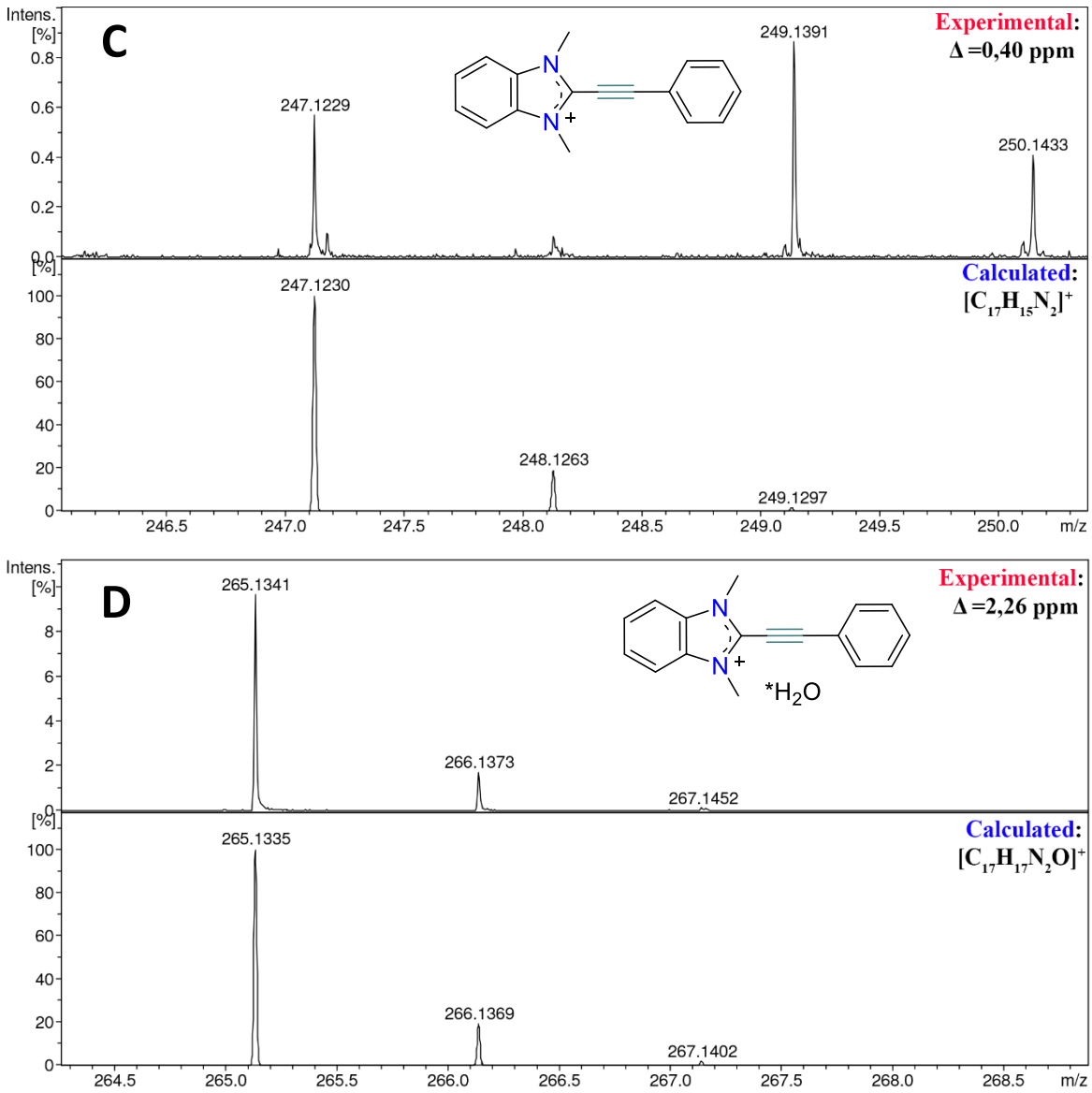

Figure S40. A) Scheme of the reaction; Experimental and theoretical ESI-(+)HRMS spectrum of the reaction mixture of NHC-C coupling reaction (NHC-Ph (B) and NHC-ethynyl (C), (D)) in NHC gold(I) alkynyl complex **3h** after 4 h in DMF-d_7 initiated by PhI, expanded to the $[NHC+R]^+$ region. Sample diluted in CH_3CN.

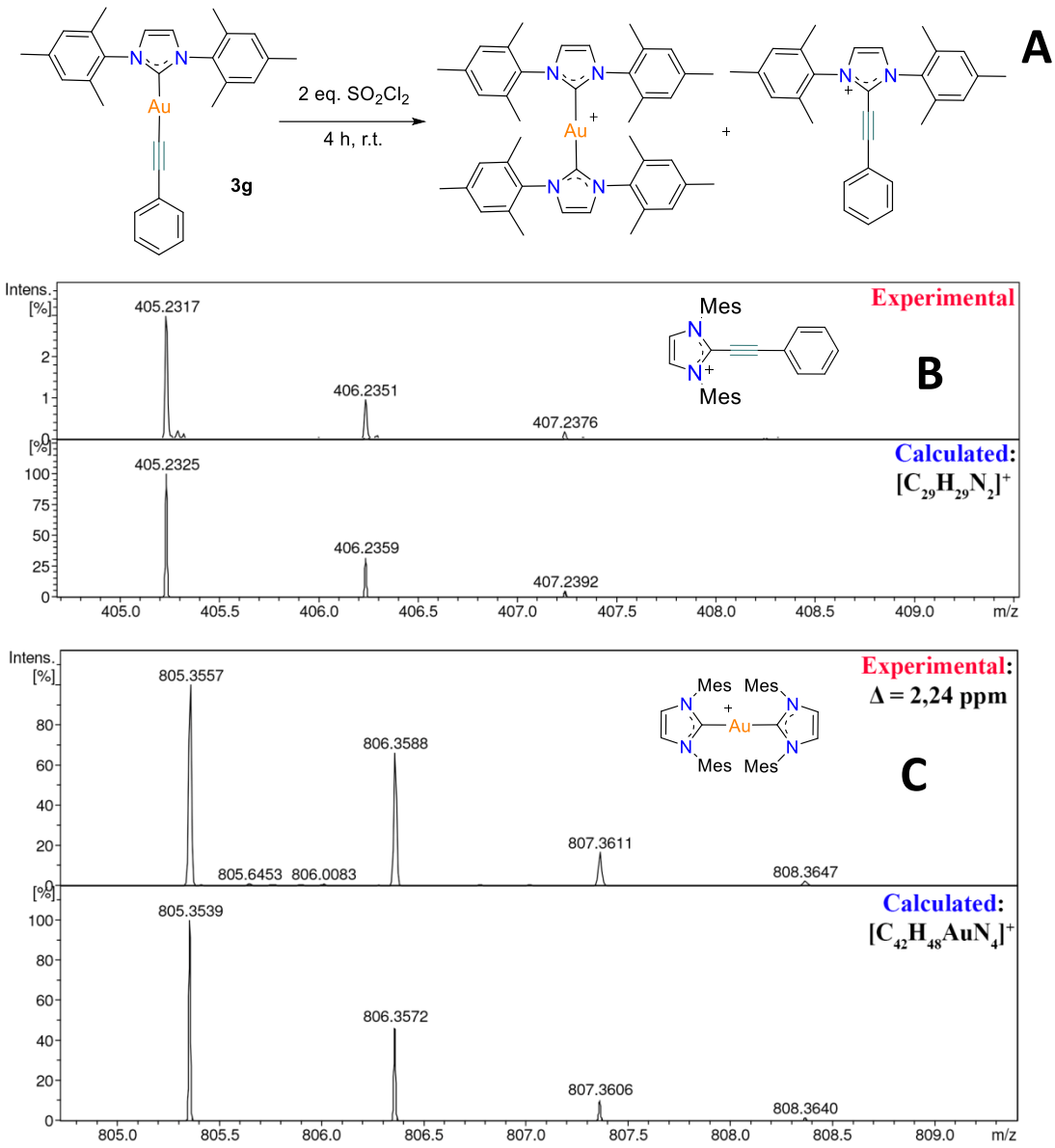

Figure S41. A) Scheme of the reaction; B) Experimental and theoretical ESI-(+)HRMS spectrum of the reaction mixture of NHC-C coupling reaction in NHC gold(I) alkynyl complex **3g** after 4 h in $CDCl_3$ initiated by 2 eq. SO_2Cl_2, expanded to the $[NHC+R]^+$ region. Sample diluted in CH_3CN. C) Experimental and theoretical ESI-(+)HRMS spectrum of the reaction mixture of simultaneous formation of homoleptic gold(I) complex in NHC gold(I) alkynyl complex **3g** after 4 h in $CDCl_3$ initiated by 2 eq. SO_2Cl_2, expanded to the $[IMes_2Au]^+$ region. Sample diluted in CH_3CN.

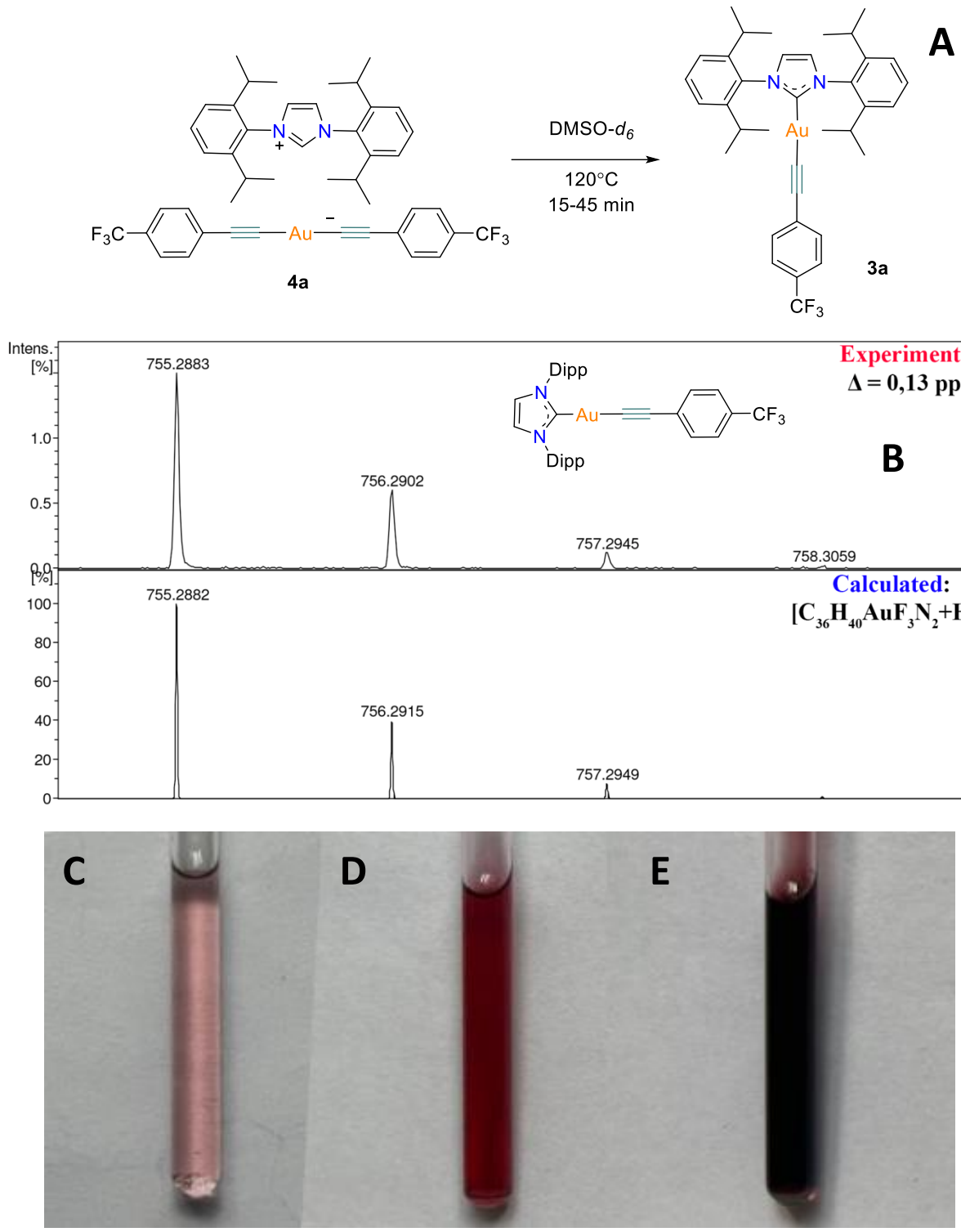

Figure S42. A) Transformation of homoleptic gold(I) complex **4a** to heteroleptic gold(I) complex **3a** in DMSO-d_6 at 120 °C; B) Experimental and theoretical ESI-(+)HRMS spectrum of the reaction mixture of formation of heteroleptic gold(I) complex **3a** from homoleptic gold(I) complex **4a** in DMSO-d_6 at 120 °C, expanded to the [NHC-Au-alkynyl+H]$^+$ region. Sample diluted in CH_3CN; Pictures of heating of complex **4a** in DMSO-d_6: C) 15 min at 80 °C; D) 30 min at 100 °C; E) 15 min at 120 °C with 1 eq. $PhI(OAc)_2$.

Table S3. The formation of bis-NHC Au(I) complex from Au NPs study.

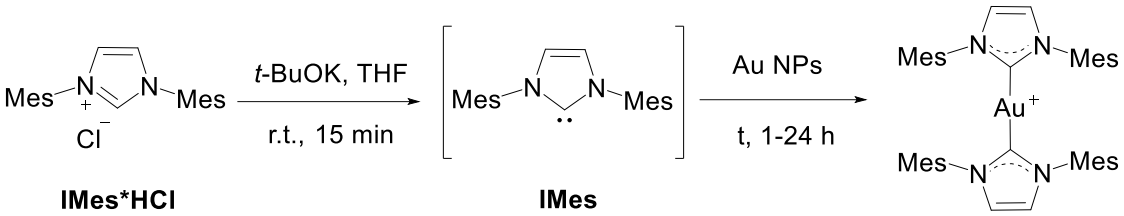

IMes*HCl **IMes**

m/z 805.3572

1. t = r.t.
2. t = 60 °C
3. t = 90 °C
4. t = 120 °C

Entry	Temperature	Time	*m/z* 805.3539 ESI-HRMS
1	r.t.	0 h	trace
2	r.t.	24 h	detected
3	60 °C	24 h	detected
4	90 °C	24 h	detected
5	120 °C	24 h	detected

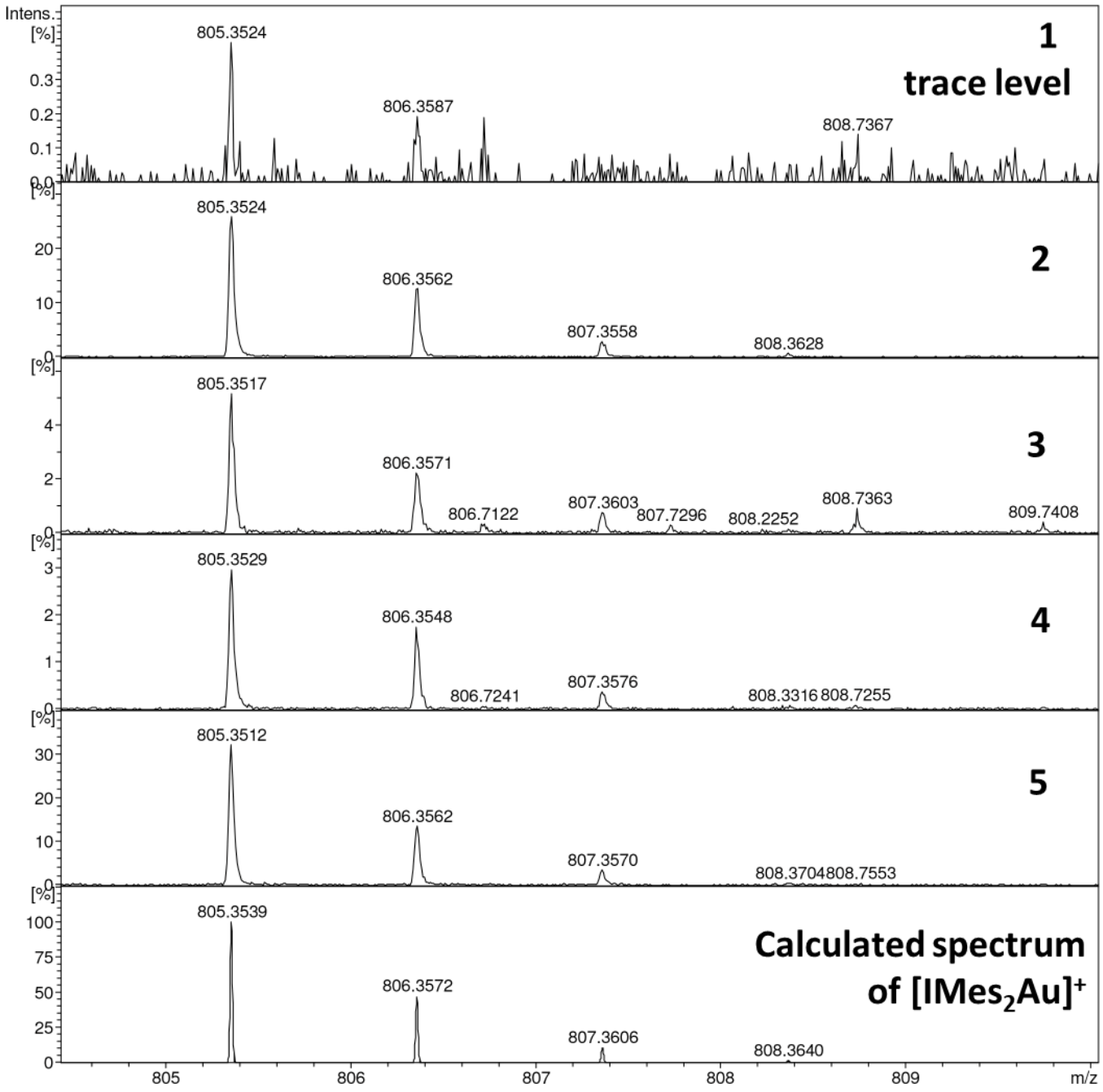

Figure S43. Experimental ESI-(+)HRMS spectrum of the reaction mixture of formation of complex $[IMes_2Au]^+$ from gold nanoparticles: the 805 *m/z* region with theoretical ESI-HRMS spectrum of investigated $[IMes_2Au]^+$ ion.

Table S4. ESI-HRMS fragments of the most common NHC-AuCl complexes.

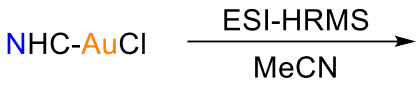

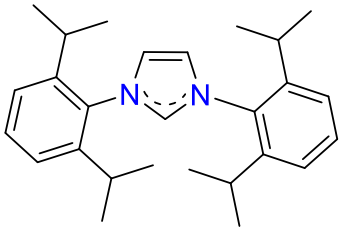

NHC = IPr

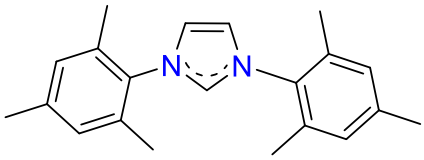

NHC = IMes

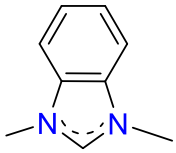

NHC = BIMe

NHC	$[NHC-H]^+$	$[M-H]^+$	$[M-H-MeCN]^+$	$[NHC-Au]^+$	$[NHC_2Au]^+$
IPr	389.2964 $[IPr-H]^+$	621.2280 $[IPrAuCl-H]^+$	626.2810 $[IPrAuCl-H-MeCN]^+$ was not detected	585.2514 $[IPr-Au]^+$ was not detected	973,5423 $[IPr_2Au]^+$ was not detected
IMes	305,2018 $[IMes-H]^+$	536,1294 $[IMesAuCl-H]^+$	543.1949 $[IMesAuCl-H-MeCN]^+$ was not detected	501,1605 $[IMes-Au]^+$ was not detected	805,3544 $[IMes_2Au]^+$ was not detected
BIMe	147.0922 $[BIMe-H]^+$	379,0276 $[BIMeAuCl-H]^+$	385.0853 $[BIMeAuCl-H-MeCN]^+$ was not detected	344,0588 $[BIMe-Au]^+$ was not detected	489,1353 $[BIMe_2Au]^+$ was not detected

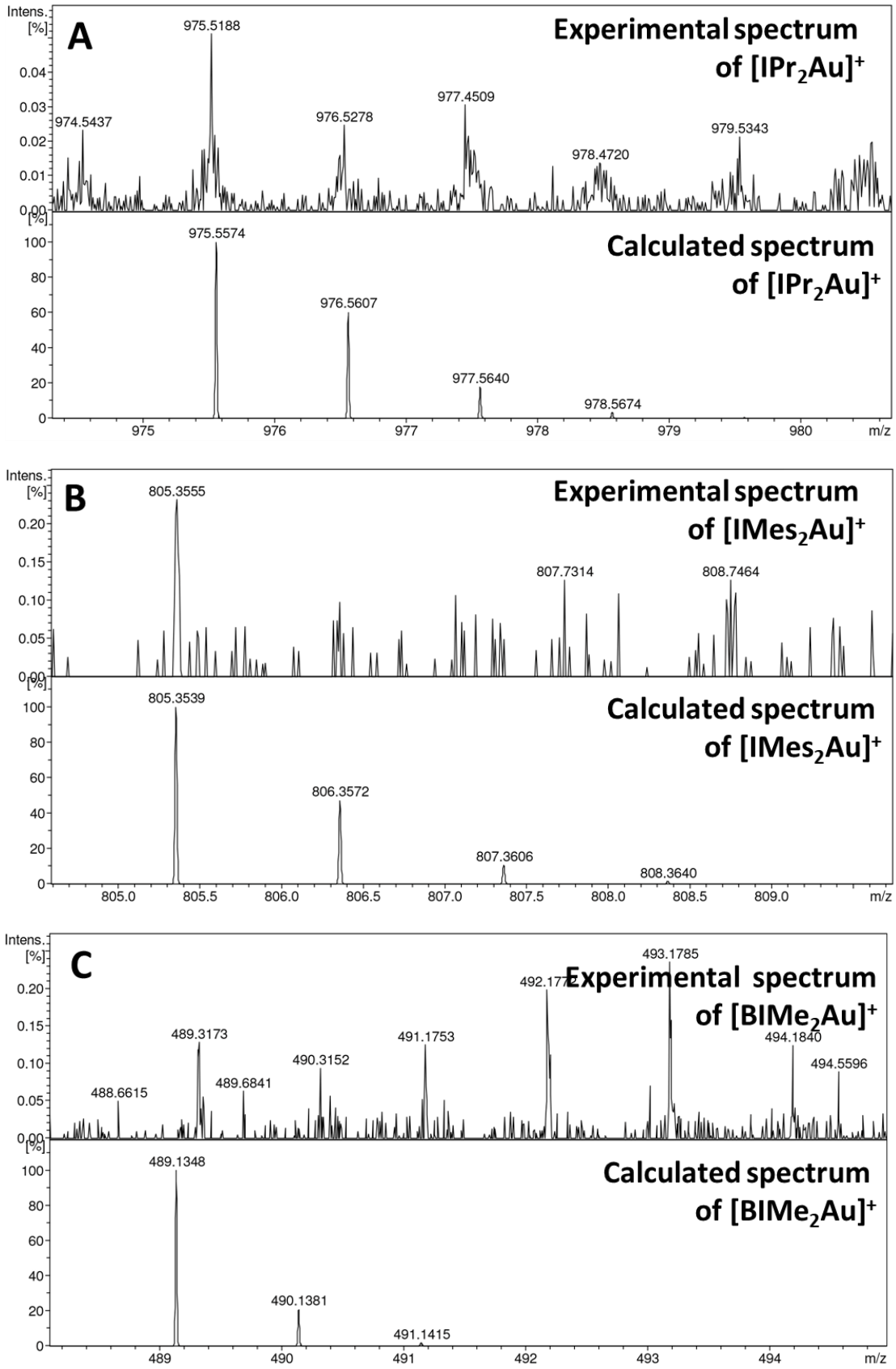

Figure S44. Experimental ESI-(+)HRMS spectrum of the $[NHC_2Au]^+$ region obtained when the registration of NHC-AuCl were carried out: A) NHC = IPr, B) NHC = IMes, C) NHC = BIMe.

9. ^{1}H NMR study of the chemical properties of homoleptic gold complex 3

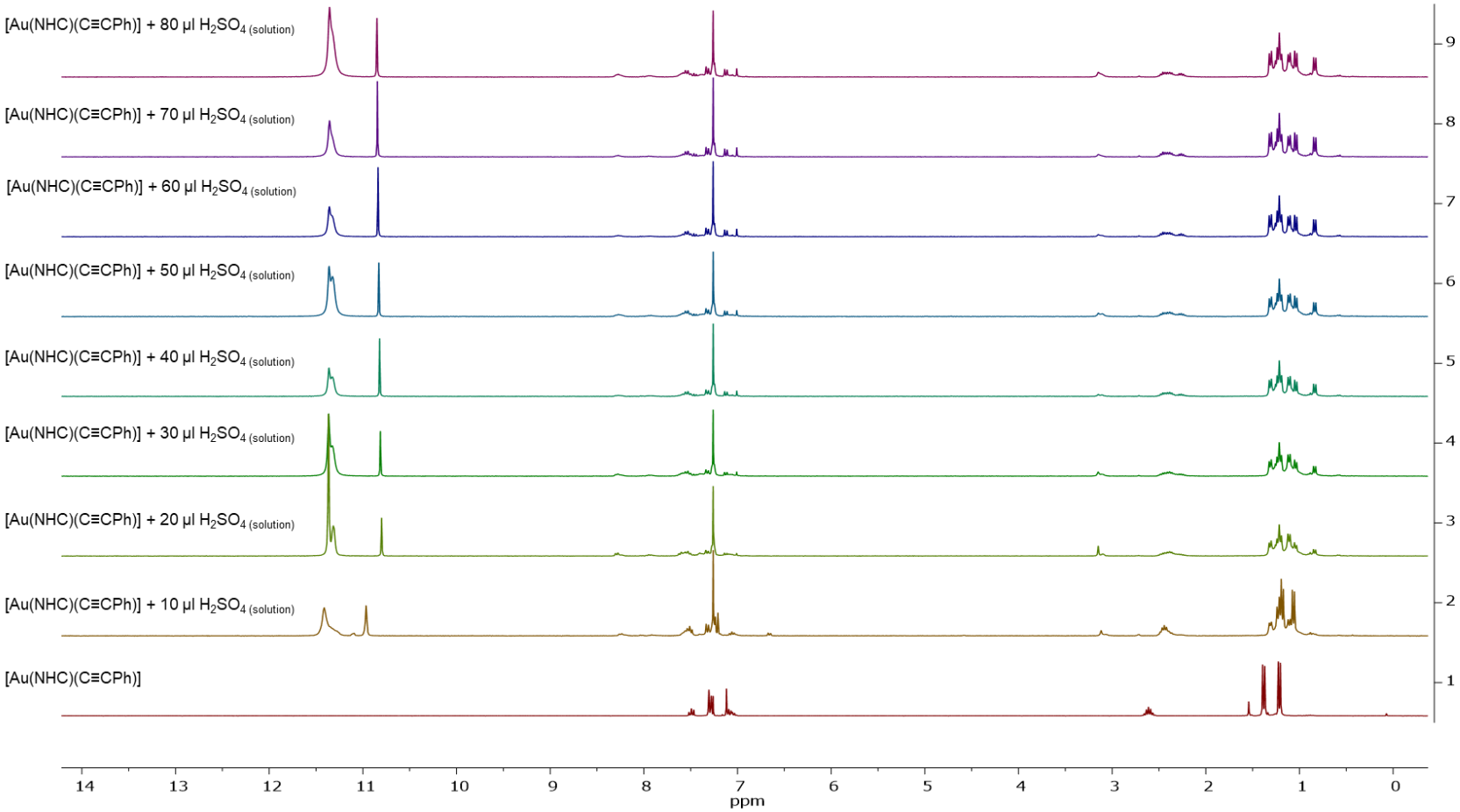

Figure S45. ^{1}H NMR spectra of the reaction mixture after the portion addition (10 µL at a time) of 1 eq. of H_2SO_4 in 100 µL $CDCl_3$ to the complex **3f** ($CDCl_3$, 300 MHz).

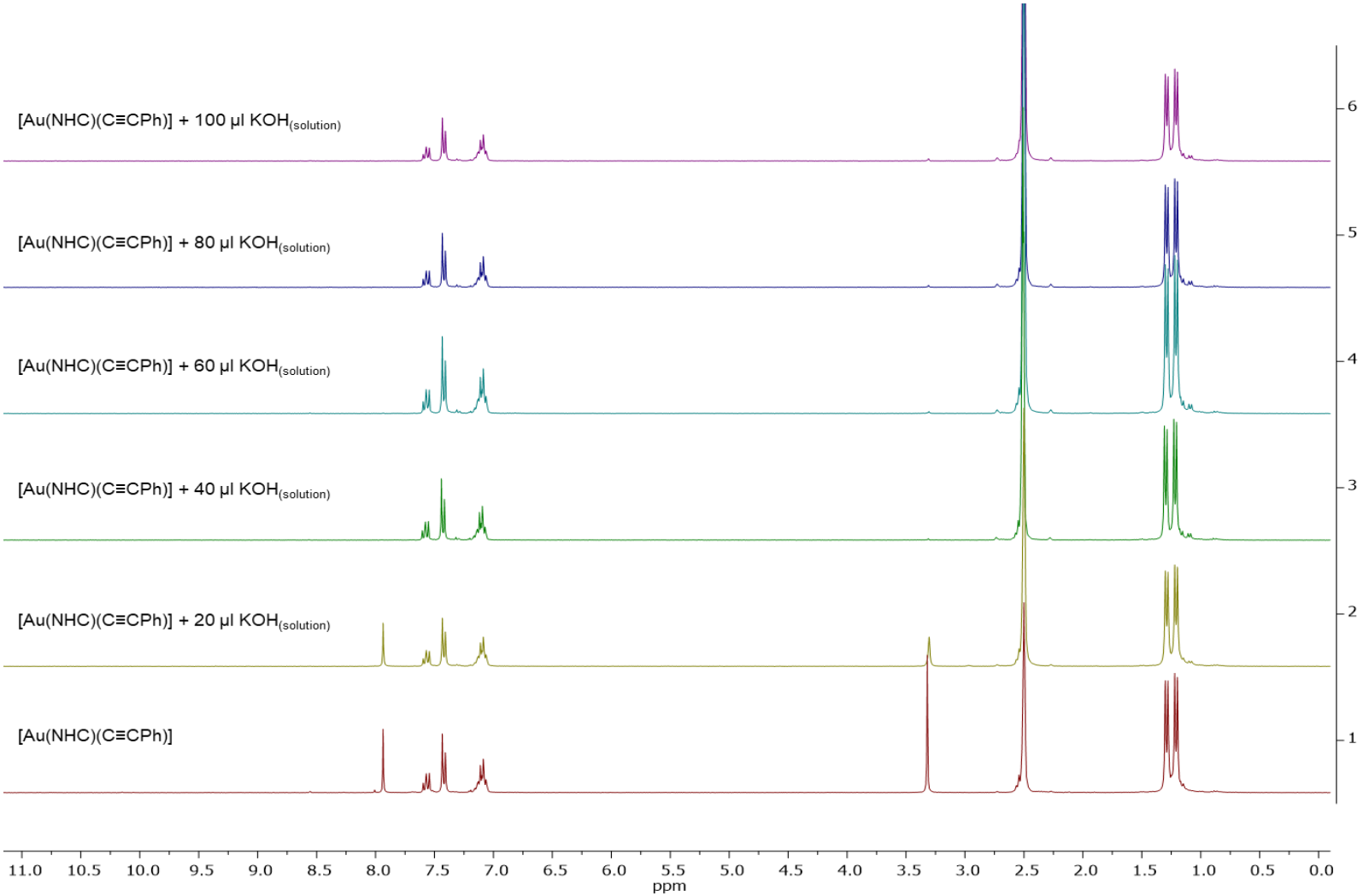

Figure S46. ^{1}H NMR spectra of the reaction mixture after the portion addition (20 µL at a time) of 1 eq. of KOH in 100 µL DMSO-d_6 to the complex **3f** (DMSO-d_6, 300 MHz).

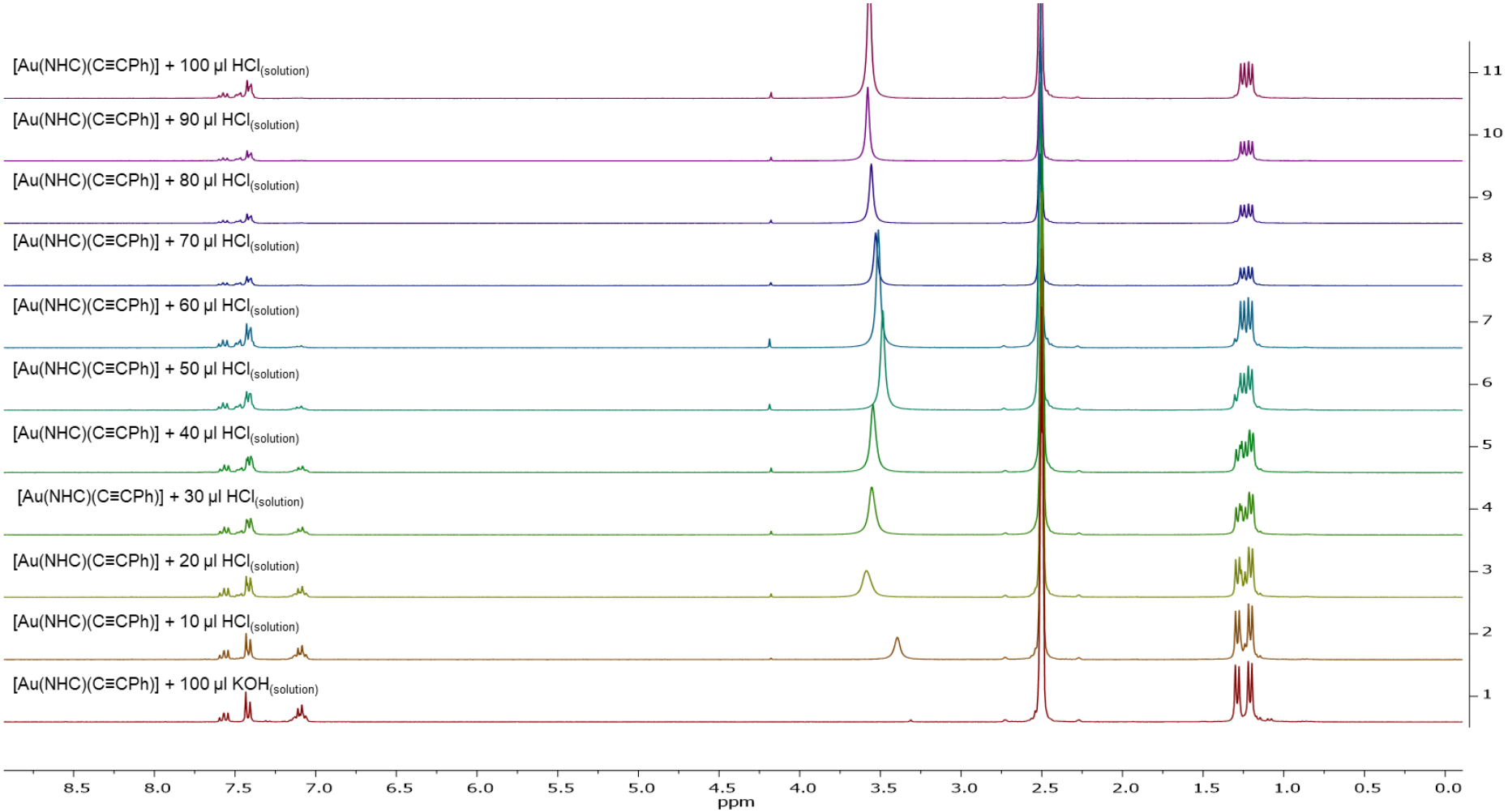

Figure S47. ^{1}H NMR spectra of the reaction mixture after the portion addition (10 µL at a time) of 1 eq. of HCl_{aq} to the mixture of 1 eq. KOH and complex **3f** in DMSO-d_6 (DMSO-d_6, 300 MHz).

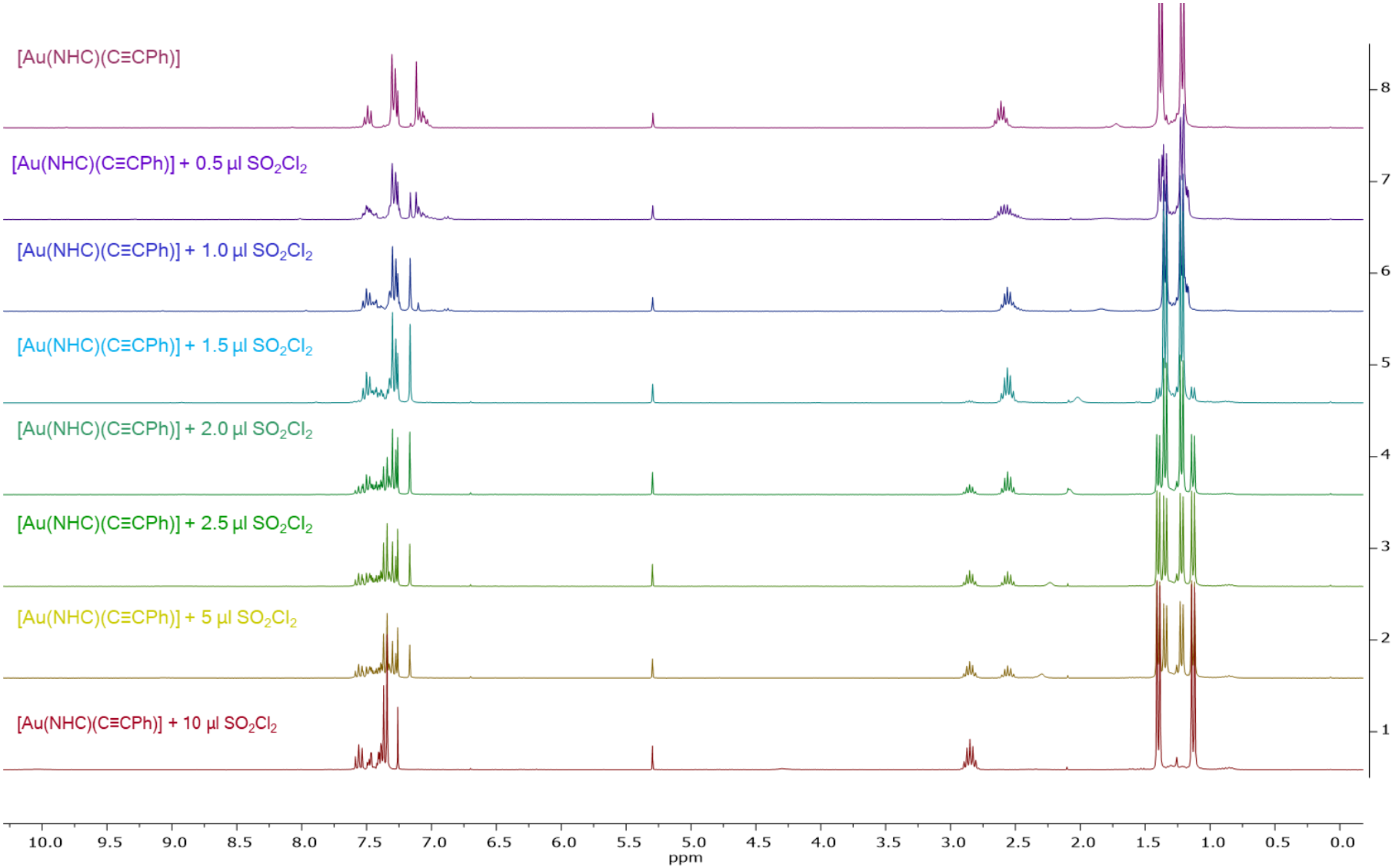

Figure S48. ^{1}H NMR spectra of the reaction mixture after the portion addition of SO_2Cl_2 to the complex **3f** ($CDCl_3$, 300 MHz).

10.TGA/DSC analysis of gold (I) complexes

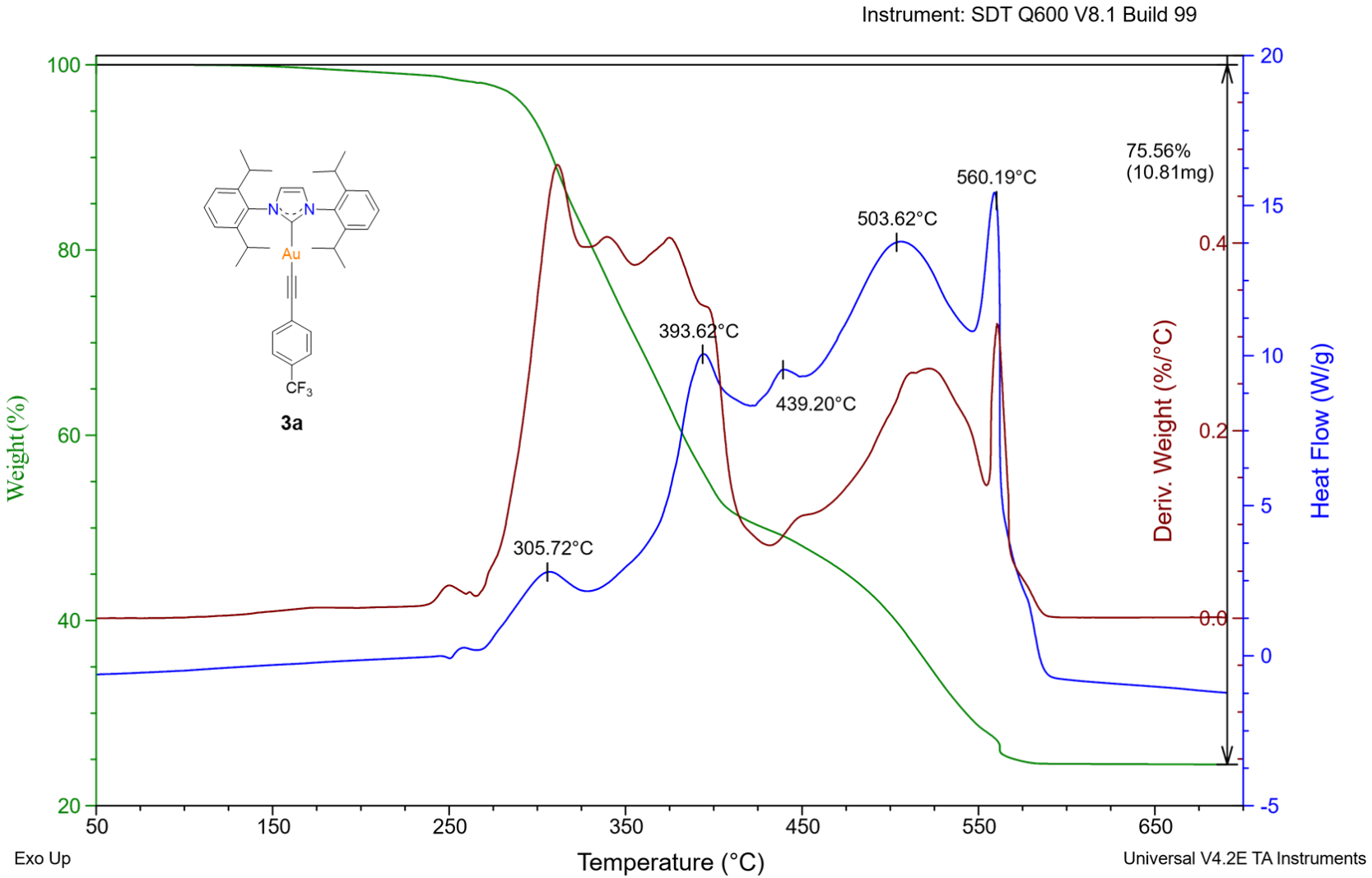

Figure S49. TGA/DSC analysis for complex **3a**.

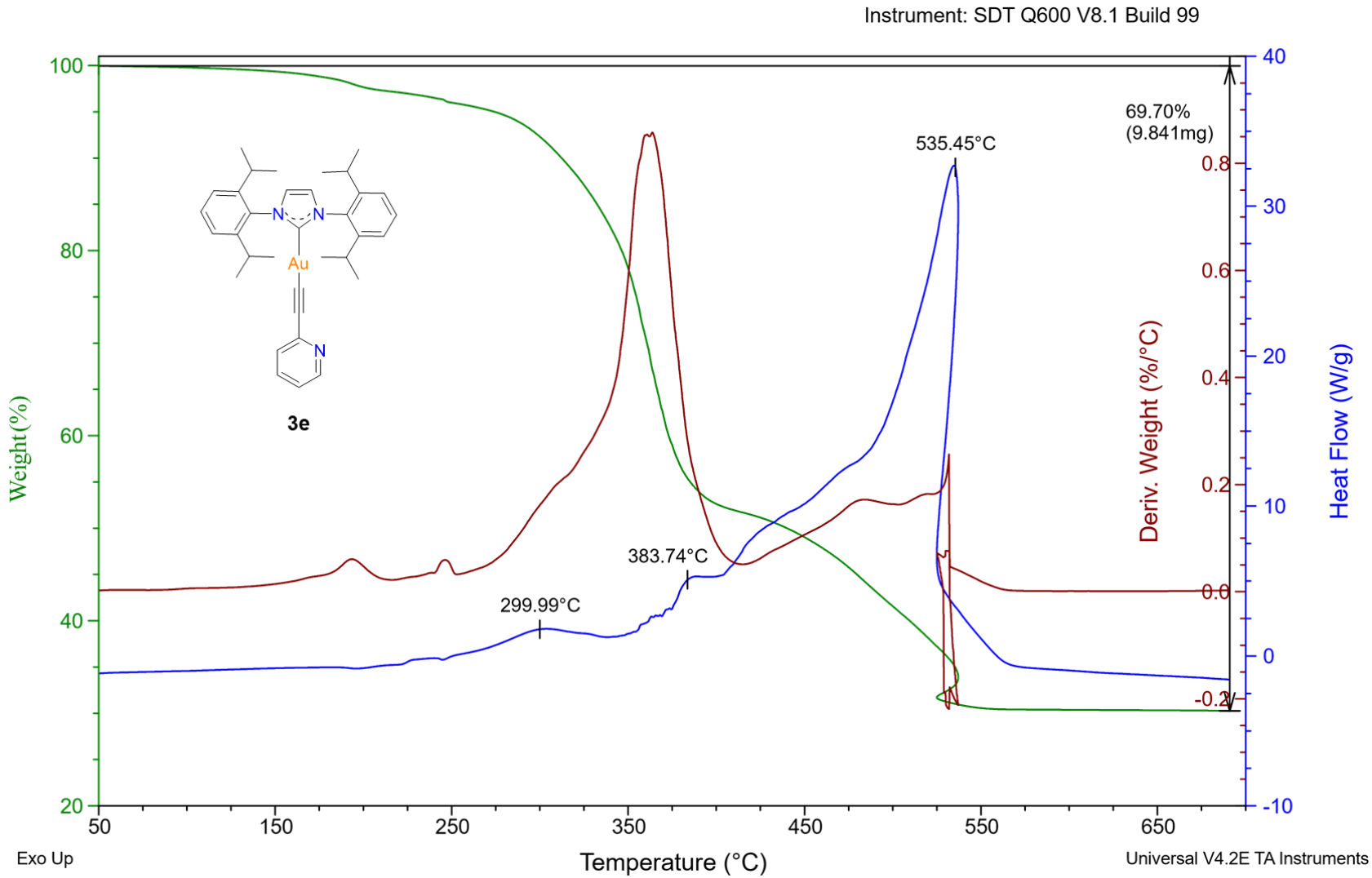

Figure S50. TGA/DSC analysis for complex **3e**.

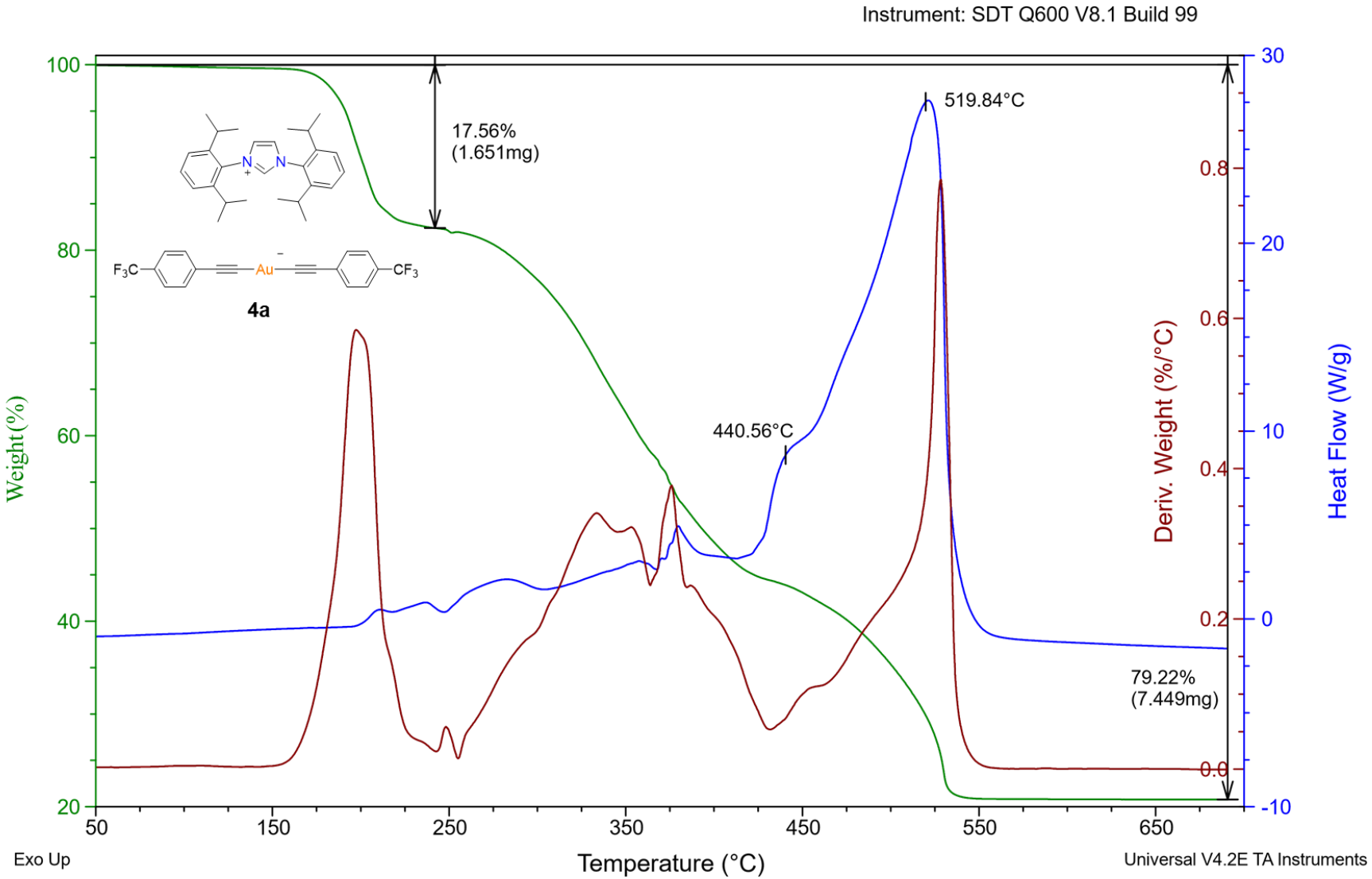

Figure S51. TGA/DSC analysis for complex **4a**.

11.X-ray diffraction study of structures of gold(I) complexes

Regardless of the relatively large number of crystallographically studied NHC-Au(I) complexes, complexes of type IPr-Au-C≡C-R (R= Alkyl, Aryl) are still poorly and irregularly studied by single-crystal X-ray diffraction analysis. According to the Cambridge Structural Database1, crystal structures of IPr-Au-C≡C-R are limited to 4 (R=Alkyl) and 13 (R=Aryl) published models, including that of **3f**•$CHCl_3$.[2] Herein, we report the structures of **3a**, **3b**, **3c, 3e** and **4a** (Fig. S52, see also Section 12 for details). The structure of closely related IPr-Au-C≡C-CH_3[3] will also be used for comparison. The crystal structure of **3h** (see below) has been already presented in the CSD.

Complex **3a** forms two different triclinic polymorph modifications. The first modification, **3a-I**, exhibits one unique (Z'=1) but entirely disordered molecule of **3a**, whereas the second modification, **3a-II**, has three crystallographically unique molecules (Z'=3). Complexes **3b** and **3c** crystalize as dichloromethane solvates **3b**•CH_2Cl_2 (Z'=1) and **3c**•0.92(CH_2Cl_2) (Z'=2). Complex **3e** crystalizes in the chiral $P2_1$ space group (Z'=2). Both crystallographically non-equivalent molecules exhibit rather large thermal motions resulting in poor accuracy in determination of bond lengths. It seems that **4a** is the sole crystallographically studied example containing both a complex anion $[Au(-C\equiv C-R)_2]^-$ and a cation of a protonated NHC ligand.

The Au atom in complexes **3a**, **3b**, **3c**, **3e** and **4a** is in a linear environment, as expected for Au(I); the C_{NHC}-Au-$C_{C\equiv C}$ angle varies from 175.1(2)° to 178.9(6)°. The C-C and C-N bond distances (within the given ESDs) in the NHC ligand are, on average, similar in complexes IPr-Au-C≡C-Aryl (**3a**, **3b**, **3c**, **3e** and **3f**) but slightly differ from those in IPr-Au-C≡C-CH_3.[3] Analysis of the Au-C_{NHC}, Au-$C_{C\equiv C}$ and C≡C distances (Table S5) indicates similar electron effects induced by C≡C-Aryl ligands. The C≡C-Aryl ligands exhibit a somewhat reduced σ-donor ability compared to that of C≡C-Me, which makes the IPr NHC ligand a somewhat stronger σ-donor, reflecting this in shorter Au-C_{NHC} bond distances (Table S5). Both longer C≡C and shorter Au-$C_{C\equiv C}$ distances indicate a stronger π-acceptor ability of the C≡C-Aryl ligands.

Both effects likely lead to a higher thermodynamic stability of complexes IPr-Au-C≡C-Aryl compared to that of IPr-Au-C≡C-Alkyl, using IPr-Au-C≡C-Me as an example. Among the subtle differences for complexes **3a**, **3b**, **3c** and **3f**, it might be noted that the smallest σ-donor ability might be attributed to **3a**, bearing the C≡C-C_6H_4-4-CF_3 ligand, whereas the smallest π-acceptor ability is observed for **3e** and **3b** (shortest C≡C bond lengths). Structure **3h** (see the CSD[1]) exhibits similar electronic and geometrical properties to those of IPr-Au-C≡C-Aryl (**3a**, **3b**, **3c** and **3f**).

Interestingly, the π-acceptor ability of the C≡C-C_6H_4-4-CF_3 ligand does not seem to change in the complex anion of Au(I) in **4a**.

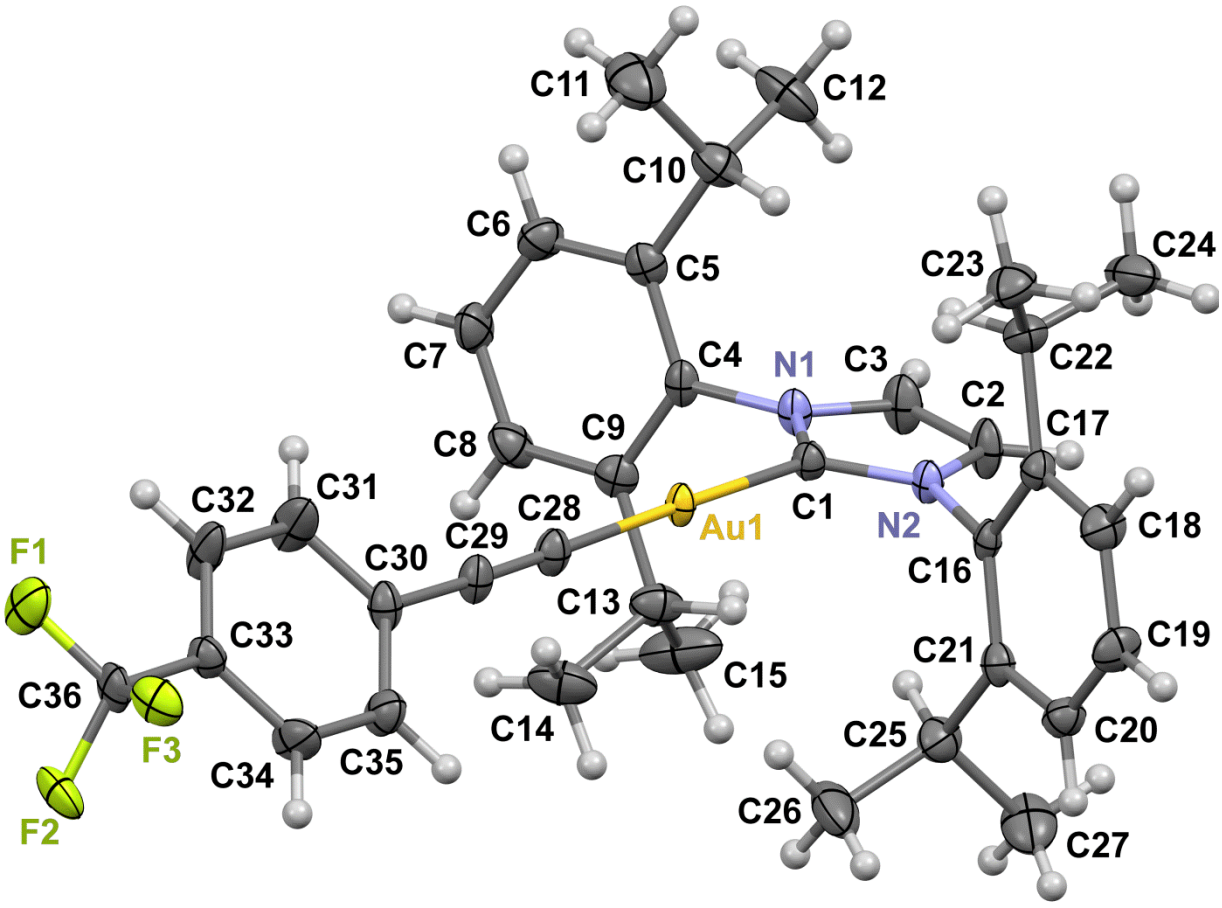

3a

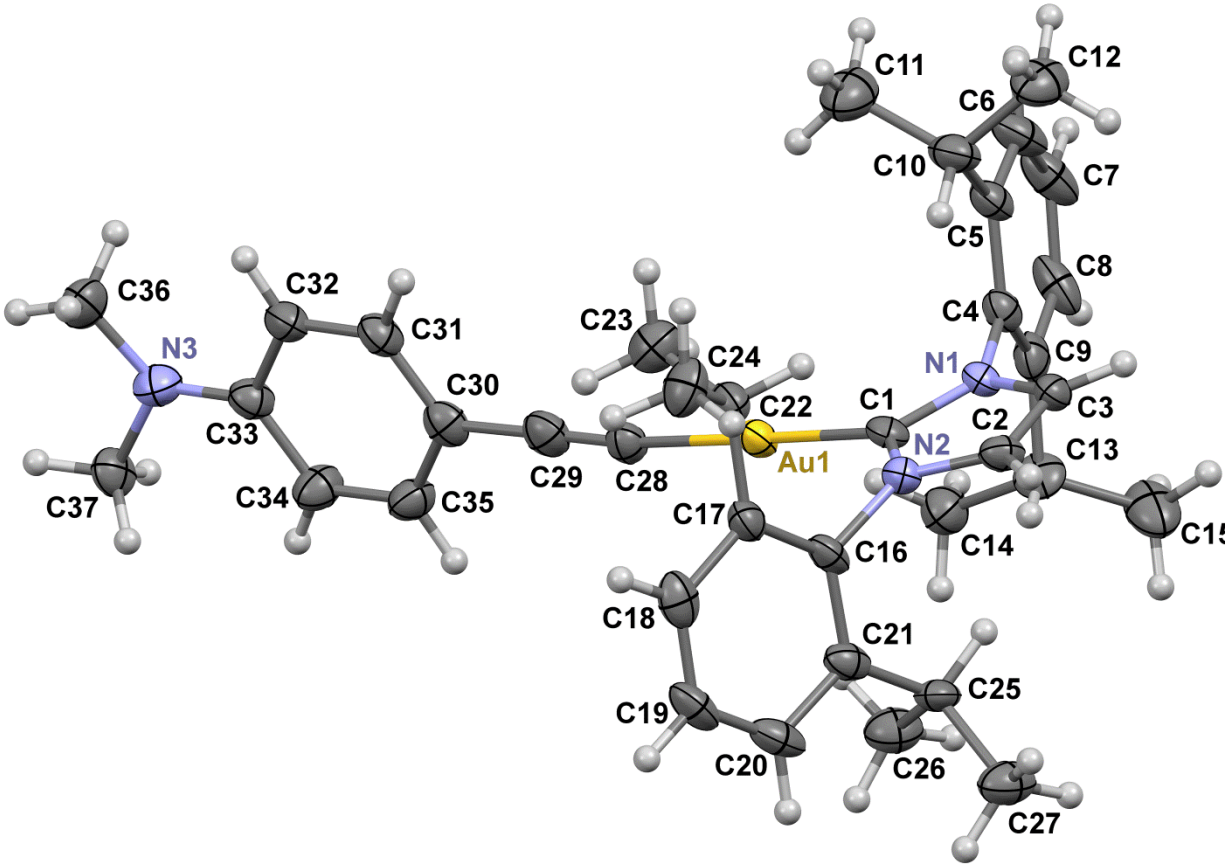
C11
C12
C6
C10
C7
C5
C8
C4
C9
N1
C3
C2
C13
C15
C14
C16
C17
C18
C21
C25
C19
C20
C26
C27
C36
N3
C32
C31
C23
C24
C30
C22
C1
N2
C33
C29
C28
Au1
C37
C34
C35

3b

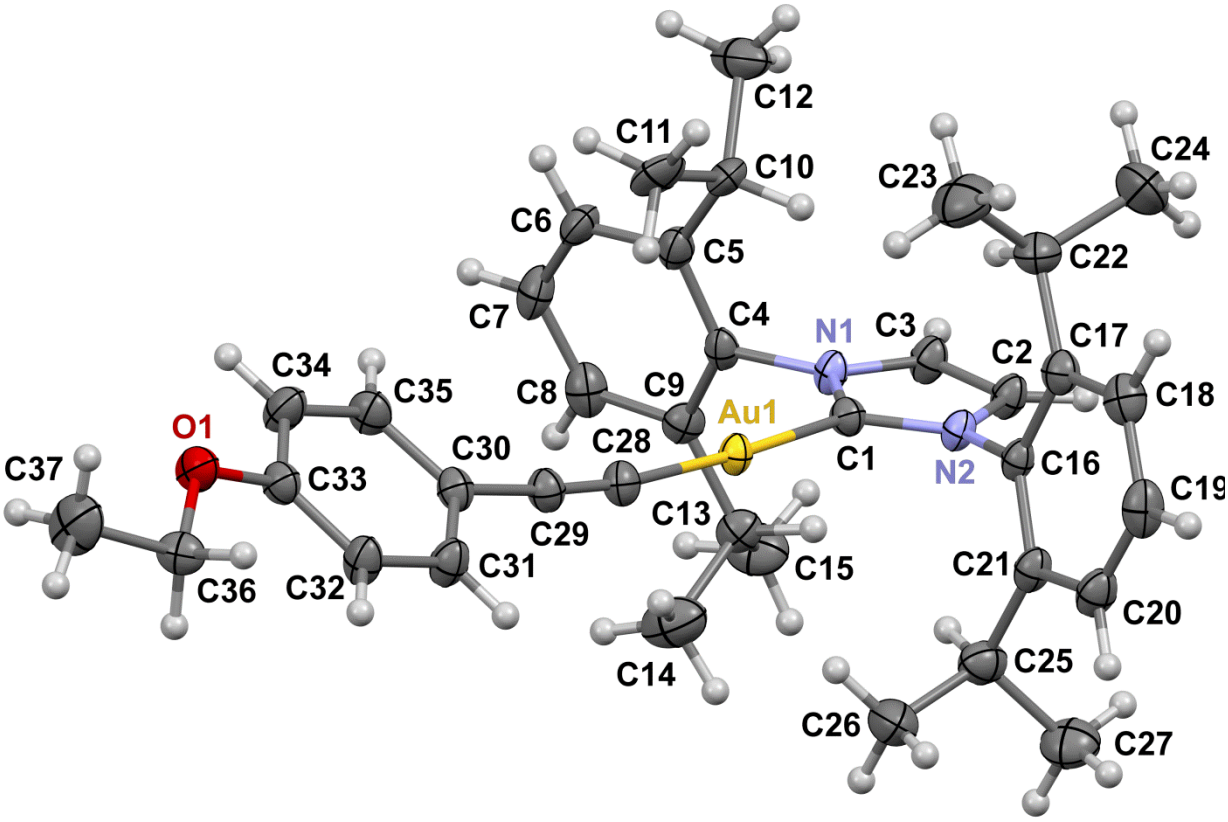
C12
C11
C10
C24
C23
C6
C5
C22
C7
C4
N1
C3
C17
C2
C34
C35
C8
C9
C18
Au1
O1
C30
C28
C1
N2
C16
C37
C33
C19
C29
C13
C31
C15
C21
C36
C32
C20
C14
C25
C26
C27

3c

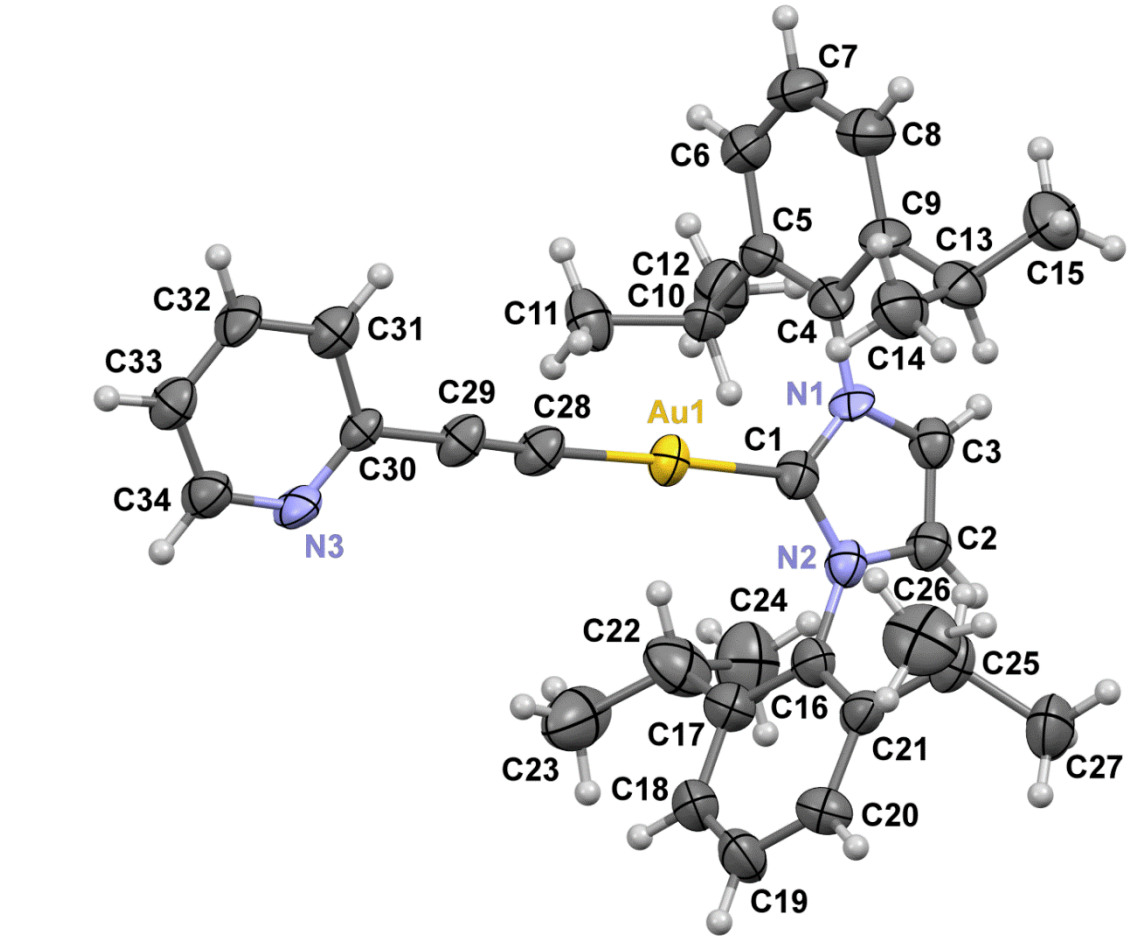

3e

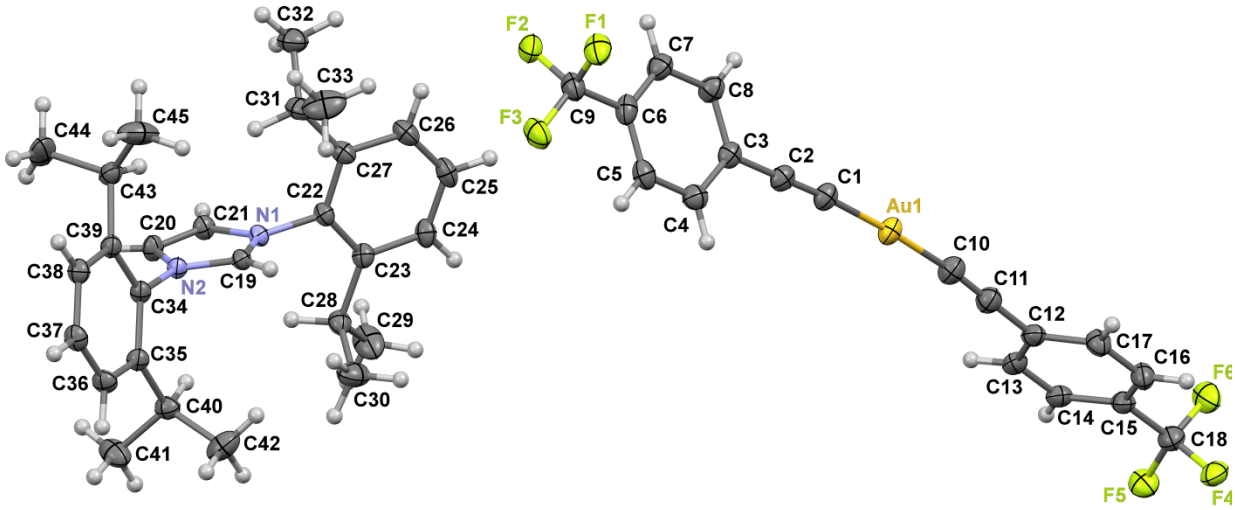

4a

Figure S52. Crystal structures of **3a**, **3b**, **3c, 3e** and **4a** (only one molecule for modification **3a-II** and in **3e** is shown). Thermal ellipsoids are set to a 50% probability level. Disorder is omitted.

Table S5. Selected bond distances (Å) and C-Au-C angles (°).

Complex	**Au-C_{NHC}**	**Au-$C_{C\equiv C}$**	**C≡C**	**$C_{\equiv}$-$C_{Me/Ar}$**	**C_{Au}-N (NHC)**	**N-$C_{=}$ (NHC)**	**C=C (NHC)**	**C-Au-C**
IPr-Au-C≡CMe[3]	2.048(13), 2.038(12)	1.998(12), 2.003(12)	1.127(18), 1.174(18)	1.51(2), 1.49(2)	1.322(17)-1.358(17)	1.329(16)-1.422(15)	1.294(19), 1.321(18)	175.9(6), 178.9(5)
3f[2]	2.018(7)	1.976(7)	1.203(10)	1.457(10)	1.348(9), 1.357(9)	1.374(9), 1.387(9)	1.349(10)	177.8(5)
3a (**3a-I**, **3a-II**)	2.003(3)-2.0088(19)	1.974(2)-1.985(3)	1.209(3)-1.220(3)	1.431(5)-1.446(3)	1.354(4)-1.359(4)	1.378(4)-1.384(2)	1.349(5)-1.353(4)	175.1(2)-178.9(6)
3b	2.017(8)	2.004(8)	1.193(12)	1.453(13)	1.370(11), 1.334(10)	1.390(10), 1.379(11)	1.352(12)	178.3(3)
3c	2.012(3), 2.014(3)	1.978(3), 1.984(4)	1.219(4), 1.213(5)	1.445(4), 1.447(5)	1.355(4)-1.369(4)	1.377(4)-1.393(4)	1.352(5), 1.352(5)	176.85(13)
3e	2.021(8), 2.007(8)	1.999(8), 2.052(10)	1.189(12), 1.143(14)	1.470(12), 1.485(15)	1.343(11)-1.386(11)	1.354(11)-1.394(10)	1.352(12), 1.341(13)	177.8(3), 178.7(4)
3h*	2.022(6)	1.994(6)	1.207(8)	1.436(8)	1.347(7), 1.358(7)	1.380(7), 1.381(7)	1.397(8)**	175.1(2)
4a	-	1.977(2), 1.980(2)	1.213(3), 1.216(3)	1.436(3), 1.431(3)	-	-	-	176.58(9)

***** According to CSD[1], the structure remains unpublished. Its CCDC deposition number is 1578124, and the CSD refcode is JIRHIE, DOI: 10.5517/ccdc.csd.cc1pz572

** This value corresponds to a C-C bond within a fused benzene ring**.**

References:

1. C. R. Groom, I. J. Bruno, M. P. Lightfoot, S. C. Ward, The Cambridge Structural Database, *Acta Cryst.*, 2016, **B72**, 171. CSD, version 5.43, updates up to November 2022.
2. S. Gaillard, A. M. Z. Slawin, S. P. Nolan, A *N*-heterocyclic carbene gold hydroxide complex: a golden synthon, *Chem. Commun.*, 2010, **46**, 2742.
3. A. S. K. Hashmi, T. Lauterbach, P. Nösel, M. H. Vilhelmsen, M. Rudolph, F. Rominger, Dual Gold Catalysis: σ,π-Propyne Acetylide and Hydroxyl-Bridged Digold Complexes as Easy-To-Prepare and Easy-To-Handle Precatalysts, *Chem.-Eur. J.*, 2013, **19**, 1058.

12.Summary of crystallographic data

Table S6. Crystal data, data collection and structure refinement details for **3a**, **3b**•CH_2Cl_2, **3c**•0.92(CH_2Cl_2), **3e** and **4a**.

Identification code	**3a-I**	**3-II**	**3b**•CH_2Cl_2	**3c**•0.92(CH_2Cl_2)	**3e**	**4a**
Empirical formula	$C_{36}H_{40}AuF_3N_2$	$C_{36}H_{40}AuF_3N_2$	$C_{38}H_{48}AuCl_2N_3$	$C_{37.92}H_{46.84}AuCl_{1.84}N_2O$	$C_{34}H_{40}AuN_3$	$C_{45}H_{45}AuF_6N_2$
Formula weight	754.66	754.66	814.66	808.76	687.65	924.79
Temperature, K	99.9(4)	100(2) K	100(2)	100(2)	100.0(5)	100(2)
Wavelength, Å	0.71073	0.71073	0.71073	0.71073	1.54184	0.71073
Crystal system	Triclinic	Triclinic	Monoclinic	Monoclinic	Monoclinic	Monoclinic
Space group	$P\bar{1}$	$P\bar{1}$	$P2_1/n$	$P2_1/n$	$P2_1$	$P2_1/c$
Unit cell dimensions						
a, Å	10.48248(7)	16.6955(4)	13.8463(11)	22.0775(11)	12.44412(8)	19.8123(3)
b, Å	11.13296(7)	18.1173(5)	15.2509(12)	15.1913(7)	17.19895(11)	12.4220(2)
c, Å	14.92534(9)	20.6902(5)	17.2099(14)	24.3230(12)	14.80376(10)	17.1873(2)
α, °	91.9967(5)	67.9350(10)	90	90	90	90
β, °	90.9661(5)	87.1560(10)	92.158(3)	115.297(2)	98.9726(6)	107.4140(10)
γ, °	101.0360(6)	63.2460(10)	90	90	90	90
Volume, $Å^3$	1708.062(19)	5124.8(2)	3631.6(5)	7375.3(6)	3129.61(4)	4036.07(10)
Z	2	6	4	8	4	4
Calculated density, g/cm^3	1.467	1.467	1.490	1.457	1.459	1.522
μ, mm^{-1}	4.348	4.347	4.228	4.153	9.011	3.706
F(000)	752	2256	1640	3252.8	1376	1848
Crystal size, mm	0.17×0.09×0.08	0.27×0.24×0.20	0.23×0.10×0.09	0.35×0.24×0.09	0.14×0.11×0.08	0.50×0.15×0.03

Table S6 (*cont.*). Crystal data, data collection and structure refinement details for **3a**, **3b**•CH_2Cl_2, **3c**•0.92(CH_2Cl_2), **3e** and **4a**.

Identification code	**3a-I**	**3a-II**	**3b**•CH_2Cl_2	**3c**•0.92(CH_2Cl_2)	**3e**	**4a**
θ range, °	2.269-34.249	1.867 to 25.250	1.854-25.049	1.629-34.465	3.022-77.864	2.057-33.157
Index ranges	$-16 \le h \le 16$	$-20 \le h \le 20$	$-16 \le h \le 16$	$-35 \le h \le 35$	$-15 \le h \le 15$	$-30 \le h \le 30$
	$-17 \le k \le 17$	$-21 \le k \le 21$	$-17 \le k \le 18$	$-24 \le k \le 24$	$-21 \le k \le 20$	$-18 \le k \le 19$
	$-23 \le l \le 23$	$-24 \le l \le 24$	$-20 \le l \le 20$	$-38 \le l \le 38$	$-18 \le l \le 18$	$-26 \le l \le 26$
Reflections						
Collected	80582	186395	62921	275992	87963	154358
Independent [R_{int}]	14035 [0.0242]	18522 [0.0333]	6443 [0.0877]	31110 [0.0629]	13201 [0.0285]	15386 [0.0441]
Observed (with $I>2\sigma(I)$)	12083	16684	5030	22723	13134	12409
Completeness to θ_{full} / θ_{max}	1.000 / 0.986	0.999 / 0.999	0.999 / 0.999	0.999 / 0.998	1.000 / 0.998	0.999 / 0.999
T_{max} / T_{min}	0.760 / 0.583	0.435 / 0.377	0.494 / 0.339	0.271 / 0.176	0.752 / 0.408	0.269 / 0.183
Data / restraints / parameters	14035 / 374 / 522	18522 / 128 / 1242	6443 / 33 / 429	31110 / 217 / 894	13201 / 347 / 849	15386 / 626 / 588
Goodness-of-fit on F^2	1.059	1.032	1.185	1.023	1.125	1.042
R1 / wR2 indices ($I>2\sigma(I)$)	0.0229 / 0.0531	0.0261 / 0.0621	0.0508 / 0.1310	0.0417 / 0.0956	0.0325 / 0.0766	0.0280 / 0.0559
R1 / wR2 indices (all data)	0.0300 / 0.0551	0.0305 / 0.0646	0.0702 / 0.1467	0.0677 / 0.1068	0.0326 / 0.0766	0.0418 / 0.0608
Absolute structure parameter	-	-	-	-	-0.001(6)	-
$\Delta\rho_{max}$ / $\Delta\rho_{max}$, ē•$Å^{-3}$	1.542 / -0.798	3.208 / -1.436	2.602 / -1.202	2.065 / -1.794	1.202 / -1.455	0.973 / -1.263
CCDC deposition number	2282626	2282627	2282628	2282629	2321627	2282630

The crystal structure of **3a**

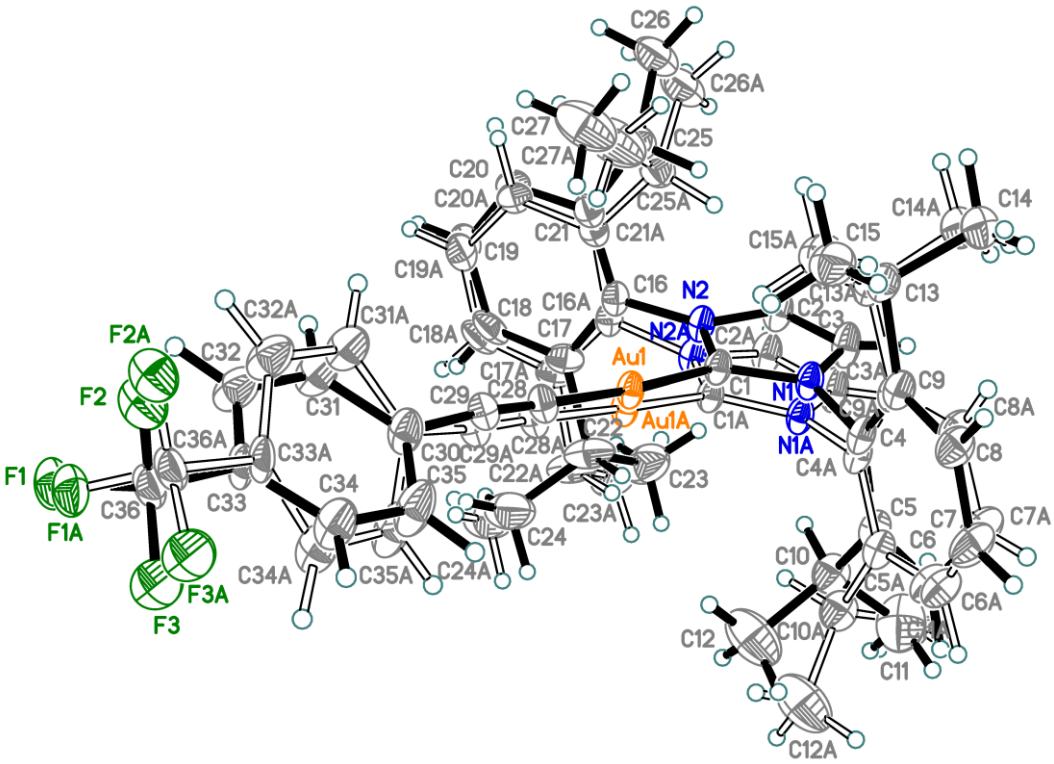

Figure S53. The molecular structure of **3a-I** (complex **3a**, 1st polymorph modification). Thermal ellipsoids are shown at a 50% probability level. Hydrogen atoms are drawn as fixed-size spheres. The entire molecule is disordered over two positions. The overlay of both components of the disorder is shown. The minor disorder component is drawn with open solid lines. The disorder ratio is 0.6011(10):0.3989(10).

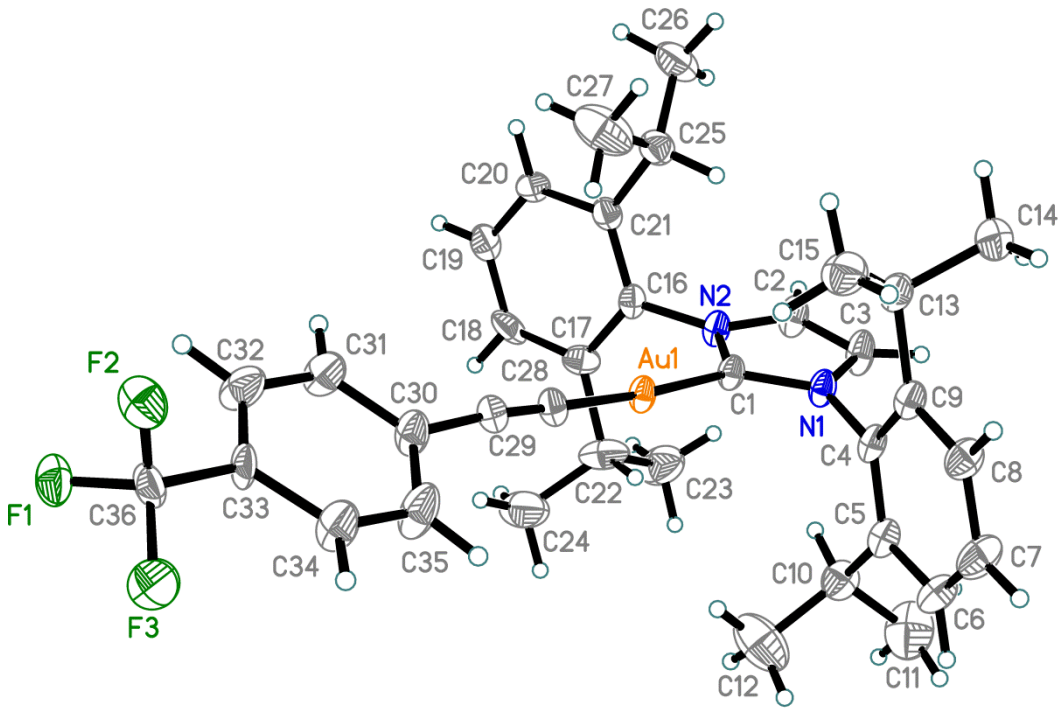

Figure S54. The major component of the disordered molecule in **3a-I**. Thermal ellipsoids are shown at a 50% probability level. Hydrogen atoms are drawn as fixed-size spheres.

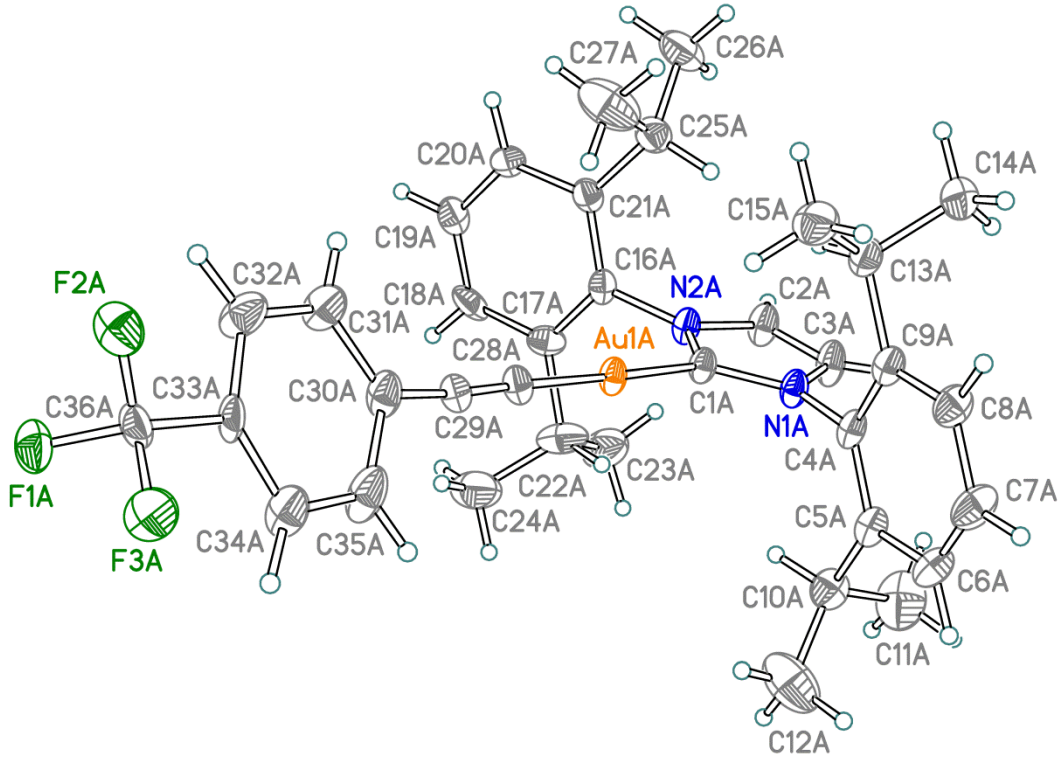

Figure S55. The minor component of the disordered molecule in **3a-I**. Thermal ellipsoids are shown at a 50% probability level. Hydrogen atoms are drawn as fixed-size spheres.

Table S7. Selected bond distances (Å) for **3a-I**.

Au1-C1	2.0088(19)	Au1A-C1A	2.006(2)
Au1-C28	1.974(2)	Au1A-C28A	1.985(3)
N1-C1	1.358(2)	N1A-C1A	1.356(2)
N1-C3	1.384(2)	N1A-C3A	1.382(3)
N1-C4	1.445(2)	N1A-C4A	1.444(3)
C1-N2	1.357(2)	C1A-N2A	1.356(2)
N2-C2	1.383(2)	N2A-C2A	1.382(3)
N2-C16	1.442(2)	N2A-C16A	1.444(3)
C2-C3	1.353(3)	C2A-C3A	1.353(4)
C4-C5	1.399(2)	C4A-C5A	1.397(2)
C4-C9	1.398(2)	C4A-C9A	1.396(2)
C5-C6	1.395(2)	C5A-C6A	1.394(3)
C5-C10	1.524(2)	C5A-C10A	1.523(3)
C6-C7	1.379(2)	C6A-C7A	1.379(2)
C7-C8	1.380(2)	C7A-C8A	1.380(2)
C8-C9	1.394(2)	C8A-C9A	1.393(3)
C9-C13	1.525(2)	C9A-C13A	1.523(2)
C10-C11	1.535(3)	C10A-C11A	1.534(3)
C10-C12	1.534(2)	C10A-C12A	1.533(3)
C13-C14	1.534(2)	C13A-C14A	1.534(2)
C13-C15	1.535(2)	C13A-C15A	1.534(3)
C16-C17	1.399(2)	C16A-C17A	1.398(2)
C16-C21	1.395(2)	C16A-C21A	1.396(2)
C17-C18	1.394(2)	C17A-C18A	1.395(3)
C17-C22	1.523(2)	C17A-C22A	1.524(3)
C18-C19	1.380(2)	C18A-C19A	1.380(2)
C19-C20	1.378(2)	C19A-C20A	1.378(2)
C20-C21	1.396(2)	C20A-C21A	1.396(3)
C21-C25	1.523(2)	C21A-C25A	1.523(3)
C22-C23	1.533(2)	C22A-C23A	1.531(3)
C22-C24	1.542(2)	C22A-C24A	1.536(3)
C25-C26	1.533(2)	C25A-C26A	1.533(3)
C25-C27	1.533(2)	C25A-C27A	1.533(3)
C28-C29	1.209(3)	C28A-C29A	1.220(3)
C29-C30	1.435(3)	C29A-C30A	1.446(3)
C30-C31	1.384(2)	C30A-C31A	1.394(3)
C30-C35	1.383(2)	C30A-C35A	1.393(3)
C31-C32	1.390(3)	C31A-C32A	1.393(3)
C32-C33	1.381(2)	C32A-C33A	1.385(3)

C33-C34	1.381(2)	C33A-C34A	1.386(3)
C33-C36	1.467(5)	C33A-C36A	1.543(9)
C34-C35	1.391(3)	C34A-C35A	1.393(3)
C36-F1	1.341(4)	C36A-F1A	1.355(7)
C36-F2	1.358(6)	C36A-F2A	1.368(9)
C36-F3	1.329(5)	C36A-F3A	1.349(8)

Table S8. Selected bond angles (°) for **3a-I**.

C28-Au1-C1	175.1(2)	C28A-Au1A-C1A	178.9(6)
C1-N1-C3	111.23(19)	C1A-N1A-C3A	110.6(3)
C1-N1-C4	123.9(5)	C1A-N1A-C4A	126.5(7)
C3-N1-C4	124.7(5)	C3A-N1A-C4A	122.7(7)
N1-C1-Au1	126.23(16)	N1A-C1A-Au1A	126.7(2)
N2-C1-Au1	128.73(16)	N1A-C1A-N2A	104.9(3)
N2-C1-N1	104.27(19)	N2A-C1A-Au1A	128.0(2)
C1-N2-C2	111.30(19)	C1A-N2A-C2A	110.9(3)
C1-N2-C16	125.9(4)	C1A-N2A-C16A	126.0(6)
C2-N2-C16	122.8(4)	C2A-N2A-C16A	123.0(6)
C3-C2-N2	106.6(2)	C3A-C2A-N2A	106.6(3)
C2-C3-N1	106.6(2)	C2A-C3A-N1A	106.9(3)
C5-C4-N1	118.2(3)	C5A-C4A-N1A	118.9(5)
C9-C4-N1	119.0(3)	C9A-C4A-N1A	117.4(5)
C9-C4-C5	122.7(3)	C9A-C4A-C5A	123.7(4)
C4-C5-C10	122.3(4)	C4A-C5A-C10A	122.8(6)
C6-C5-C4	117.1(7)	C6A-C5A-C4A	117.4(10)
C6-C5-C10	120.6(7)	C6A-C5A-C10A	119.8(10)
C7-C6-C5	121.9(13)	C7A-C6A-C5A	119.4(19)
C6-C7-C8	119.2(13)	C6A-C7A-C8A	123(2)
C7-C8-C9	122.0(9)	C7A-C8A-C9A	119.7(14)
C4-C9-C13	122.4(3)	C4A-C9A-C13A	123.5(5)
C8-C9-C4	117.1(4)	C8A-C9A-C4A	117.2(7)
C8-C9-C13	120.5(4)	C8A-C9A-C13A	119.3(7)
C5-C10-C11	112.1(13)	C5A-C10A-C11A	109.5(19)
C5-C10-C12	109.4(5)	C5A-C10A-C12A	111.4(7)
C12-C10-C11	111.3(7)	C12A-C10A-C11A	114.3(9)
C9-C13-C14	110.4(4)	C9A-C13A-C14A	110.0(6)
C9-C13-C15	110.5(3)	C9A-C13A-C15A	110.9(5)
C14-C13-C15	111.5(3)	C14A-C13A-C15A	110.7(4)
C17-C16-N2	120.5(4)	C17A-C16A-N2A	117.4(7)

C21-C16-N2	118.0(3)	C21A-C16A-N2A	117.3(6)
C21-C16-C17	121.5(4)	C21A-C16A-C17A	125.2(6)
C16-C17-C22	123.5(4)	C16A-C17A-C22A	123.7(8)
C18-C17-C16	116.9(6)	C18A-C17A-C16A	117.6(10)
C18-C17-C22	119.5(5)	C18A-C17A-C22A	118.6(9)
C19-C18-C17	123.4(9)	C19A-C18A-C17A	117.6(15)
C20-C19-C18	117.6(10)	C20A-C19A-C18A	124.4(18)
C19-C20-C21	122.2(9)	C19A-C20A-C21A	119.7(16)
C16-C21-C20	118.1(5)	C16A-C21A-C25A	123.5(7)
C16-C21-C25	122.4(4)	C20A-C21A-C16A	115.5(9)
C20-C21-C25	119.4(5)	C20A-C21A-C25A	120.9(9)
C17-C22-C23	111.8(5)	C17A-C22A-C23A	110.2(9)
C17-C22-C24	112.0(6)	C17A-C22A-C24A	111.6(11)
C23-C22-C24	107.1(5)	C23A-C22A-C24A	106.5(8)
C21-C25-C26	111.7(4)	C21A-C25A-C26A	112.3(8)
C21-C25-C27	109.6(7)	C21A-C25A-C27A	109.8(11)
C27-C25-C26	112.7(5)	C26A-C25A-C27A	110.4(7)
C29-C28-Au1	177.8(11)	C29A-C28A-Au1A	178.4(16)
C28-C29-C30	172.8(7)	C28A-C29A-C30A	173.9(13)
C31-C30-C29	120.4(5)	C31A-C30A-C29A	125.2(8)
C35-C30-C29	121.7(5)	C35A-C30A-C29A	114.8(8)
C35-C30-C31	117.9(3)	C35A-C30A-C31A	119.7(4)
C30-C31-C32	120.3(3)	C32A-C31A-C30A	121.8(4)
C33-C32-C31	122.5(3)	C33A-C32A-C31A	115.3(5)
C32-C33-C36	122.6(3)	C32A-C33A-C34A	125.9(6)
C34-C33-C32	116.3(4)	C32A-C33A-C36A	113.5(5)
C34-C33-C36	121.1(3)	C34A-C33A-C36A	120.3(5)
C33-C34-C35	122.1(4)	C33A-C34A-C35A	116.1(6)
C30-C35-C34	120.7(3)	C34A-C35A-C30A	120.9(5)
F1-C36-C33	111.9(4)	F1A-C36A-C33A	112.7(7)
F1-C36-F2	105.2(5)	F1A-C36A-F2A	104.9(8)
F2-C36-C33	110.2(4)	F2A-C36A-C33A	116.0(7)
F3-C36-C33	113.6(4)	F3A-C36A-C33A	112.4(6)
F3-C36-F1	108.5(3)	F3A-C36A-F1A	104.7(6)
F3-C36-F2	107.1(4)	F3A-C36A-F2A	105.2(7)

Table S9. Torsion angles (°) for **3a-I**.

Au1-C1-N2-C2	169.6(2)	Au1A-C1A-N2A-C2A	173.6(4)
Au1-C1-N2-C16	-12.2(5)	Au1A-C1A-N2A-C16A	-2.7(8)
N1-C1-N2-C2	-0.8(3)	N1A-C1A-N2A-C2A	0.0(6)
N1-C1-N2-C16	177.4(3)	N1A-C1A-N2A-C16A	-176.2(5)
N1-C4-C5-C6	177.9(10)	N1A-C4A-C5A-C6A	177.5(16)
N1-C4-C5-C10	-4.3(13)	N1A-C4A-C5A-C10A	-3(2)
N1-C4-C9-C8	-178.4(7)	N1A-C4A-C9A-C8A	-177.1(12)
N1-C4-C9-C13	1.3(11)	N1A-C4A-C9A-C13A	2.3(19)
C1-N1-C3-C2	-0.6(4)	C1A-N1A-C3A-C2A	0.4(6)
C1-N1-C4-C5	91.9(8)	C1A-N1A-C4A-C5A	101.5(13)
C1-N1-C4-C9	-89.0(8)	C1A-N1A-C4A-C9A	-80.0(14)
C1-N2-C2-C3	0.5(4)	C1A-N2A-C2A-C3A	0.2(6)
C1-N2-C16-C17	-83.6(7)	C1A-N2A-C16A-C17A	-95.3(11)
C1-N2-C16-C21	98.9(8)	C1A-N2A-C16A-C21A	87.8(13)
N2-C2-C3-N1	0.1(4)	N2A-C2A-C3A-N1A	-0.4(6)
N2-C16-C17-C18	-174.0(8)	N2A-C16A-C17A-C18A	-177.9(13)
N2-C16-C17-C22	4.3(10)	N2A-C16A-C17A-C22A	5.9(16)
N2-C16-C21-C20	172.7(9)	N2A-C16A-C21A-C20A	179.5(14)
N2-C16-C21-C25	-10.4(13)	N2A-C16A-C21A-C25A	-3(2)
C2-N2-C16-C17	94.4(7)	C2A-N2A-C16A-C17A	88.8(11)
C2-N2-C16-C21	-83.1(8)	C2A-N2A-C16A-C21A	-88.0(13)
C3-N1-C1-Au1	-169.8(2)	C3A-N1A-C1A-Au1A	-173.9(4)
C3-N1-C1-N2	0.9(3)	C3A-N1A-C1A-N2A	-0.3(6)
C3-N1-C4-C5	-82.6(9)	C3A-N1A-C4A-C5A	-83.5(14)
C3-N1-C4-C9	96.4(8)	C3A-N1A-C4A-C9A	94.9(13)
C4-N1-C1-Au1	15.0(4)	C4A-N1A-C1A-Au1A	1.5(8)
C4-N1-C1-N2	-174.3(3)	C4A-N1A-C1A-N2A	175.2(5)
C4-N1-C3-C2	174.6(3)	C4A-N1A-C3A-C2A	-175.2(5)
C4-C5-C6-C7	0.3(12)	C4A-C5A-C6A-C7A	0.0(17)
C4-C5-C10-C11	128.1(10)	C4A-C5A-C10A-C11A	98.0(19)
C4-C5-C10-C12	-107.9(9)	C4A-C5A-C10A-C12A	-134.6(13)
C4-C9-C13-C14	-114.3(7)	C4A-C9A-C13A-C14A	-115.9(12)
C4-C9-C13-C15	121.8(7)	C4A-C9A-C13A-C15A	121.4(11)
C5-C4-C9-C8	0.6(11)	C5A-C4A-C9A-C8A	1.3(19)
C5-C4-C9-C13	-179.6(8)	C5A-C4A-C9A-C13A	-179.3(13)
C5-C6-C7-C8	1.0(19)	C5A-C6A-C7A-C8A	0(3)
C6-C5-C10-C11	-54.1(10)	C6A-C5A-C10A-C11A	-82.4(17)
C6-C5-C10-C12	69.8(8)	C6A-C5A-C10A-C12A	44.9(14)
C6-C7-C8-C9	-1.6(19)	C6A-C7A-C8A-C9A	0(3)

C7-C8-C9-C4	0.8(13)	C7A-C8A-C9A-C4A	-1(2)
C7-C8-C9-C13	-179.0(10)	C7A-C8A-C9A-C13A	179.6(16)
C8-C9-C13-C14	65.4(7)	C8A-C9A-C13A-C14A	63.5(11)
C8-C9-C13-C15	-58.4(7)	C8A-C9A-C13A-C15A	-59.2(11)
C9-C4-C5-C6	-1.1(9)	C9A-C4A-C5A-C6A	-0.8(14)
C9-C4-C5-C10	176.7(9)	C9A-C4A-C5A-C10A	178.7(15)
C10-C5-C6-C7	-177.6(14)	C10A-C5A-C6A-C7A	-180(2)
C16-N2-C2-C3	-177.8(3)	C16A-N2A-C2A-C3A	176.6(5)
C16-C17-C18-C19	1.2(10)	C16A-C17A-C18A-C19A	-1.1(15)
C16-C17-C22-C23	-87.3(8)	C16A-C17A-C22A-C23A	-98.4(13)
C16-C17-C22-C24	152.5(8)	C16A-C17A-C22A-C24A	143.5(13)
C16-C21-C25-C26	132.0(8)	C16A-C21A-C25A-C26A	126.4(14)
C16-C21-C25-C27	-102.3(10)	C16A-C21A-C25A-C27A	-110.4(16)
C17-C16-C21-C20	-4.7(13)	C17A-C16A-C21A-C20A	3(2)
C17-C16-C21-C25	172.1(8)	C17A-C16A-C21A-C25A	-179.8(14)
C17-C18-C19-C20	-4.1(15)	C17A-C18A-C19A-C20A	2(3)
C18-C17-C22-C23	91.0(7)	C18A-C17A-C22A-C23A	85.4(12)
C18-C17-C22-C24	-29.2(9)	C18A-C17A-C22A-C24A	-32.7(15)
C18-C19-C20-C21	2.7(17)	C18A-C19A-C20A-C21A	0(3)
C19-C20-C21-C16	1.6(16)	C19A-C20A-C21A-C16A	-2(3)
C19-C20-C21-C25	-175.3(10)	C19A-C20A-C21A-C25A	-179.5(16)
C20-C21-C25-C26	-51.2(11)	C20A-C21A-C25A-C26A	-56.5(18)
C20-C21-C25-C27	74.5(11)	C20A-C21A-C25A-C27A	66.7(18)
C21-C16-C17-C18	3.4(9)	C21A-C16A-C17A-C18A	-1.3(14)
C21-C16-C17-C22	-178.3(9)	C21A-C16A-C17A-C22A	-177.5(15)
C22-C17-C18-C19	-177.2(11)	C22A-C17A-C18A-C19A	175.3(17)
C29-C30-C31-C32	-176.6(5)	C29A-C30A-C31A-C32A	174.1(10)
C29-C30-C35-C34	174.8(5)	C29A-C30A-C35A-C34A	-174.4(9)
C30-C31-C32-C33	-1.3(7)	C30A-C31A-C32A-C33A	2.6(9)
C31-C30-C35-C34	-3.5(8)	C31A-C30A-C35A-C34A	0.0(12)
C31-C32-C33-C34	2.4(7)	C31A-C32A-C33A-C34A	-6.7(11)
C31-C32-C33-C36	-179.1(4)	C31A-C32A-C33A-C36A	178.5(6)
C32-C33-C34-C35	-4.2(7)	C32A-C33A-C34A-C35A	7.1(12)
C32-C33-C36-F1	42.4(7)	C32A-C33A-C36A-F1A	86.4(9)
C32-C33-C36-F2	-74.2(6)	C32A-C33A-C36A-F2A	-34.5(11)
C32-C33-C36-F3	165.7(4)	C32A-C33A-C36A-F3A	-155.6(6)
C33-C34-C35-C30	4.9(8)	C33A-C34A-C35A-C30A	-3.4(10)
C34-C33-C36-F1	-139.2(5)	C34A-C33A-C36A-F1A	-88.7(10)
C34-C33-C36-F2	104.1(6)	C34A-C33A-C36A-F2A	150.4(9)
C34-C33-C36-F3	-16.0(6)	C34A-C33A-C36A-F3A	29.3(10)

C35-C30-C31-C32	1.7(8)	C35A-C30A-C31A-C32A	0.4(11)
C36-C33-C34-C35	177.3(4)	C36A-C33A-C34A-C35A	-178.4(7)

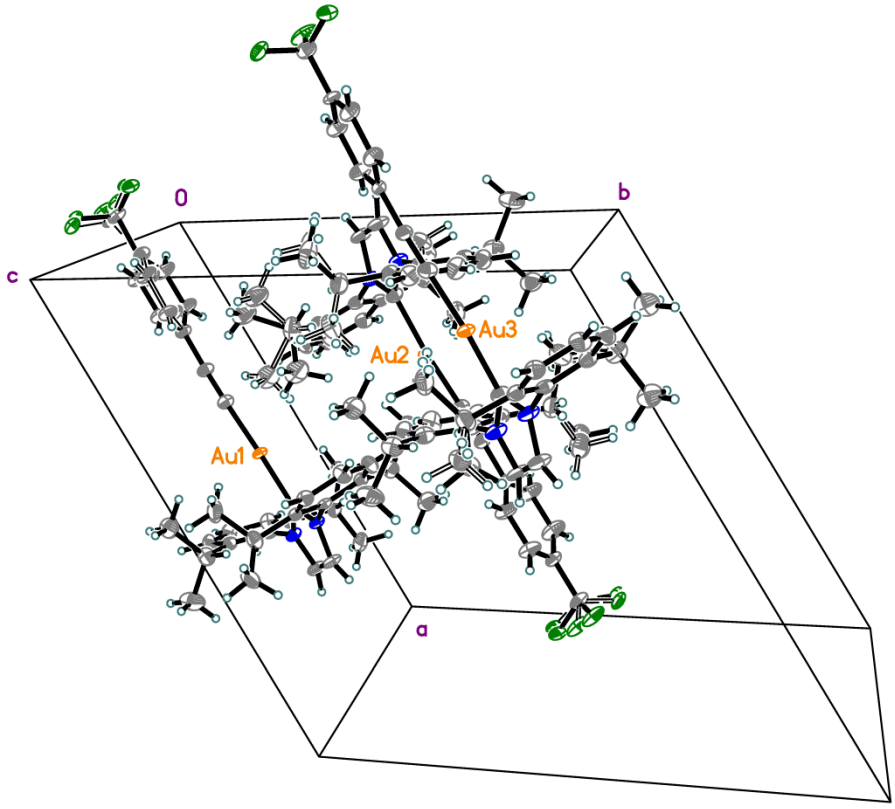

Figure S56. The crystal structure of **3a-II** (complex **3a**, 2nd polymorph modification). Three crystallographically inequivalent molecules are shown in the unit cell. Thermal ellipsoids are shown at a 50% probability level. Hydrogen atoms are drawn as fixed-size spheres.

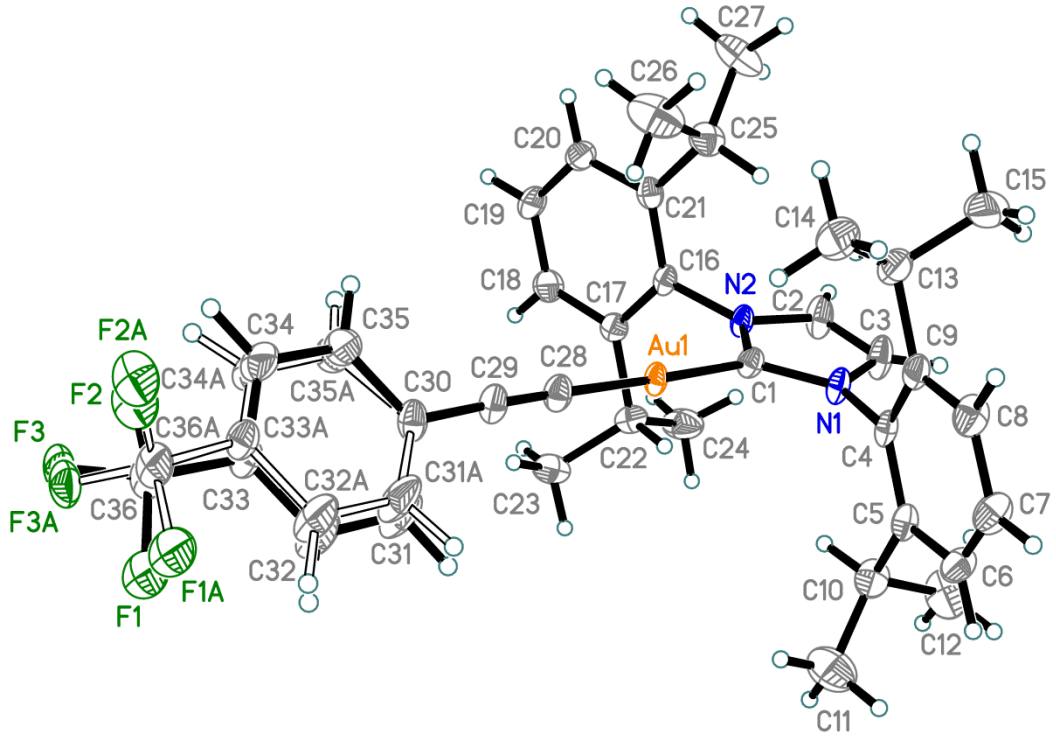

Figure S57. The 1st molecule **3a** in **3a-II**. Thermal ellipsoids are shown at a 50% probability level. Hydrogen atoms are drawn as fixed-size spheres. The disorder ratio for atoms C31..C36, F1..F3 / C31A..C36A, F1A..F3A is 0.862(17):0.138(17). The minor component of the disorder is drawn with open solid lines.

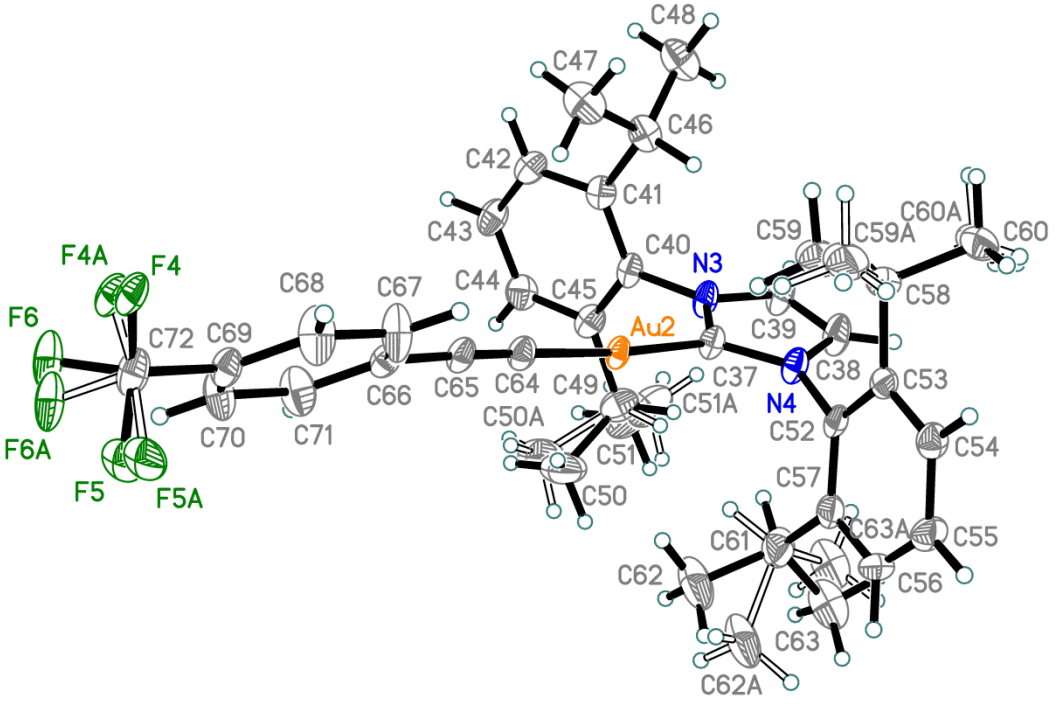

Figure S58. The 2nd molecule **3a** in **3a-II**. Thermal ellipsoids are shown at a 50% probability level. Hydrogen atoms are drawn as fixed-size spheres. The disorder ratios for groups of atoms are 0.88(2) : 0.12(2) for C50, C51 / C50A, C51A; 0.82(4) : 0.18(4) for C59, C60 / C59A, C60A; 0.503(7) : 0.497(7) for C62, C63 / C62A, C63A; 0.79(3) : 0.21(3) for F4..F6 / F4A..F6A.

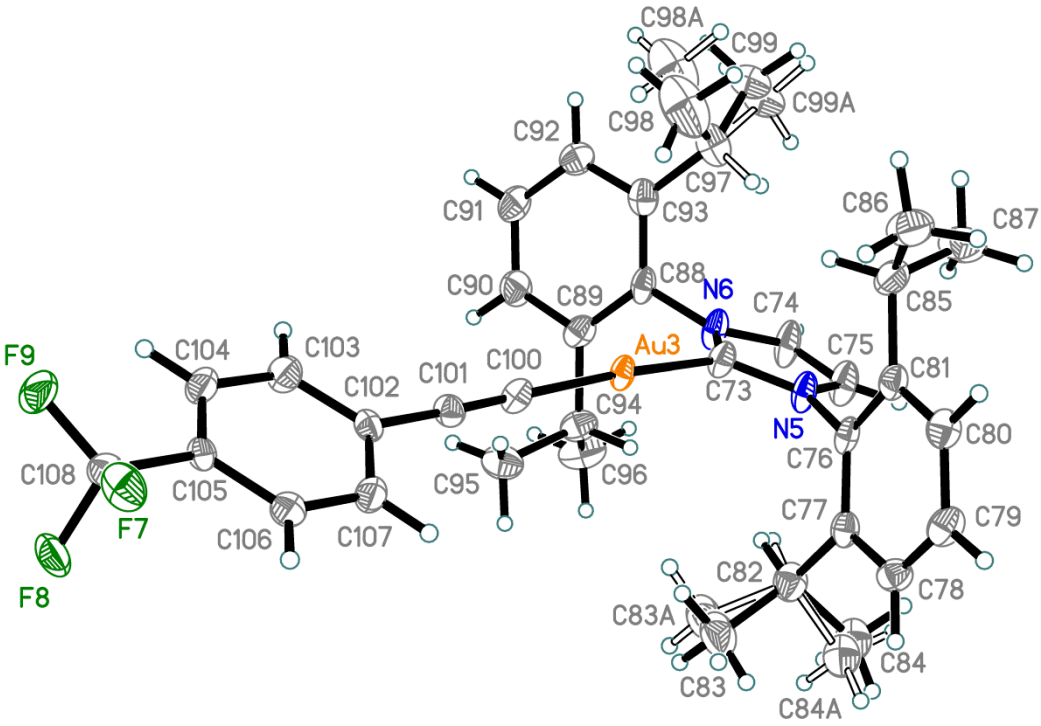

Figure S59. The 3rd molecule **3a** in **3a-II**. Thermal ellipsoids are shown at a 50% probability level. Hydrogen atoms are drawn as fixed-size spheres. The disorder ratios for groups of atoms are 0.30(8) : 0.70(8) for C83, C84 / C83A, C84A; 0.56(2) : 0.44(2) for C98, C99 / C98A, C99A.

Table S10. Selected bond distances (Å) for **3a-II**.

Au1-C1	2.004(3)	C13-C15	1.525(5)	C30-C35A	1.393(17)
Au1-C28	1.975(3)	C13-C14	1.536(5)	C30-C31	1.395(6)
N1-C1	1.359(4)	C16-C17	1.397(4)	C31-C32	1.386(6)
N1-C3	1.378(4)	C16-C21	1.397(5)	C32-C33	1.373(6)
N1-C4	1.447(4)	C17-C18	1.389(5)	C33-C34	1.390(6)
N2-C1	1.354(4)	C17-C22	1.527(4)	C33-C36	1.487(5)
N2-C2	1.380(4)	C18-C19	1.379(5)	C34-C35	1.379(6)
N2-C16	1.449(4)	C19-C20	1.383(5)	C36-F1	1.336(5)
C2-C3	1.349(5)	C20-C21	1.394(5)	C36-F3	1.344(5)
C4-C5	1.392(5)	C21-C25	1.516(5)	C36-F2	1.355(5)
C4-C9	1.399(5)	C22-C23	1.526(5)	C31A-C32A	1.378(17)
C5-C6	1.392(5)	C22-C24	1.535(5)	C32A-C33A	1.379(17)
C5-C10	1.522(5)	C25-C26	1.529(5)	C33A-C34A	1.384(17)
C6-C7	1.380(5)	C25-C27	1.531(5)	C33A-C36A	1.487(19)
C7-C8	1.382(5)	C28-C29	1.212(5)	C34A-C35A	1.380(17)
C8-C9	1.390(5)	C29-C30	1.432(5)	C36A-F1A	1.337(15)
C9-C13	1.517(5)	C30-C35	1.380(5)	C36A-F3A	1.342(15)
C10-C12	1.524(5)	C30-C31A	1.384(16)	C36A-F2A	1.343(15)
C10-C11	1.532(6)				

Au2-C37	2.008(3)	C46-C47	1.534(5)	C61-C63A	1.492(10)
Au2-C64	1.975(3)	C49-C50	1.531(6)	C61-C63	1.540(10)
N3-C37	1.359(4)	C49-C51	1.537(6)	C61-C62A	1.637(9)
N3-C39	1.379(4)	C49-C51A	1.545(16)	C64-C65	1.216(5)
N3-C40	1.444(4)	C49-C50A	1.560(16)	C65-C66	1.432(5)
N4-C37	1.356(4)	C52-C53	1.386(5)	C66-C71	1.387(5)
N4-C38	1.383(4)	C52-C57	1.399(5)	C66-C67	1.392(5)
N4-C52	1.446(4)	C53-C54	1.395(5)	C67-C68	1.387(5)
C38-C39	1.351(5)	C53-C58	1.520(5)	C68-C69	1.378(5)
C40-C41	1.392(5)	C54-C55	1.377(5)	C69-C70	1.369(5)
C40-C45	1.402(5)	C55-C56	1.382(5)	C69-C72	1.507(5)
C41-C42	1.391(5)	C56-C57	1.382(5)	C70-C71	1.380(5)
C41-C46	1.521(5)	C57-C61	1.512(5)	C72-F4A	1.329(14)
C42-C43	1.383(5)	C58-C60A	1.515(15)	C72-F5	1.347(6)
C43-C44	1.386(5)	C58-C59A	1.525(16)	C72-F6	1.349(5)
C44-C45	1.392(5)	C58-C60	1.530(6)	C72-F4	1.351(5)
C45-C49	1.525(5)	C58-C59	1.533(7)	C72-F6A	1.361(12)
C46-C48	1.529(5)	C61-C62	1.466(8)	C72-F5A	1.369(14)
Au3-C73	2.003(3)	C82-C84	1.529(14)	C97-C98	1.517(9)
Au3-C100	1.974(4)	C82-C84A	1.531(8)	C97-C99	1.519(11)
N5-C73	1.356(4)	C82-C83	1.532(15)	C97-C99A	1.539(12)
N5-C75	1.382(4)	C82-C83A	1.538(8)	C97-C98A	1.579(12)
N5-C76	1.445(4)	C85-C87	1.530(5)	C100-C101	1.217(5)
N6-C73	1.356(4)	C85-C86	1.543(6)	C101-C102	1.431(5)
N6-C74	1.379(4)	C88-C89	1.396(5)	C102-C103	1.384(5)
N6-C88	1.448(4)	C88-C93	1.402(5)	C102-C107	1.399(5)
C74-C75	1.351(5)	C89-C90	1.392(5)	C103-C104	1.382(5)
C76-C77	1.395(5)	C89-C94	1.528(5)	C104-C105	1.380(5)
C76-C81	1.404(5)	C90-C91	1.383(5)	C105-C106	1.380(5)
C77-C78	1.389(5)	C91-C92	1.389(5)	C105-C108	1.492(5)
C77-C82	1.524(5)	C92-C93	1.382(5)	C106-C107	1.377(5)
C78-C79	1.382(5)	C93-C97	1.520(5)	C108-F9	1.338(4)
C79-C80	1.379(5)	C94-C95	1.528(5)	C108-F7	1.347(4)
C80-C81	1.390(5)	C94-C96	1.533(5)	C108-F8	1.359(4)
C81-C85	1.521(5)				

Table S11. Selected bond angles (°) for **3a-II**.

C28-Au1-C1	178.27(14)	C9-C13-C14	110.7(3)	C31-C30-C29	119.8(4)
C1-N1-C3	110.8(3)	C15-C13-C14	110.3(3)	C32-C31-C30	120.2(6)
C1-N1-C4	125.4(3)	C17-C16-C21	123.3(3)	C33-C32-C31	120.4(7)
C3-N1-C4	123.5(3)	C17-C16-N2	118.3(3)	C32-C33-C34	120.0(7)
C1-N2-C2	111.4(3)	C21-C16-N2	118.3(3)	C32-C33-C36	121.8(6)
C1-N2-C16	126.1(3)	C18-C17-C16	117.1(3)	C34-C33-C36	118.2(6)
C2-N2-C16	122.4(3)	C18-C17-C22	120.3(3)	C35-C34-C33	119.3(8)
N2-C1-N1	104.4(3)	C16-C17-C22	122.6(3)	C34-C35-C30	121.5(8)
N2-C1-Au1	128.3(2)	C19-C18-C17	121.2(3)	F1-C36-F3	106.9(4)
N1-C1-Au1	127.1(2)	C18-C19-C20	120.5(3)	F1-C36-F2	106.4(4)
C3-C2-N2	106.3(3)	C19-C20-C21	120.8(3)	F3-C36-F2	104.0(4)
C2-C3-N1	107.1(3)	C20-C21-C16	117.1(3)	F1-C36-C33	112.8(5)
C5-C4-C9	123.5(3)	C20-C21-C25	120.5(3)	F3-C36-C33	113.4(5)
C5-C4-N1	118.4(3)	C16-C21-C25	122.4(3)	F2-C36-C33	112.7(6)
C9-C4-N1	118.0(3)	C23-C22-C17	112.1(3)	C32A-C31A-C30	128(5)
C6-C5-C4	117.0(3)	C23-C22-C24	109.7(3)	C31A-C32A-C33A	117(5)
C6-C5-C10	119.6(3)	C17-C22-C24	110.6(3)	C32A-C33A-C34A	113(5)
C4-C5-C10	123.4(3)	C21-C25-C26	110.4(3)	C32A-C33A-C36A	112(4)
C7-C6-C5	121.1(3)	C21-C25-C27	111.4(3)	C34A-C33A-C36A	134(5)
C6-C7-C8	120.3(3)	C26-C25-C27	110.5(3)	C35A-C34A-C33A	128(6)
C7-C8-C9	121.2(3)	C29-C28-Au1	178.1(3)	C34A-C35A-C30	117(5)
C8-C9-C4	116.9(3)	C28-C29-C30	177.7(4)	F1A-C36A-F3A	108(2)
C8-C9-C13	120.0(3)	C31A-C30-C35A	114(3)	F1A-C36A-F2A	107(2)
C4-C9-C13	123.2(3)	C35-C30-C31	118.6(5)	F3A-C36A-F2A	108(2)
C5-C10-C12	111.3(3)	C35-C30-C29	121.5(4)	F1A-C36A-C33A	115(3)
C5-C10-C11	111.4(3)	C31A-C30-C29	128(2)	F3A-C36A-C33A	110(4)
C12-C10-C11	110.1(3)	C35A-C30-C29	118(3)	F2A-C36A-C33A	110(4)
C9-C13-C15	110.6(3)				
C64-Au2-C37	175.42(14)	C45-C49-C50	110.1(4)	C57-C61-C63	114.1(6)
C37-N3-C39	111.2(3)	C45-C49-C51	112.4(5)	C63A-C61-C62A	106.4(6)
C37-N3-C40	124.1(3)	C50-C49-C51	111.0(5)	C57-C61-C62A	105.9(4)
C39-N3-C40	124.5(3)	C45-C49-C51A	109(4)	C65-C64-Au2	178.2(3)
C37-N4-C38	111.1(3)	C45-C49-C50A	102.3(18)	C64-C65-C66	178.1(4)
C37-N4-C52	125.9(3)	C51A-C49-C50A	107(2)	C71-C66-C67	118.4(3)
C38-N4-C52	122.9(3)	C53-C52-C57	123.0(3)	C71-C66-C65	121.0(3)
N4-C37-N3	104.3(3)	C53-C52-N4	118.2(3)	C67-C66-C65	120.6(3)
N4-C37-Au2	129.5(2)	C57-C52-N4	118.8(3)	C68-C67-C66	120.7(4)
N3-C37-Au2	125.6(2)	C52-C53-C54	117.3(3)	C69-C68-C67	119.5(3)
C39-C38-N4	106.7(3)	C52-C53-C58	122.7(3)	C70-C69-C68	120.6(3)

C38-C39-N3	106.7(3)	C54-C53-C58	119.9(3)	C70-C69-C72	119.7(3)
C41-C40-C45	123.2(3)	C55-C54-C53	120.9(3)	C68-C69-C72	119.7(3)
C41-C40-N3	118.5(3)	C54-C55-C56	120.3(3)	C69-C70-C71	119.9(3)
C45-C40-N3	118.3(3)	C55-C56-C57	121.0(3)	C70-C71-C66	120.9(3)
C42-C41-C40	116.9(3)	C56-C57-C52	117.4(3)	F5-C72-F6	108.0(4)
C42-C41-C46	119.8(3)	C56-C57-C61	120.3(3)	F5-C72-F4	105.4(5)
C40-C41-C46	123.2(3)	C52-C57-C61	122.3(3)	F6-C72-F4	105.3(4)
C43-C42-C41	121.6(3)	C60A-C58-C53	111.9(17)	F4A-C72-F6A	111.9(15)
C42-C43-C44	120.2(4)	C60A-C58-C59A	114.0(19)	F4A-C72-F5A	105.3(19)
C43-C44-C45	120.6(3)	C53-C58-C59A	108(2)	F6A-C72-F5A	98.7(15)
C44-C45-C40	117.6(3)	C53-C58-C60	112.5(4)	F4A-C72-C69	120.0(19)
C44-C45-C49	120.8(3)	C53-C58-C59	109.1(5)	F5-C72-C69	114.2(5)
C40-C45-C49	121.6(3)	C60-C58-C59	112.0(4)	F6-C72-C69	112.3(3)
C41-C46-C48	110.3(3)	C62-C61-C57	113.6(5)	F4-C72-C69	111.1(5)
C41-C46-C47	111.1(3)	C63A-C61-C57	112.4(6)	F6A-C72-C69	112.9(9)
C48-C46-C47	111.4(3)	C62-C61-C63	113.6(6)	F5A-C72-C69	105.1(18)
C100-Au3-C73	175.60(14)	C77-C82-C84	108(2)	C98-C97-C99	115.1(10)
C73-N5-C75	111.2(3)	C77-C82-C84A	113.9(10)	C98-C97-C93	110.0(6)
C73-N5-C76	125.9(3)	C77-C82-C83	108(3)	C99-C97-C93	113.1(15)
C75-N5-C76	122.9(3)	C84-C82-C83	113.6(19)	C93-C97-C99A	111(2)
C73-N6-C74	111.3(3)	C77-C82-C83A	109.8(10)	C93-C97-C98A	109.5(8)
C73-N6-C88	124.8(3)	C84A-C82-C83A	110.9(7)	C99A-C97-C98A	105.4(12)
C74-N6-C88	123.9(3)	C81-C85-C87	111.0(3)	C101-C100-Au3	179.1(3)
N6-C73-N5	104.3(3)	C81-C85-C86	112.1(3)	C100-C101-C102	177.3(4)
N6-C73-Au3	127.1(2)	C87-C85-C86	109.1(3)	C103-C102-C107	117.8(3)
N5-C73-Au3	127.9(2)	C89-C88-C93	123.0(3)	C103-C102-C101	121.5(3)
C75-C74-N6	106.6(3)	C89-C88-N6	118.6(3)	C107-C102-C101	120.8(3)
C74-C75-N5	106.6(3)	C93-C88-N6	118.4(3)	C104-C103-C102	121.7(3)
C77-C76-C81	123.1(3)	C90-C89-C88	117.1(3)	C105-C104-C103	119.4(3)
C77-C76-N5	117.9(3)	C90-C89-C94	119.5(3)	C104-C105-C106	120.2(3)
C81-C76-N5	118.9(3)	C88-C89-C94	123.4(3)	C104-C105-C108	120.2(3)
C78-C77-C76	117.3(3)	C91-C90-C89	121.2(4)	C106-C105-C108	119.6(3)
C78-C77-C82	119.7(3)	C90-C91-C92	120.2(4)	C107-C106-C105	119.9(3)
C76-C77-C82	122.9(3)	C93-C92-C91	120.9(4)	C106-C107-C102	121.0(3)
C79-C78-C77	121.0(3)	C92-C93-C88	117.6(3)	F9-C108-F7	106.6(3)
C80-C79-C78	120.5(3)	C92-C93-C97	120.0(4)	F9-C108-F8	105.8(3)
C79-C80-C81	121.1(3)	C88-C93-C97	122.4(3)	F7-C108-F8	105.2(3)
C80-C81-C76	116.9(3)	C95-C94-C89	110.8(3)	F9-C108-C105	113.5(3)
C80-C81-C85	120.9(3)	C95-C94-C96	111.4(3)	F7-C108-C105	113.0(3)
C76-C81-C85	122.2(3)	C89-C94-C96	110.2(3)	F8-C108-C105	112.1(3)

Table S12. Torsion angles (°) for **3a-II**.

C2-N2-C1-N1	-0.8(4)	C17-C18-C19-C20	-0.8(6)
C16-N2-C1-N1	-175.9(3)	C18-C19-C20-C21	1.1(6)
C2-N2-C1-Au1	174.1(3)	C19-C20-C21-C16	-0.4(5)
C16-N2-C1-Au1	-1.0(5)	C19-C20-C21-C25	-179.3(3)
C3-N1-C1-N2	0.5(4)	C17-C16-C21-C20	-0.8(5)
C4-N1-C1-N2	174.5(3)	N2-C16-C21-C20	175.2(3)
C3-N1-C1-Au1	-174.4(3)	C17-C16-C21-C25	178.1(3)
C4-N1-C1-Au1	-0.5(5)	N2-C16-C21-C25	-5.8(5)
C1-N2-C2-C3	0.7(4)	C18-C17-C22-C23	-38.4(5)
C16-N2-C2-C3	176.0(3)	C16-C17-C22-C23	142.9(3)
N2-C2-C3-N1	-0.3(4)	C18-C17-C22-C24	84.4(4)
C1-N1-C3-C2	-0.1(4)	C16-C17-C22-C24	-94.3(4)
C4-N1-C3-C2	-174.2(3)	C20-C21-C25-C26	70.3(4)
C1-N1-C4-C5	103.1(4)	C16-C21-C25-C26	-108.6(4)
C3-N1-C4-C5	-83.7(4)	C20-C21-C25-C27	-52.8(5)
C1-N1-C4-C9	-79.2(4)	C16-C21-C25-C27	128.3(4)
C3-N1-C4-C9	94.0(4)	C35-C30-C31-C32	-0.29(19)
C9-C4-C5-C6	-0.9(5)	C29-C30-C31-C32	179.6(3)
N1-C4-C5-C6	176.6(3)	C30-C31-C32-C33	0.1(2)
C9-C4-C5-C10	179.0(3)	C31-C32-C33-C34	-0.2(5)
N1-C4-C5-C10	-3.5(5)	C31-C32-C33-C36	179.5(5)
C4-C5-C6-C7	0.2(5)	C32-C33-C34-C35	0.5(6)
C10-C5-C6-C7	-179.7(3)	C36-C33-C34-C35	-179.1(5)
C5-C6-C7-C8	0.4(6)	C33-C34-C35-C30	-0.7(5)
C6-C7-C8-C9	-0.4(6)	C31-C30-C35-C34	0.6(4)
C7-C8-C9-C4	-0.3(5)	C29-C30-C35-C34	-179.3(3)
C7-C8-C9-C13	-179.3(3)	C32-C33-C36-F1	5.4(7)
C5-C4-C9-C8	1.0(5)	C34-C33-C36-F1	-174.9(4)
N1-C4-C9-C8	-176.6(3)	C32-C33-C36-F3	-116.2(5)
C5-C4-C9-C13	179.9(3)	C34-C33-C36-F3	63.4(6)
N1-C4-C9-C13	2.4(5)	C32-C33-C36-F2	125.9(5)
C6-C5-C10-C12	-77.9(5)	C34-C33-C36-F2	-54.4(7)
C4-C5-C10-C12	102.2(4)	C35A-C30-C31A-C32A	0.0(2)
C6-C5-C10-C11	45.4(5)	C29-C30-C31A-C32A	179.8(4)
C4-C5-C10-C11	-134.5(4)	C30-C31A-C32A-C33A	-10(3)
C8-C9-C13-C15	62.9(5)	C31A-C32A-C33A-C34A	19(5)
C4-C9-C13-C15	-116.0(4)	C31A-C32A-C33A-C36A	-175(3)
C8-C9-C13-C14	-59.7(4)	C32A-C33A-C34A-C35A	-21(6)
C4-C9-C13-C14	121.4(4)	C36A-C33A-C34A-C35A	176(4)

C1-N2-C16-C17	-95.6(4)	C33A-C34A-C35A-C30	12(4)
C2-N2-C16-C17	89.7(4)	C31A-C30-C35A-C34A	-0.1(5)
C1-N2-C16-C21	88.1(4)	C29-C30-C35A-C34A	-179.9(5)
C2-N2-C16-C21	-86.6(4)	C32A-C33A-C36A-F1A	11(6)
C21-C16-C17-C18	1.2(5)	C34A-C33A-C36A-F1A	174(5)
N2-C16-C17-C18	-174.9(3)	C32A-C33A-C36A-F3A	-110(4)
C21-C16-C17-C22	179.9(3)	C34A-C33A-C36A-F3A	52(7)
N2-C16-C17-C22	3.9(5)	C32A-C33A-C36A-F2A	131(4)
C16-C17-C18-C19	-0.4(5)	C34A-C33A-C36A-F2A	-66(7)
C22-C17-C18-C19	-179.1(3)		
C38-N4-C37-N3	1.5(4)	N4-C52-C53-C58	7.9(5)
C52-N4-C37-N3	-175.3(3)	C52-C53-C54-C55	-0.4(5)
C38-N4-C37-Au2	-169.6(3)	C58-C53-C54-C55	176.1(3)
C52-N4-C37-Au2	13.5(5)	C53-C54-C55-C56	-1.3(6)
C39-N3-C37-N4	-1.5(4)	C54-C55-C56-C57	1.6(6)
C40-N3-C37-N4	173.7(3)	C55-C56-C57-C52	-0.2(6)
C39-N3-C37-Au2	170.2(3)	C55-C56-C57-C61	-179.6(4)
C40-N3-C37-Au2	-14.7(5)	C53-C52-C57-C56	-1.6(5)
C37-N4-C38-C39	-1.0(4)	N4-C52-C57-C56	176.1(3)
C52-N4-C38-C39	175.9(3)	C53-C52-C57-C61	177.8(3)
N4-C38-C39-N3	0.1(4)	N4-C52-C57-C61	-4.5(5)
C37-N3-C39-C38	0.9(5)	C52-C53-C58-C60A	-114(2)
C40-N3-C39-C38	-174.2(3)	C54-C53-C58-C60A	70(2)
C37-N3-C40-C41	88.6(4)	C52-C53-C58-C59A	119(3)
C39-N3-C40-C41	-97.0(4)	C54-C53-C58-C59A	-57(3)
C37-N3-C40-C45	-91.3(4)	C52-C53-C58-C60	-134.4(8)
C39-N3-C40-C45	83.2(4)	C54-C53-C58-C60	49.3(8)
C45-C40-C41-C42	-1.8(5)	C52-C53-C58-C59	100.7(8)
N3-C40-C41-C42	178.3(3)	C54-C53-C58-C59	-75.6(8)
C45-C40-C41-C46	179.0(3)	C56-C57-C61-C62	76.7(7)
N3-C40-C41-C46	-0.8(5)	C52-C57-C61-C62	-102.7(6)
C40-C41-C42-C43	0.5(5)	C56-C57-C61-C63A	-84.7(7)
C46-C41-C42-C43	179.7(3)	C52-C57-C61-C63A	95.9(7)
C41-C42-C43-C44	0.7(6)	C56-C57-C61-C63	-55.7(7)
C42-C43-C44-C45	-0.7(6)	C52-C57-C61-C63	124.9(6)
C43-C44-C45-C40	-0.5(6)	C56-C57-C61-C62A	31.0(6)
C43-C44-C45-C49	177.0(4)	C52-C57-C61-C62A	-148.4(5)
C41-C40-C45-C44	1.8(5)	C71-C66-C67-C68	-1.0(6)
N3-C40-C45-C44	-178.3(3)	C65-C66-C67-C68	178.4(4)
C41-C40-C45-C49	-175.7(3)	C66-C67-C68-C69	0.6(6)

N3-C40-C45-C49	4.1(5)	C67-C68-C69-C70	0.1(6)
C42-C41-C46-C48	-67.2(5)	C67-C68-C69-C72	179.6(4)
C40-C41-C46-C48	111.9(4)	C68-C69-C70-C71	-0.4(6)
C42-C41-C46-C47	56.7(4)	C72-C69-C70-C71	-179.9(4)
C40-C41-C46-C47	-124.1(4)	C69-C70-C71-C66	0.0(6)
C44-C45-C49-C50	-70.3(6)	C67-C66-C71-C70	0.7(6)
C40-C45-C49-C50	107.2(6)	C65-C66-C71-C70	-178.7(4)
C44-C45-C49-C51	54.0(6)	C70-C69-C72-F4A	-138(2)
C40-C45-C49-C51	-128.5(5)	C68-C69-C72-F4A	42(2)
C44-C45-C49-C51A	71(3)	C70-C69-C72-F5	94.8(6)
C40-C45-C49-C51A	-112(3)	C68-C69-C72-F5	-84.7(6)
C44-C45-C49-C50A	-43(3)	C70-C69-C72-F6	-28.5(7)
C40-C45-C49-C50A	135(3)	C68-C69-C72-F6	152.0(6)
C37-N4-C52-C53	-98.1(4)	C70-C69-C72-F4	-146.2(6)
C38-N4-C52-C53	85.4(4)	C68-C69-C72-F4	34.3(6)
C37-N4-C52-C57	84.1(4)	C70-C69-C72-F6A	-3.0(15)
C38-N4-C52-C57	-92.4(4)	C68-C69-C72-F6A	177.5(14)
C57-C52-C53-C54	1.9(5)	C70-C69-C72-F5A	103.5(17)
N4-C52-C53-C54	-175.8(3)	C68-C69-C72-F5A	-76.0(17)
C57-C52-C53-C58	-174.5(3)		
C74-N6-C73-N5	1.6(4)	C73-N6-C88-C93	93.1(4)
C88-N6-C73-N5	-175.7(3)	C74-N6-C88-C93	-83.8(5)
C74-N6-C73-Au3	-169.1(3)	C93-C88-C89-C90	0.5(5)
C88-N6-C73-Au3	13.7(5)	N6-C88-C89-C90	-178.4(3)
C75-N5-C73-N6	-2.0(4)	C93-C88-C89-C94	-179.5(3)
C76-N5-C73-N6	-179.6(3)	N6-C88-C89-C94	1.5(5)
C75-N5-C73-Au3	168.5(3)	C88-C89-C90-C91	0.1(6)
C76-N5-C73-Au3	-9.0(5)	C94-C89-C90-C91	-179.8(4)
C73-N6-C74-C75	-0.6(5)	C89-C90-C91-C92	-0.5(6)
C88-N6-C74-C75	176.7(3)	C90-C91-C92-C93	0.2(6)
N6-C74-C75-N5	-0.7(5)	C91-C92-C93-C88	0.5(6)
C73-N5-C75-C74	1.7(5)	C91-C92-C93-C97	-178.0(4)
C76-N5-C75-C74	179.4(3)	C89-C88-C93-C92	-0.8(5)
C73-N5-C76-C77	95.8(4)	N6-C88-C93-C92	178.2(3)
C75-N5-C76-C77	-81.5(4)	C89-C88-C93-C97	177.6(3)
C73-N5-C76-C81	-86.4(4)	N6-C88-C93-C97	-3.4(5)
C75-N5-C76-C81	96.3(4)	C90-C89-C94-C95	-61.3(5)
C81-C76-C77-C78	-2.6(5)	C88-C89-C94-C95	118.7(4)
N5-C76-C77-C78	175.1(3)	C90-C89-C94-C96	62.4(5)
C81-C76-C77-C82	174.4(3)	C88-C89-C94-C96	-117.5(4)

N5-C76-C77-C82	-7.9(5)	C92-C93-C97-C98	75.9(10)
C76-C77-C78-C79	0.5(5)	C88-C93-C97-C98	-102.5(10)
C82-C77-C78-C79	-176.6(3)	C92-C93-C97-C99	-54.4(10)
C77-C78-C79-C80	1.8(6)	C88-C93-C97-C99	127.2(10)
C78-C79-C80-C81	-2.2(6)	C92-C93-C97-C99A	-69.9(13)
C79-C80-C81-C76	0.2(5)	C88-C93-C97-C99A	111.7(13)
C79-C80-C81-C85	-179.5(3)	C92-C93-C97-C98A	46.1(10)
C77-C76-C81-C80	2.2(5)	C88-C93-C97-C98A	-132.3(10)
N5-C76-C81-C80	-175.5(3)	C107-C102-C103-C104	0.9(5)
C77-C76-C81-C85	-178.0(3)	C101-C102-C103-C104	-178.3(3)
N5-C76-C81-C85	4.3(5)	C102-C103-C104-C105	-0.3(6)
C78-C77-C82-C84	-62(2)	C103-C104-C105-C106	0.0(5)
C76-C77-C82-C84	121(2)	C103-C104-C105-C108	-179.7(3)
C78-C77-C82-C84A	-50.9(13)	C104-C105-C106-C107	-0.4(5)
C76-C77-C82-C84A	132.2(13)	C108-C105-C106-C107	179.3(3)
C78-C77-C82-C83	61(2)	C105-C106-C107-C102	1.0(5)
C76-C77-C82-C83	-116(2)	C103-C102-C107-C106	-1.3(5)
C78-C77-C82-C83A	74.2(14)	C101-C102-C107-C106	177.9(3)
C76-C77-C82-C83A	-102.7(14)	C104-C105-C108-F9	-19.7(5)
C80-C81-C85-C87	97.0(4)	C106-C105-C108-F9	160.6(3)
C76-C81-C85-C87	-82.8(4)	C104-C105-C108-F7	-141.2(3)
C80-C81-C85-C86	-25.3(5)	C106-C105-C108-F7	39.1(4)
C76-C81-C85-C86	154.9(3)	C104-C105-C108-F8	100.1(4)
C73-N6-C88-C89	-87.9(4)	C106-C105-C108-F8	-79.6(4)
C74-N6-C88-C89	95.2(4)		

The crystal structure of **3b**

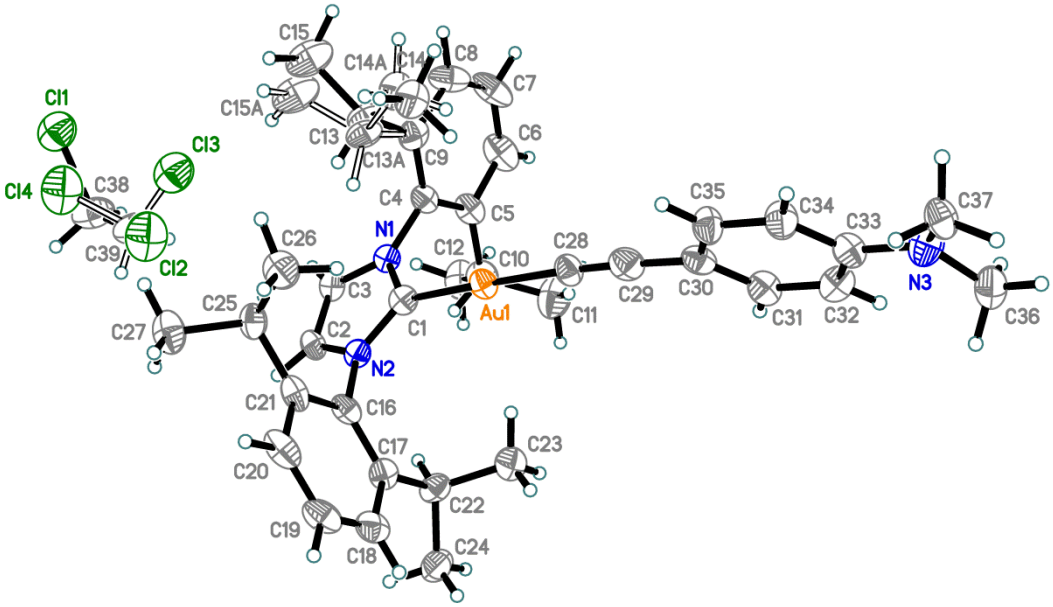

Figure S60. The crystal structure of **3b**. Thermal ellipsoids are shown at a 50% probability level. Hydrogen atoms are drawn as fixed-size spheres. The disorder ratios are 0.62(3) : 0.38(3) for atoms C13..C15 / C13A..C15A of the *iso*-propyl group and 0.557(4) : 0.443(4) for a non-coordinating dichloromethane molecule. Minor components of the disorders are drawn with open solid lines.

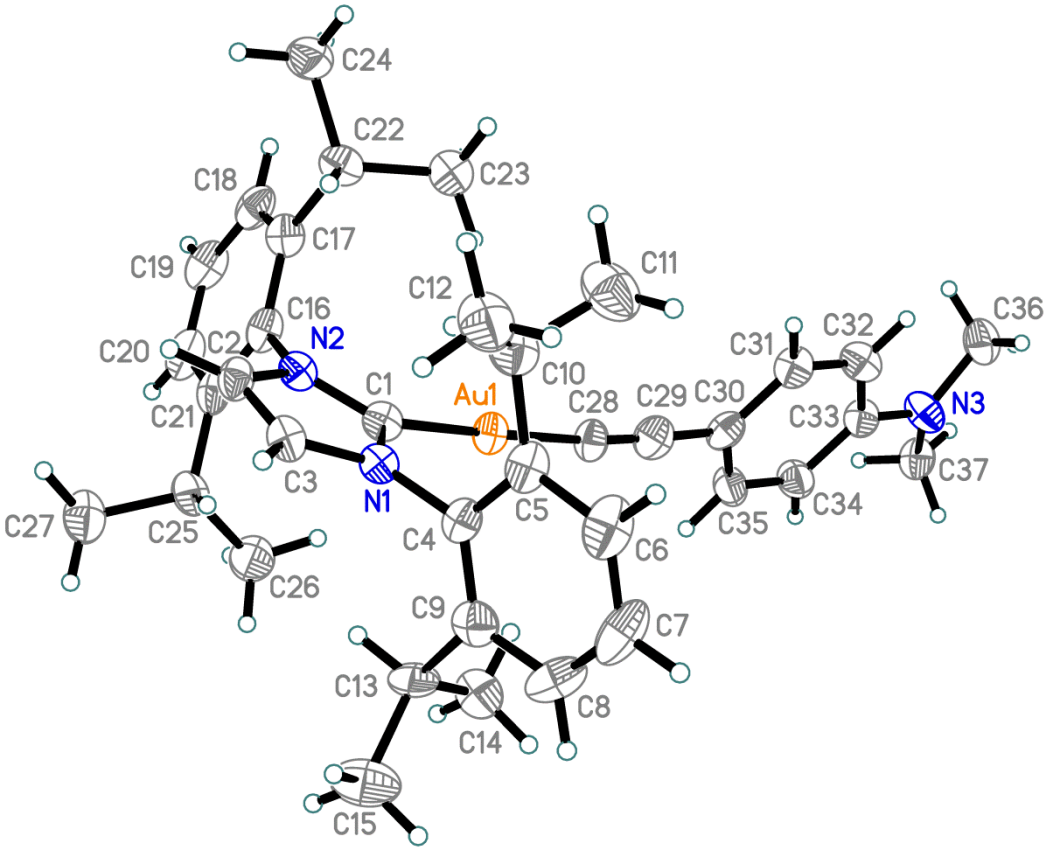

Figure S61. The structure of complex **3b**. Thermal ellipsoids are shown at a 50% probability level. Hydrogen atoms are drawn as fixed-size spheres. Disorder is omitted.

Table S13. Selected bond lengths (Å) for **3b**.

Au1-C1	2.017(8)	C6-C7	1.365(15)	C19-C20	1.383(14)
Au1-C28	2.004(8)	C7-C8	1.369(15)	C20-C21	1.406(12)
N1-C1	1.370(11)	C8-C9	1.411(13)	C21-C25	1.507(13)
N1-C3	1.390(10)	C9-C13	1.528(14)	C22-C23	1.535(13)
N1-C4	1.443(10)	C9-C13A	1.528(14)	C22-C24	1.536(13)
N2-C1	1.334(10)	C10-C11	1.521(14)	C25-C27	1.523(12)
N2-C2	1.379(11)	C10-C12	1.540(13)	C25-C26	1.529(13)
N2-C16	1.476(10)	C13-C14	1.570(15)	C28-C29	1.193(12)
N3-C33	1.373(11)	C13-C15	1.571(15)	C29-C30	1.453(13)
N3-C36	1.425(13)	C13A-C14A	1.53(3)	C30-C35	1.391(12)
N3-C37	1.466(12)	C13A-C15A	1.53(3)	C30-C31	1.394(13)
C2-C3	1.352(12)	C16-C17	1.391(12)	C31-C32	1.378(13)
C4-C9	1.397(12)	C16-C21	1.401(12)	C32-C33	1.405(12)
C4-C5	1.398(12)	C17-C18	1.396(12)	C33-C34	1.399(13)
C5-C6	1.399(13)	C17-C22	1.535(12)	C34-C35	1.371(13)
C5-C10	1.508(13)	C18-C19	1.380(14)		

Table S14. Selected bond angles (°) for **3b**.

C28-Au1-C1	178.3(3)	C7-C8-C9	120.9(9)	C19-C20-C21	120.9(9)
C1-N1-C3	111.1(7)	C4-C9-C8	116.3(9)	C16-C21-C20	116.6(9)
C1-N1-C4	125.5(7)	C4-C9-C13	126.7(12)	C16-C21-C25	122.5(8)
C3-N1-C4	123.2(7)	C8-C9-C13	117.0(12)	C20-C21-C25	120.9(8)
C1-N2-C2	112.3(7)	C4-C9-C13A	115.1(16)	C23-C22-C17	111.6(7)
C1-N2-C16	123.8(7)	C8-C9-C13A	128.6(17)	C23-C22-C24	108.7(8)
C2-N2-C16	123.0(7)	C5-C10-C11	110.0(8)	C17-C22-C24	113.0(8)
C33-N3-C36	120.7(8)	C5-C10-C12	112.8(8)	C21-C25-C27	112.7(8)
C33-N3-C37	120.7(7)	C11-C10-C12	111.8(8)	C21-C25-C26	110.2(8)
C36-N3-C37	115.5(8)	C9-C13-C14	110.0(18)	C27-C25-C26	110.9(7)
N2-C1-N1	104.0(7)	C9-C13-C15	112.7(14)	C29-C28-Au1	172.6(8)
N2-C1-Au1	129.0(6)	C14-C13-C15	113.1(16)	C28-C29-C30	177.5(10)
N1-C1-Au1	127.0(6)	C14A-C13A-C15A	104(3)	C35-C30-C31	116.6(8)
C3-C2-N2	106.8(8)	C14A-C13A-C9	111(3)	C35-C30-C29	122.8(8)
C2-C3-N1	105.9(7)	C15A-C13A-C9	111(3)	C31-C30-C29	120.6(8)
C9-C4-C5	123.7(8)	C17-C16-C21	123.8(8)	C32-C31-C30	122.0(8)
C9-C4-N1	119.1(8)	C17-C16-N2	120.1(7)	C31-C32-C33	121.1(9)
C5-C4-N1	117.2(7)	C21-C16-N2	116.1(8)	N3-C33-C34	122.3(8)
C4-C5-C6	116.5(9)	C16-C17-C18	116.9(8)	N3-C33-C32	121.0(8)

C4-C5-C10	122.3(8)	C16-C17-C22	122.5(7)	C34-C33-C32	116.6(8)
C6-C5-C10	121.2(8)	C18-C17-C22	120.6(8)	C35-C34-C33	121.6(9)
C7-C6-C5	121.2(9)	C19-C18-C17	121.3(9)	C34-C35-C30	122.1(9)
C6-C7-C8	121.2(9)	C18-C19-C20	120.5(8)		

Table S15. Torsion angles (°) for **3b**.

C2-N2-C1-N1	-1.2(9)	C8-C9-C13A-C14A	-46(4)
C16-N2-C1-N1	-170.1(7)	C4-C9-C13A-C15A	-113(3)
C2-N2-C1-Au1	-179.8(6)	C8-C9-C13A-C15A	69(4)
C16-N2-C1-Au1	11.4(12)	C1-N2-C16-C17	-94.2(10)
C3-N1-C1-N2	1.2(9)	C2-N2-C16-C17	98.1(10)
C4-N1-C1-N2	-173.8(7)	C1-N2-C16-C21	86.2(10)
C3-N1-C1-Au1	179.8(6)	C2-N2-C16-C21	-81.5(10)
C4-N1-C1-Au1	4.8(12)	C21-C16-C17-C18	-2.3(13)
C1-N2-C2-C3	0.8(10)	N2-C16-C17-C18	178.2(7)
C16-N2-C2-C3	169.8(7)	C21-C16-C17-C22	178.6(8)
N2-C2-C3-N1	0.0(9)	N2-C16-C17-C22	-0.9(12)
C1-N1-C3-C2	-0.7(9)	C16-C17-C18-C19	2.2(13)
C4-N1-C3-C2	174.4(7)	C22-C17-C18-C19	-178.7(8)
C1-N1-C4-C9	-81.8(11)	C17-C18-C19-C20	-0.7(13)
C3-N1-C4-C9	103.7(9)	C18-C19-C20-C21	-0.9(14)
C1-N1-C4-C5	98.5(9)	C17-C16-C21-C20	0.8(12)
C3-N1-C4-C5	-76.0(10)	N2-C16-C21-C20	-179.7(7)
C9-C4-C5-C6	-3.8(13)	C17-C16-C21-C25	-179.0(8)
N1-C4-C5-C6	175.9(8)	N2-C16-C21-C25	0.6(12)
C9-C4-C5-C10	177.0(8)	C19-C20-C21-C16	0.9(12)
N1-C4-C5-C10	-3.3(12)	C19-C20-C21-C25	-179.3(8)
C4-C5-C6-C7	3.0(14)	C16-C17-C22-C23	89.3(10)
C10-C5-C6-C7	-177.8(9)	C18-C17-C22-C23	-89.8(10)
C5-C6-C7-C8	-1.6(16)	C16-C17-C22-C24	-147.8(8)
C6-C7-C8-C9	0.8(16)	C18-C17-C22-C24	33.2(11)
C5-C4-C9-C8	3.1(13)	C16-C21-C25-C27	128.1(9)
N1-C4-C9-C8	-176.6(8)	C20-C21-C25-C27	-51.7(11)
C5-C4-C9-C13	-176.6(13)	C16-C21-C25-C26	-107.5(9)
N1-C4-C9-C13	3.7(16)	C20-C21-C25-C26	72.8(10)
C5-C4-C9-C13A	-175(2)	C35-C30-C31-C32	-0.4(13)
N1-C4-C9-C13A	6(2)	C29-C30-C31-C32	178.1(8)
C7-C8-C9-C4	-1.5(13)	C30-C31-C32-C33	1.2(14)
C7-C8-C9-C13	178.3(12)	C36-N3-C33-C34	169.8(9)

C7-C8-C9-C13A	176(2)	C37-N3-C33-C34	10.5(14)
C4-C5-C10-C11	-116.9(10)	C36-N3-C33-C32	-11.8(14)
C6-C5-C10-C11	63.9(12)	C37-N3-C33-C32	-171.1(9)
C4-C5-C10-C12	117.5(9)	C31-C32-C33-N3	-179.9(9)
C6-C5-C10-C12	-61.6(12)	C31-C32-C33-C34	-1.5(13)
C4-C9-C13-C14	107.6(16)	N3-C33-C34-C35	179.5(9)
C8-C9-C13-C14	-72.1(16)	C32-C33-C34-C35	1.0(14)
C4-C9-C13-C15	-125.2(15)	C33-C34-C35-C30	-0.2(15)
C8-C9-C13-C15	55.1(19)	C31-C30-C35-C34	-0.1(14)
C4-C9-C13A-C14A	131(2)	C29-C30-C35-C34	-178.5(9)

The crystal structure of **3c**

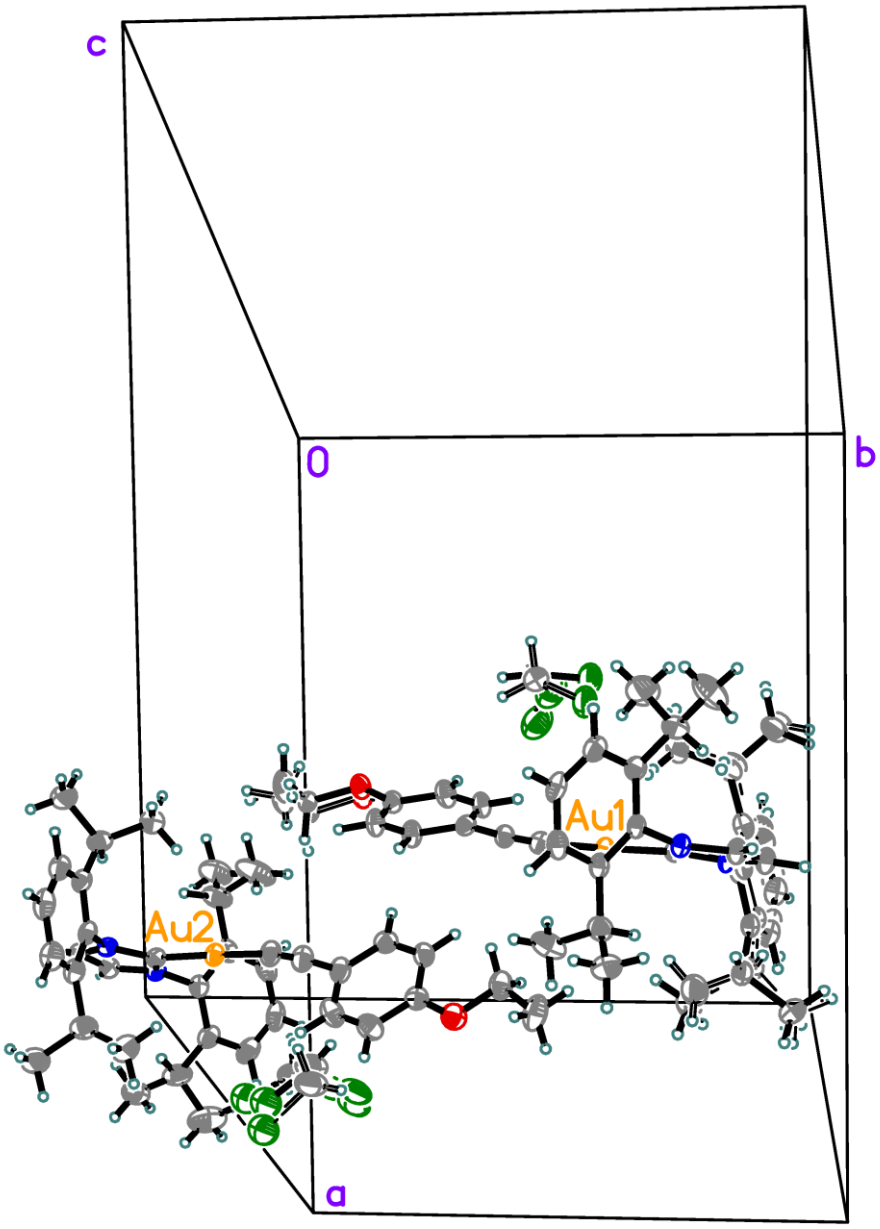

Figure S62. The crystal structure of **3c**. Two crystallographically inequivalent molecules are shown in the unit cell. Thermal ellipsoids are shown at a 50% probability level. Hydrogen atoms are drawn as fixed-size spheres. The site occupancies of the disordered dichloromethane molecules are 0.973(3) : 0.027(3) for the upper molecule and 0.625(6) : 0.161(3) : 0.052(4) for the lower molecule.

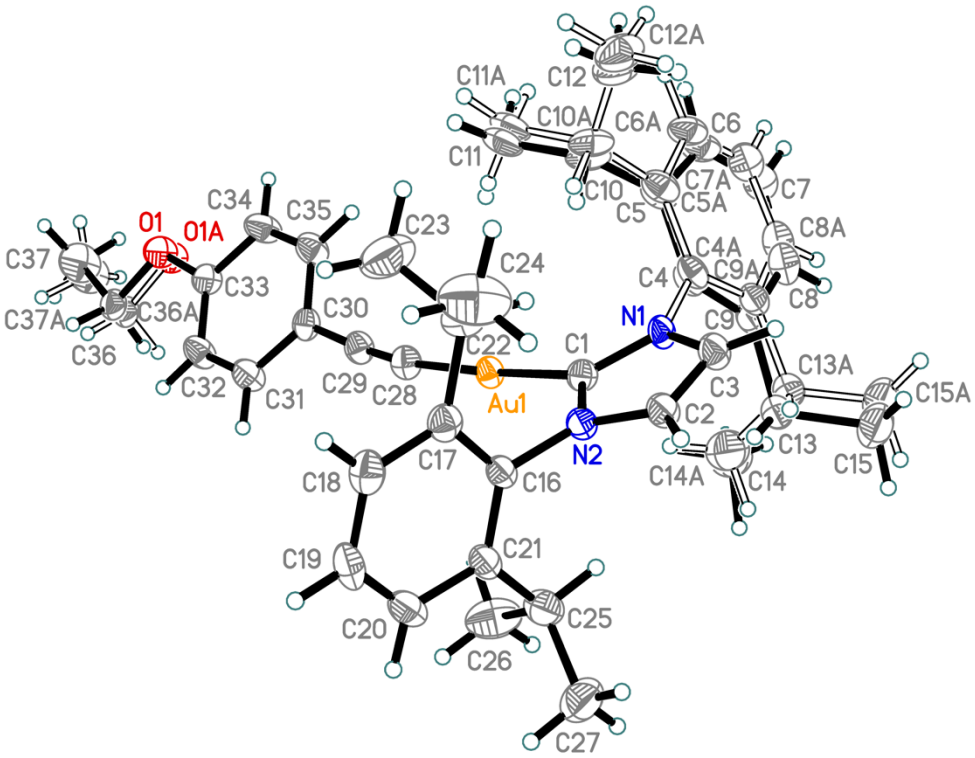

Figure S63. The 1st molecule of **3c**. Thermal ellipsoids are shown at a 50% probability level. Hydrogen atoms are drawn as fixed-size spheres. The disorder ratio for 2,6-di-isopropylphenyl atoms C4..C15 / C4A..C15A is 0.556(12) : 0.444(12). The disorder ratio for the OEt fragment (atoms O1, C36, C37 / O1A, C36A, C37A) is 0.61(6) : 0.39(6). The minor components of the disorder are drawn with open solid lines.

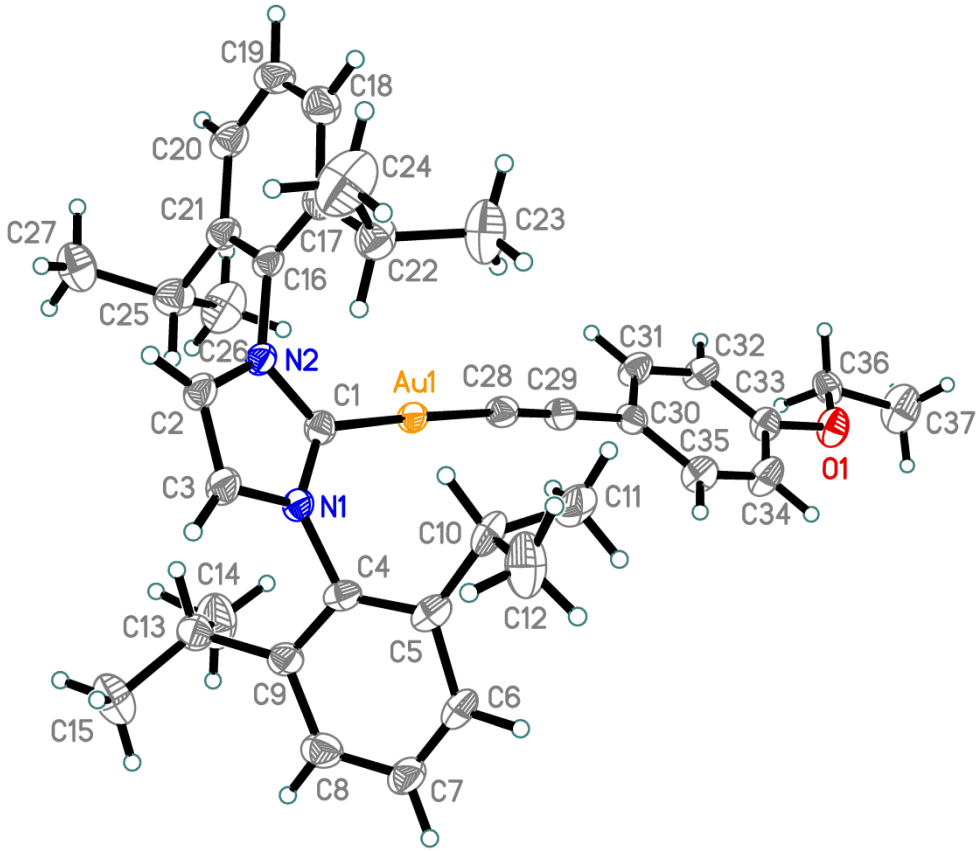

Figure S64. The 1st molecule of **3c**. Thermal ellipsoids are shown at a 50% probability level. Hydrogen atoms are drawn as fixed-size spheres. Disorder is omitted.

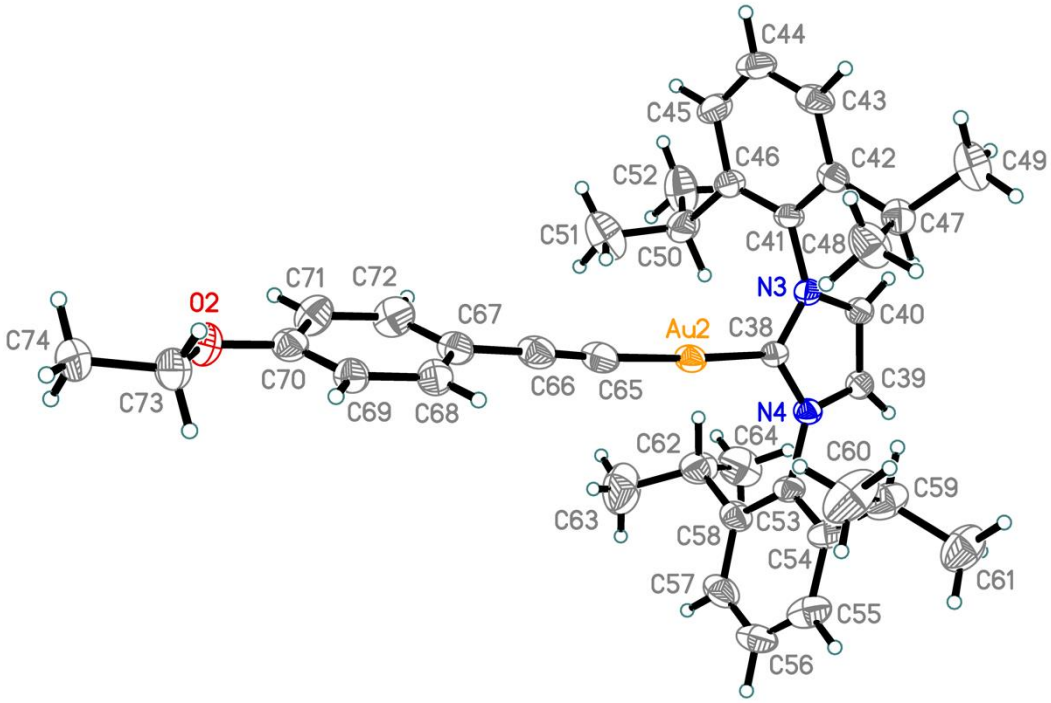

Figure S65. The 2nd molecule of **3c**. Thermal ellipsoids are shown at a 50% probability level. Hydrogen atoms are drawn as fixed-size spheres.

Table S16. Selected bond lengths (Å) for **3c**.

Au1-C1	2.012(3)	C13-C15	1.529(4)	C20-C21	1.406(5)
Au1-C28	1.978(3)	C13-C14	1.530(4)	C21-C25	1.518(5)
N1-C1	1.355(4)	C4A-C5A	1.402(3)	C22-C24	1.513(6)
N1-C3	1.393(4)	C4A-C9A	1.402(4)	C22-C23	1.527(6)
N1-C4A	1.450(4)	C5A-C6A	1.411(4)	C25-C26	1.528(6)
N1-C4	1.451(4)	C5A-C10A	1.515(4)	C25-C27	1.532(6)
C1-N2	1.369(4)	C6A-C7A	1.373(4)	C28-C29	1.219(4)
N2-C2	1.377(4)	C7A-C8A	1.372(4)	C29-C30	1.445(4)
N2-C16	1.443(4)	C8A-C9A	1.410(4)	C30-C31	1.387(5)
C2-C3	1.352(5)	C9A-C13A	1.514(4)	C30-C35	1.404(5)
C4-C5	1.402(3)	C10A-C12A	1.530(4)	C31-C32	1.394(5)
C4-C9	1.403(3)	C10A-C11A	1.532(4)	C32-C33	1.379(5)
C5-C6	1.411(4)	C13A-C15A	1.529(4)	C33-O1	1.374(5)
C5-C10	1.516(4)	C13A-C14A	1.530(4)	C33-O1A	1.374(5)
C6-C7	1.374(4)	C16-C21	1.391(4)	C33-C34	1.393(5)
C7-C8	1.373(4)	C16-C17	1.400(4)	C34-C35	1.379(5)
C8-C9	1.411(4)	C17-C18	1.390(5)	O1-C36	1.431(5)
C9-C13	1.514(4)	C17-C22	1.522(5)	C36-C37	1.511(6)
C10-C12	1.530(4)	C18-C19	1.392(5)	O1A-C36A	1.431(5)
C10-C11	1.532(4)	C19-C20	1.381(5)	C36A-C37A	1.511(6)

Au2-C38	2.014(3)	C45-C46	1.397(5)	C59-C60	1.547(7)
Au2-C65	1.984(4)	C46-C50	1.526(5)	C62-C63	1.531(7)
N3-C38	1.357(4)	C47-C49	1.527(6)	C62-C64	1.535(8)
N3-C40	1.386(4)	C47-C48	1.530(6)	C65-C66	1.213(5)
N3-C41	1.436(4)	C50-C51	1.519(7)	C66-C67	1.447(5)
C38-N4	1.363(4)	C50-C52	1.534(7)	C67-C68	1.385(5)
N4-C39	1.387(4)	C53-C54	1.395(5)	C67-C72	1.410(6)
N4-C53	1.442(4)	C53-C58	1.404(5)	C68-C69	1.392(5)
C39-C40	1.352(5)	C54-C55	1.402(6)	C69-C70	1.390(5)
C41-C46	1.397(5)	C54-C59	1.506(6)	C70-O2	1.376(5)
C41-C42	1.400(5)	C55-C56	1.370(7)	C70-C71	1.390(5)
C42-C43	1.392(5)	C56-C57	1.376(7)	C71-C72	1.384(6)
C42-C47	1.518(5)	C57-C58	1.396(5)	O2-C73	1.426(5)
C43-C44	1.376(6)	C58-C62	1.517(6)	C73-C74	1.515(6)
C44-C45	1.387(6)	C59-C61	1.535(6)		

Table S17. Selected bond angles (°) for **3c**.

C28-Au1-C1	176.85(13)	C8A-C9A-C13A	122.9(11)
C1-N1-C3	111.6(3)	C5A-C10A-C12A	116(3)
C1-N1-C4A	127.2(5)	C5A-C10A-C11A	109(2)
C3-N1-C4A	121.2(5)	C12A-C10A-C11A	109.3(11)
C1-N1-C4	122.1(4)	C9A-C13A-C15A	114.7(10)
C3-N1-C4	126.2(4)	C9A-C13A-C14A	110.4(14)
N1-C1-N2	103.6(3)	C15A-C13A-C14A	111.4(10)
N1-C1-Au1	128.3(2)	C21-C16-C17	124.3(3)
N2-C1-Au1	128.0(2)	C21-C16-N2	119.6(3)
C1-N2-C2	111.7(3)	C17-C16-N2	116.0(3)
C1-N2-C16	124.2(3)	C18-C17-C16	116.8(3)
C2-N2-C16	123.4(3)	C18-C17-C22	121.1(3)
C3-C2-N2	106.8(3)	C16-C17-C22	122.1(3)
C2-C3-N1	106.3(3)	C17-C18-C19	120.7(3)
C5-C4-C9	127.8(8)	C20-C19-C18	120.9(3)
C5-C4-N1	116.7(9)	C19-C20-C21	120.5(3)
C9-C4-N1	114.7(9)	C16-C21-C20	116.7(3)
C4-C5-C6	111.7(10)	C16-C21-C25	123.1(3)
C4-C5-C10	121.8(12)	C20-C21-C25	120.2(3)
C6-C5-C10	126.4(13)	C24-C22-C17	111.9(3)
C7-C6-C5	124.8(11)	C24-C22-C23	112.0(4)
C8-C7-C6	119.3(11)	C17-C22-C23	110.4(4)

C7-C8-C9	122.0(11)	C21-C25-C26	111.8(3)
C4-C9-C8	114.4(8)	C21-C25-C27	111.2(3)
C4-C9-C13	123.5(10)	C26-C25-C27	110.9(3)
C8-C9-C13	122.1(8)	C29-C28-Au1	172.7(3)
C5-C10-C12	111(2)	C28-C29-C30	175.5(4)
C5-C10-C11	112.0(16)	C31-C30-C35	117.1(3)
C12-C10-C11	108.5(9)	C31-C30-C29	121.8(3)
C9-C13-C15	113.2(7)	C35-C30-C29	121.1(3)
C9-C13-C14	107.9(11)	C30-C31-C32	122.0(3)
C15-C13-C14	113.4(8)	C33-C32-C31	119.7(3)
C5A-C4A-C9A	118.2(10)	O1-C33-C32	124.1(9)
C5A-C4A-N1	121.2(11)	O1A-C33-C32	124.0(14)
C9A-C4A-N1	120.6(12)	O1-C33-C34	116.3(9)
C4A-C5A-C6A	123.0(14)	O1A-C33-C34	115.8(15)
C4A-C5A-C10A	125.9(15)	C32-C33-C34	119.5(3)
C6A-C5A-C10A	111.2(16)	C35-C34-C33	120.3(3)
C7A-C6A-C5A	117.0(15)	C34-C35-C30	121.3(3)
C8A-C7A-C6A	121.7(15)	C33-O1-C36	117.7(14)
C7A-C8A-C9A	121.6(14)	O1-C36-C37	106.4(19)
C4A-C9A-C8A	118.5(10)	C33-O1A-C36A	117(2)
C4A-C9A-C13A	118.7(13)	O1A-C36A-C37A	108(3)
C65-Au2-C38	176.40(15)	C54-C53-N4	118.8(3)
C38-N3-C40	110.9(3)	C58-C53-N4	117.8(3)
C38-N3-C41	124.7(3)	C53-C54-C55	116.4(4)
C40-N3-C41	124.4(3)	C53-C54-C59	122.0(3)
N3-C38-N4	104.6(3)	C55-C54-C59	121.6(4)
N3-C38-Au2	126.8(2)	C56-C55-C54	121.3(4)
N4-C38-Au2	128.6(2)	C55-C56-C57	121.2(4)
C38-N4-C39	111.0(3)	C56-C57-C58	120.5(4)
C38-N4-C53	124.9(3)	C57-C58-C53	117.1(4)
C39-N4-C53	124.1(3)	C57-C58-C62	120.9(4)
C40-C39-N4	106.5(3)	C53-C58-C62	122.0(3)
C39-C40-N3	107.1(3)	C54-C59-C61	111.7(4)
C46-C41-C42	123.1(3)	C54-C59-C60	110.0(4)
C46-C41-N3	118.5(3)	C61-C59-C60	111.2(4)
C42-C41-N3	118.4(3)	C58-C62-C63	113.0(4)
C43-C42-C41	116.7(3)	C58-C62-C64	110.8(4)
C43-C42-C47	121.9(3)	C63-C62-C64	110.3(4)
C41-C42-C47	121.4(3)	C66-C65-Au2	171.1(4)
C44-C43-C42	122.2(4)	C65-C66-C67	174.8(4)

C43-C44-C45	119.7(3)	C68-C67-C72	118.2(4)
C44-C45-C46	121.0(4)	C68-C67-C66	122.3(4)
C45-C46-C41	117.3(4)	C72-C67-C66	119.5(4)
C45-C46-C50	119.7(3)	C67-C68-C69	121.1(4)
C41-C46-C50	122.9(3)	C70-C69-C68	120.1(3)
C42-C47-C49	113.3(4)	O2-C70-C69	124.5(3)
C42-C47-C48	110.7(3)	O2-C70-C71	115.8(3)
C49-C47-C48	109.0(3)	C69-C70-C71	119.6(4)
C51-C50-C46	110.2(4)	C72-C71-C70	120.1(4)
C51-C50-C52	109.9(4)	C71-C72-C67	120.8(4)
C46-C50-C52	112.4(4)	C70-O2-C73	117.7(3)
C54-C53-C58	123.5(3)	O2-C73-C74	107.6(4)

Table S18. Torsion angles (°) for **3c**.

C3-N1-C1-N2	0.7(3)	C5A-C4A-C9A-C13A	-179.3(3)
C4A-N1-C1-N2	-177.4(8)	N1-C4A-C9A-C13A	-0.2(11)
C4-N1-C1-N2	177.2(6)	C7A-C8A-C9A-C4A	0.7(6)
C3-N1-C1-Au1	-179.1(2)	C7A-C8A-C9A-C13A	179.5(4)
C4A-N1-C1-Au1	2.8(9)	C4A-C5A-C10A-C12A	122(2)
C4-N1-C1-Au1	-2.6(7)	C6A-C5A-C10A-C12A	-58(2)
N1-C1-N2-C2	-0.5(3)	C4A-C5A-C10A-C11A	-114.5(16)
Au1-C1-N2-C2	179.3(2)	C6A-C5A-C10A-C11A	65.0(16)
N1-C1-N2-C16	170.1(3)	C4A-C9A-C13A-C15A	-148.7(11)
Au1-C1-N2-C16	-10.1(4)	C8A-C9A-C13A-C15A	32.4(12)
C1-N2-C2-C3	0.2(4)	C4A-C9A-C13A-C14A	84.5(14)
C16-N2-C2-C3	-170.5(3)	C8A-C9A-C13A-C14A	-94.4(14)
N2-C2-C3-N1	0.3(4)	C1-N2-C16-C21	88.4(4)
C1-N1-C3-C2	-0.6(4)	C2-N2-C16-C21	-102.0(4)
C4A-N1-C3-C2	177.6(8)	C1-N2-C16-C17	-94.4(4)
C4-N1-C3-C2	-177.0(7)	C2-N2-C16-C17	75.2(4)
C1-N1-C4-C5	84.7(5)	C21-C16-C17-C18	1.9(5)
C3-N1-C4-C5	-99.3(6)	N2-C16-C17-C18	-175.2(3)
C1-N1-C4-C9	-104.6(5)	C21-C16-C17-C22	-177.3(3)
C3-N1-C4-C9	71.3(8)	N2-C16-C17-C22	5.6(4)
C9-C4-C5-C6	0.2(2)	C16-C17-C18-C19	-1.2(5)
N1-C4-C5-C6	169.5(7)	C22-C17-C18-C19	178.0(3)
C9-C4-C5-C10	179.7(3)	C17-C18-C19-C20	-0.7(5)
N1-C4-C5-C10	-11.0(7)	C18-C19-C20-C21	2.2(5)
C4-C5-C6-C7	-0.1(2)	C17-C16-C21-C20	-0.5(5)

C10-C5-C6-C7	-179.5(3)	N2-C16-C21-C20	176.5(3)
C5-C6-C7-C8	0.2(4)	C17-C16-C21-C25	178.4(3)
C6-C7-C8-C9	-0.6(6)	N2-C16-C21-C25	-4.7(5)
C5-C4-C9-C8	-0.6(4)	C19-C20-C21-C16	-1.5(5)
N1-C4-C9-C8	-170.0(8)	C19-C20-C21-C25	179.5(3)
C5-C4-C9-C13	-179.2(2)	C18-C17-C22-C24	56.4(5)
N1-C4-C9-C13	11.4(8)	C16-C17-C22-C24	-124.4(4)
C7-C8-C9-C4	0.7(5)	C18-C17-C22-C23	-69.0(5)
C7-C8-C9-C13	179.4(4)	C16-C17-C22-C23	110.2(4)
C4-C5-C10-C12	129.3(17)	C16-C21-C25-C26	-111.0(4)
C6-C5-C10-C12	-51.3(17)	C20-C21-C25-C26	67.9(4)
C4-C5-C10-C11	-109.2(12)	C16-C21-C25-C27	124.4(4)
C6-C5-C10-C11	70.2(12)	C20-C21-C25-C27	-56.7(5)
C4-C9-C13-C15	-131.2(9)	C35-C30-C31-C32	-0.3(5)
C8-C9-C13-C15	50.2(9)	C29-C30-C31-C32	178.7(3)
C4-C9-C13-C14	102.4(10)	C30-C31-C32-C33	-0.9(6)
C8-C9-C13-C14	-76.2(10)	C31-C32-C33-O1	-175.1(15)
C1-N1-C4A-C5A	74.9(8)	C31-C32-C33-O1A	172(2)
C3-N1-C4A-C5A	-103.0(6)	C31-C32-C33-C34	1.8(6)
C1-N1-C4A-C9A	-104.2(8)	O1-C33-C34-C35	175.7(14)
C3-N1-C4A-C9A	77.9(9)	O1A-C33-C34-C35	-172.3(18)
C9A-C4A-C5A-C6A	0.2(2)	C32-C33-C34-C35	-1.4(6)
N1-C4A-C5A-C6A	-178.9(10)	C33-C34-C35-C30	0.2(6)
C9A-C4A-C5A-C10A	179.6(3)	C31-C30-C35-C34	0.7(5)
N1-C4A-C5A-C10A	0.6(10)	C29-C30-C35-C34	-178.4(4)
C4A-C5A-C6A-C7A	-0.1(2)	C32-C33-O1-C36	-13(2)
C10A-C5A-C6A-C7A	-179.7(3)	C34-C33-O1-C36	170.2(12)
C5A-C6A-C7A-C8A	0.3(5)	C33-O1-C36-C37	-173(2)
C6A-C7A-C8A-C9A	-0.6(7)	C32-C33-O1A-C36A	-1(4)
C5A-C4A-C9A-C8A	-0.4(5)	C34-C33-O1A-C36A	169(2)
N1-C4A-C9A-C8A	178.7(10)	C33-O1A-C36A-C37A	174(3)
C40-N3-C38-N4	0.1(3)	C38-N4-C53-C54	-89.0(4)
C41-N3-C38-N4	177.8(3)	C39-N4-C53-C54	92.8(4)
C40-N3-C38-Au2	-179.7(2)	C38-N4-C53-C58	92.1(4)
C41-N3-C38-Au2	-2.0(5)	C39-N4-C53-C58	-86.1(4)
N3-C38-N4-C39	0.1(4)	C58-C53-C54-C55	2.0(5)
Au2-C38-N4-C39	179.9(2)	N4-C53-C54-C55	-176.8(3)
N3-C38-N4-C53	-178.3(3)	C58-C53-C54-C59	-177.4(4)
Au2-C38-N4-C53	1.5(5)	N4-C53-C54-C59	3.8(5)
C38-N4-C39-C40	-0.3(4)	C53-C54-C55-C56	-0.8(6)

C53-N4-C39-C40	178.1(3)	C59-C54-C55-C56	178.6(4)
N4-C39-C40-N3	0.3(4)	C54-C55-C56-C57	-0.6(6)
C38-N3-C40-C39	-0.3(4)	C55-C56-C57-C58	0.8(6)
C41-N3-C40-C39	-178.0(3)	C56-C57-C58-C53	0.4(6)
C38-N3-C41-C46	-84.6(4)	C56-C57-C58-C62	179.7(4)
C40-N3-C41-C46	92.8(4)	C54-C53-C58-C57	-1.8(5)
C38-N3-C41-C42	96.3(4)	N4-C53-C58-C57	177.0(3)
C40-N3-C41-C42	-86.3(4)	C54-C53-C58-C62	178.9(4)
C46-C41-C42-C43	-2.2(5)	N4-C53-C58-C62	-2.3(5)
N3-C41-C42-C43	176.8(3)	C53-C54-C59-C61	-130.8(4)
C46-C41-C42-C47	176.2(3)	C55-C54-C59-C61	49.8(6)
N3-C41-C42-C47	-4.8(5)	C53-C54-C59-C60	105.3(5)
C41-C42-C43-C44	0.5(5)	C55-C54-C59-C60	-74.1(5)
C47-C42-C43-C44	-177.8(4)	C57-C58-C62-C63	36.5(6)
C42-C43-C44-C45	1.0(6)	C53-C58-C62-C63	-144.2(4)
C43-C44-C45-C46	-0.9(6)	C57-C58-C62-C64	-87.9(5)
C44-C45-C46-C41	-0.7(6)	C53-C58-C62-C64	91.4(5)
C44-C45-C46-C50	177.6(4)	C72-C67-C68-C69	0.5(6)
C42-C41-C46-C45	2.3(5)	C66-C67-C68-C69	-177.5(4)
N3-C41-C46-C45	-176.7(3)	C67-C68-C69-C70	1.2(6)
C42-C41-C46-C50	-176.0(4)	C68-C69-C70-O2	176.5(3)
N3-C41-C46-C50	5.0(5)	C68-C69-C70-C71	-2.0(6)
C43-C42-C47-C49	-41.1(5)	O2-C70-C71-C72	-177.5(4)
C41-C42-C47-C49	140.7(4)	C69-C70-C71-C72	1.1(6)
C43-C42-C47-C48	81.7(5)	C70-C71-C72-C67	0.5(7)
C41-C42-C47-C48	-96.6(4)	C68-C67-C72-C71	-1.3(6)
C45-C46-C50-C51	-67.5(5)	C66-C67-C72-C71	176.7(4)
C41-C46-C50-C51	110.7(5)	C69-C70-O2-C73	6.7(5)
C45-C46-C50-C52	55.5(5)	C71-C70-O2-C73	-174.8(4)

The crystal structure of **3e**

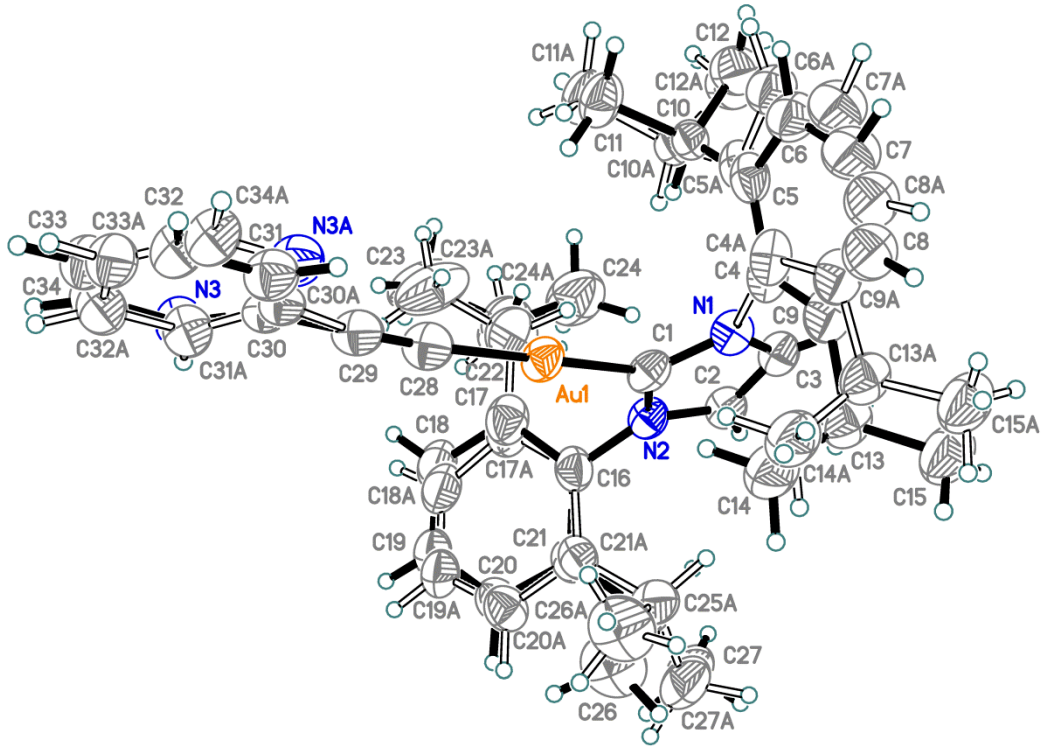

Figure S66. The 1st molecule of **3e**. Thermal ellipsoids are shown at a 50% probability level. Hydrogen atoms are drawn as fixed-size spheres.

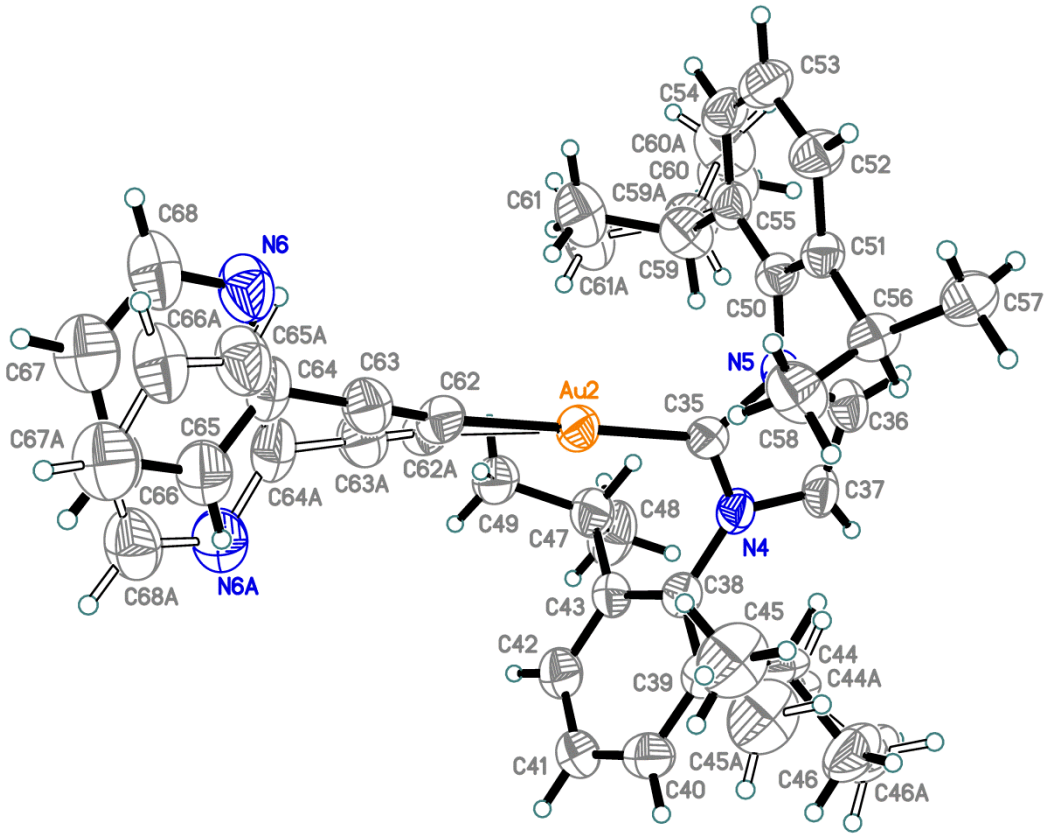

Figure S67. The 2nd molecule of **3e**. Thermal ellipsoids are shown at a 50% probability level. Hydrogen atoms are drawn as fixed-size spheres.

Table S19. Selected bond lengths (Å) for **3e**.

Au1-C1	2.021(8)	C5A-C10A	1.51(3)	C17A-C22A	1.52(2)
Au1-C28	1.999(8)	C6A-C7A	1.38(2)	C18A-C19A	1.37(2)
N1-C1	1.344(11)	C7A-C8A	1.39(2)	C19A-C20A	1.38(2)
N1-C3	1.368(10)	C8A-C9A	1.39(2)	C20A-C21A	1.41(2)
N1-C4	1.416(12)	C9A-C13A	1.44(5)	C21A-C25A	1.51(2)
N1-C4A	1.48(2)	C10A-C11A	1.53(2)	C22A-C23A	1.54(2)
C1-N2	1.361(10)	C10A-C12A	1.53(2)	C22A-C24A	1.55(2)
N2-C2	1.379(10)	C13A-C14A	1.52(2)	C25A-C26A	1.55(2)
N2-C16	1.440(10)	C13A-C15A	1.53(2)	C25A-C27A	1.55(2)
C2-C3	1.352(12)	C16-C17	1.417(17)	C28-C29	1.189(12)
C4-C5	1.404(14)	C16-C21	1.395(16)	C29-C30	1.470(12)
C4-C9	1.421(15)	C16-C17A	1.407(19)	C29-C30A	1.43(2)
C5-C6	1.396(14)	C16-C21A	1.403(19)	C30-C31	1.43(2)
C5-C10	1.514(15)	C17-C18	1.413(18)	C30-N3	1.304(19)
C6-C7	1.380(15)	C17-C22	1.52(2)	C31-C32	1.38(2)
C7-C8	1.379(15)	C18-C19	1.373(18)	C32-C33	1.366(19)
C8-C9	1.390(16)	C19-C20	1.385(17)	C33-C34	1.390(17)
C9-C13	1.52(2)	C20-C21	1.406(17)	C34-N3	1.315(18)
C10-C11	1.533(15)	C21-C25	1.503(19)	C30A-C31A	1.42(3)
C10-C12	1.531(16)	C22-C23	1.55(2)	C30A-N3A	1.29(3)
C13-C14	1.523(17)	C22-C24	1.55(2)	C31A-C32A	1.38(3)
C13-C15	1.502(15)	C25-C26	1.544(18)	C32A-C33A	1.37(3)
C4A-C5A	1.42(2)	C25-C27	1.536(18)	C33A-C34A	1.39(3)
C4A-C9A	1.43(2)	C17A-C18A	1.41(2)	C34A-N3A	1.31(3)
C5A-C6A	1.40(2)				
Au2-C35	2.007(8)	C44-C45	1.51(2)	C59A-C60A	1.55(2)
Au2-C62	2.052(10)	C44-C46	1.54(2)	C59A-C61A	1.55(2)
Au2-C62A	2.11(2)	C44A-C45A	1.52(2)	C62-C63	1.143(14)
N4-C35	1.349(10)	C44A-C46A	1.53(2)	C63-C64	1.485(16)
N4-C37	1.393(10)	C47-C48	1.487(16)	C64-C65	1.384(19)
N4-C38	1.430(10)	C47-C49	1.527(14)	C64-N6	1.364(18)
C35-N5	1.386(11)	C50-C51	1.387(11)	C65-C66	1.36(2)
N5-C36	1.354(11)	C50-C55	1.406(11)	C66-C67	1.42(2)
N5-C50	1.472(10)	C51-C52	1.405(12)	C67-C68	1.39(2)
C36-C37	1.341(13)	C51-C56	1.514(11)	C68-N6	1.344(18)
C38-C39	1.401(12)	C52-C53	1.391(12)	C62A-C63A	1.11(2)
C38-C43	1.391(12)	C53-C54	1.375(14)	C63A-C64A	1.48(2)
C39-C40	1.382(12)	C54-C55	1.378(12)	C64A-C65A	1.39(3)

C39-C44	1.530(19)	C55-C59	1.509(15)	C64A-N6A	1.36(3)
C39-C44A	1.53(2)	C55-C59A	1.51(2)	C65A-C66A	1.35(3)
C40-C41	1.375(13)	C56-C57	1.528(13)	C66A-C67A	1.39(3)
C41-C42	1.404(14)	C56-C58	1.534(13)	C67A-C68A	1.37(3)
C42-C43	1.374(13)	C59-C60	1.537(16)	C68A-N6A	1.36(3)
C43-C47	1.535(13)	C59-C61	1.558(18)		

Table S20. Selected bond angles (°) for **3e**.

C28-Au1-C1	177.8(3)	C17A-C16-N2	121.7(19)
C1-N1-C3	112.4(7)	C21A-C16-N2	111.8(14)
C1-N1-C4	124.9(7)	C21A-C16-C17A	126(2)
C1-N1-C4A	126.3(12)	C16-C17-C22	127.9(19)
C3-N1-C4	122.7(8)	C18-C17-C16	118(2)
C3-N1-C4A	121.0(12)	C18-C17-C22	113.8(19)
N1-C1-Au1	129.6(6)	C19-C18-C17	120(3)
N1-C1-N2	103.6(6)	C18-C19-C20	120(3)
N2-C1-Au1	126.7(6)	C19-C20-C21	122(2)
C1-N2-C2	111.3(7)	C16-C21-C20	116.7(17)
C1-N2-C16	122.5(6)	C16-C21-C25	120.2(16)
C2-N2-C16	126.2(6)	C20-C21-C25	123.1(16)
C3-C2-N2	106.3(7)	C17-C22-C23	118(2)
C2-C3-N1	106.4(7)	C17-C22-C24	115(2)
N1-C4-C9	115.4(15)	C23-C22-C24	105.5(19)
C5-C4-N1	120.6(15)	C21-C25-C26	109.1(18)
C5-C4-C9	124.0(11)	C21-C25-C27	111.4(16)
C4-C5-C10	121.0(18)	C27-C25-C26	114.9(17)
C6-C5-C4	116.8(11)	C16-C17A-C22A	116(3)
C6-C5-C10	122.2(18)	C18A-C17A-C16	114(3)
C7-C6-C5	120.0(12)	C18A-C17A-C22A	129(3)
C8-C7-C6	122.3(11)	C19A-C18A-C17A	122(4)
C7-C8-C9	120.8(12)	C18A-C19A-C20A	120(4)
C4-C9-C13	123.5(13)	C19A-C20A-C21A	122(3)
C8-C9-C4	116.0(12)	C16-C21A-C20A	114(2)
C8-C9-C13	120.5(13)	C16-C21A-C25A	126(2)
C5-C10-C11	108.6(11)	C20A-C21A-C25A	120(2)
C5-C10-C12	115(3)	C17A-C22A-C23A	111(3)
C12-C10-C11	110.6(14)	C17A-C22A-C24A	100(3)
C9-C13-C14	107.9(10)	C23A-C22A-C24A	110(2)
C15-C13-C9	116.3(12)	C21A-C25A-C26A	108(3)

C15-C13-C14	108.9(12)	C21A-C25A-C27A	108(2)
C5A-C4A-N1	116(4)	C27A-C25A-C26A	114(2)
C5A-C4A-C9A	116.0(18)	C29-C28-Au1	176.4(8)
C9A-C4A-N1	128(4)	C28-C29-C30	177.4(11)
C4A-C5A-C10A	123(5)	C28-C29-C30A	169(2)
C6A-C5A-C4A	122(2)	C31-C30-C29	119.2(12)
C6A-C5A-C10A	115(5)	N3-C30-C29	120.3(13)
C7A-C6A-C5A	120(2)	N3-C30-C31	120.4(10)
C6A-C7A-C8A	120(2)	C32-C31-C30	119.2(14)
C7A-C8A-C9A	120(2)	C33-C32-C31	119.0(13)
C4A-C9A-C13A	113(3)	C32-C33-C34	117.5(10)
C8A-C9A-C4A	121(2)	N3-C34-C33	124.5(14)
C8A-C9A-C13A	126(4)	C30-N3-C34	119.4(12)
C5A-C10A-C11A	118(4)	C31A-C30A-C29	109(3)
C5A-C10A-C12A	102(10)	N3A-C30A-C29	126(4)
C11A-C10A-C12A	111(3)	N3A-C30A-C31A	125(2)
C9A-C13A-C14A	110(3)	C32A-C31A-C30A	116(3)
C9A-C13A-C15A	118(3)	C33A-C32A-C31A	119(3)
C14A-C13A-C15A	104(3)	C32A-C33A-C34A	120(2)
C17-C16-N2	114.6(13)	N3A-C34A-C33A	122(3)
C21-C16-N2	122.9(11)	C30A-N3A-C34A	118(3)
C21-C16-C17	122.4(18)		
C35-Au2-C62	178.7(4)	C50-C51-C56	122.2(7)
C35-Au2-C62A	166.7(9)	C52-C51-C56	121.3(8)
C35-N4-C37	111.0(7)	C53-C52-C51	120.8(9)
C35-N4-C38	122.5(6)	C54-C53-C52	120.6(9)
C37-N4-C38	126.5(7)	C53-C54-C55	121.1(8)
N4-C35-Au2	125.0(6)	C50-C55-C59	120.7(12)
N4-C35-N5	103.3(6)	C50-C55-C59A	128(3)
N5-C35-Au2	131.5(6)	C54-C55-C50	117.3(8)
C35-N5-C50	121.0(7)	C54-C55-C59	121.8(12)
C36-N5-C35	111.7(7)	C54-C55-C59A	115(3)
C36-N5-C50	127.1(7)	C51-C56-C57	113.1(7)
C37-C36-N5	107.1(8)	C51-C56-C58	111.2(7)
C36-C37-N4	106.9(7)	C57-C56-C58	109.4(7)
C39-C38-N4	118.0(8)	C55-C59-C60	110.3(16)
C43-C38-N4	119.1(8)	C55-C59-C61	107.3(16)
C43-C38-C39	122.9(8)	C60-C59-C61	111.0(14)
C38-C39-C44	117.9(14)	C55-C59A-C60A	113(4)
C38-C39-C44A	126.1(16)	C55-C59A-C61A	123(4)

C40-C39-C38	117.6(8)	C60A-C59A-C61A	108(3)
C40-C39-C44	124.1(14)	C63-C62-Au2	170.9(8)
C40-C39-C44A	116.0(16)	C62-C63-C64	179.5(10)
C41-C40-C39	121.0(9)	C65-C64-C63	120.3(11)
C40-C41-C42	120.1(9)	N6-C64-C63	116.8(10)
C43-C42-C41	120.7(9)	N6-C64-C65	122.7(12)
C38-C43-C47	122.5(8)	C66-C65-C64	120.4(15)
C42-C43-C38	117.7(8)	C65-C66-C67	117.5(15)
C42-C43-C47	119.8(8)	C68-C67-C66	119.5(16)
C39-C44-C46	107(2)	N6-C68-C67	122.4(18)
C45-C44-C39	111(2)	C68-N6-C64	117.3(14)
C45-C44-C46	112(2)	C63A-C62A-Au2	149.7(18)
C39-C44A-C46A	114(2)	C62A-C63A-C64A	180(4)
C45A-C44A-C39	112(2)	C65A-C64A-C63A	117(2)
C45A-C44A-C46A	113(2)	N6A-C64A-C63A	118(2)
C48-C47-C43	111.8(9)	N6A-C64A-C65A	125(2)
C48-C47-C49	112.2(8)	C66A-C65A-C64A	121(3)
C49-C47-C43	110.6(8)	C65A-C66A-C67A	114(3)
C51-C50-N5	119.5(7)	C68A-C67A-C66A	123(3)
C51-C50-C55	123.7(7)	N6A-C68A-C67A	122(3)
C55-C50-N5	116.7(7)	C68A-N6A-C64A	114(2)
C50-C51-C52	116.4(7)		

Table S21. Torsion angles (°) for **3e**.

Au1-C1-N2-C2	177.5(5)	C4A-C9A-C13A-C15A	157(3)
Au1-C1-N2-C16	-3.3(10)	C5A-C4A-C9A-C8A	0.0(7)
N1-C1-N2-C2	0.1(8)	C5A-C4A-C9A-C13A	179.9(4)
N1-C1-N2-C16	179.3(7)	C5A-C6A-C7A-C8A	0.1(7)
N1-C4-C5-C6	-177.9(9)	C6A-C5A-C10A-C11A	-57(6)
N1-C4-C5-C10	2.1(9)	C6A-C5A-C10A-C12A	64(7)
N1-C4-C9-C8	178.0(9)	C6A-C7A-C8A-C9A	-0.2(10)
N1-C4-C9-C13	-2.7(11)	C7A-C8A-C9A-C4A	0.1(10)
N1-C4A-C5A-C6A	-180(2)	C7A-C8A-C9A-C13A	-179.8(7)
N1-C4A-C5A-C10A	0(2)	C8A-C9A-C13A-C14A	96(3)
N1-C4A-C9A-C8A	179(3)	C8A-C9A-C13A-C15A	-23(3)
N1-C4A-C9A-C13A	-1(3)	C9A-C4A-C5A-C6A	0.0(3)
C1-N1-C3-C2	-1.1(9)	C9A-C4A-C5A-C10A	180.0(4)
C1-N1-C4-C5	-86.7(10)	C10A-C5A-C6A-C7A	-180.0(4)

C1-N1-C4-C9	95.4(10)	C16-N2-C2-C3	-179.9(7)
C1-N1-C4A-C5A	-79(2)	C16-C17-C18-C19	0.1(3)
C1-N1-C4A-C9A	102(2)	C16-C17-C22-C23	-170(2)
C1-N2-C2-C3	-0.7(9)	C16-C17-C22-C24	64(3)
C1-N2-C16-C17	81.3(13)	C16-C21-C25-C26	115.0(19)
C1-N2-C16-C21	-101.2(12)	C16-C21-C25-C27	-117(2)
C1-N2-C16-C17A	89.1(19)	C16-C17A-C18A-C19A	0.1(3)
C1-N2-C16-C21A	-89.2(14)	C16-C17A-C22A-C23A	-114(3)
N2-C2-C3-N1	1.1(9)	C16-C17A-C22A-C24A	129(3)
N2-C16-C17-C18	177.5(8)	C16-C21A-C25A-C26A	112(3)
N2-C16-C17-C22	5(3)	C16-C21A-C25A-C27A	-125(3)
N2-C16-C21-C20	-177.3(9)	C17-C16-C21-C20	0.0(7)
N2-C16-C21-C25	1(2)	C17-C16-C21-C25	179(2)
N2-C16-C17A-C18A	-178.1(13)	C17-C18-C19-C20	-0.2(7)
N2-C16-C17A-C22A	-8(4)	C18-C17-C22-C23	17(3)
N2-C16-C21A-C20A	178.3(13)	C18-C17-C22-C24	-108(2)
N2-C16-C21A-C25A	-5(3)	C18-C19-C20-C21	0.2(9)
C2-N2-C16-C17	-99.6(13)	C19-C20-C21-C16	-0.1(9)
C2-N2-C16-C21	77.9(13)	C19-C20-C21-C25	-179(2)
C2-N2-C16-C17A	-92(2)	C20-C21-C25-C26	-66.4(19)
C2-N2-C16-C21A	89.9(15)	C20-C21-C25-C27	61(2)
C3-N1-C1-Au1	-176.7(6)	C21-C16-C17-C18	0.0(3)
C3-N1-C1-N2	0.6(9)	C21-C16-C17-C22	-173(3)
C3-N1-C4-C5	91.7(10)	C22-C17-C18-C19	174(2)
C3-N1-C4-C9	-86.1(11)	C17A-C16-C21A-C20A	0.0(7)
C3-N1-C4A-C5A	95.1(17)	C17A-C16-C21A-C25A	177(3)
C3-N1-C4A-C9A	-84(3)	C17A-C18A-C19A-C20A	-0.2(7)
C4-N1-C1-Au1	1.9(16)	C18A-C17A-C22A-C23A	54(3)
C4-N1-C1-N2	179.2(12)	C18A-C17A-C22A-C24A	-63(3)
C4-N1-C3-C2	-179.7(12)	C18A-C19A-C20A-C21A	0.2(10)
C4-C5-C6-C7	-0.1(3)	C19A-C20A-C21A-C16	-0.1(9)
C4-C5-C10-C11	113.3(17)	C19A-C20A-C21A-C25A	-177(3)
C4-C5-C10-C12	-122(3)	C20A-C21A-C25A-C26A	-72(3)
C4-C9-C13-C14	-91.8(12)	C20A-C21A-C25A-C27A	52(3)
C4-C9-C13-C15	145.6(11)	C21A-C16-C17A-C18A	0.0(3)
C5-C4-C9-C8	0.2(6)	C21A-C16-C17A-C22A	170(3)
C5-C4-C9-C13	179.5(4)	C22A-C17A-C18A-C19A	-168(3)
C5-C6-C7-C8	0.4(7)	C28-C29-C30A-C31A	168(10)
C6-C5-C10-C11	-66.7(17)	C28-C29-C30A-N3A	-12(13)
C6-C5-C10-C12	58(3)	C29-C30-C31-C32	177.0(13)

C6-C7-C8-C9	-0.4(9)	C29-C30-N3-C34	-176.8(13)
C7-C8-C9-C4	0.1(9)	C29-C30A-C31A-C32A	-180(3)
C7-C8-C9-C13	-179.2(6)	C29-C30A-N3A-C34A	180(4)
C8-C9-C13-C14	87.5(12)	C30-C31-C32-C33	0.1(3)
C8-C9-C13-C15	-35.1(13)	C31-C30-N3-C34	0.3(7)
C9-C4-C5-C6	-0.2(3)	C31-C32-C33-C34	-0.3(6)
C9-C4-C5-C10	179.8(4)	C32-C33-C34-N3	0.5(9)
C10-C5-C6-C7	179.9(4)	C33-C34-N3-C30	-0.5(9)
C4A-N1-C1-Au1	-2(3)	N3-C30-C31-C32	-0.1(3)
C4A-N1-C1-N2	175(3)	C30A-C31A-C32A-C33A	0.0(3)
C4A-N1-C3-C2	-176(3)	C31A-C30A-N3A-C34A	-0.1(8)
C4A-C5A-C6A-C7A	0.0(3)	C31A-C32A-C33A-C34A	0.1(7)
C4A-C5A-C10A-C11A	123(6)	C32A-C33A-C34A-N3A	-0.1(10)
C4A-C5A-C10A-C12A	-116(7)	C33A-C34A-N3A-C30A	0.1(10)
C4A-C9A-C13A-C14A	-84(3)	N3A-C30A-C31A-C32A	0.0(4)
Au2-C35-N5-C36	-173.4(7)	C42-C43-C47-C49	60.1(12)
Au2-C35-N5-C50	2.4(12)	C43-C38-C39-C40	-0.2(14)
N4-C35-N5-C36	1.0(9)	C43-C38-C39-C44	-172.8(14)
N4-C35-N5-C50	176.9(7)	C43-C38-C39-C44A	172.5(15)
N4-C38-C39-C40	178.4(8)	C44-C39-C40-C41	172.0(14)
N4-C38-C39-C44	5.8(16)	C44A-C39-C40-C41	-173.6(14)
N4-C38-C39-C44A	-8.8(18)	C50-N5-C36-C37	-176.3(8)
N4-C38-C43-C42	-177.8(8)	C50-C51-C52-C53	0.0(13)
N4-C38-C43-C47	2.2(13)	C50-C51-C56-C57	149.0(8)
C35-N4-C37-C36	0.5(10)	C50-C51-C56-C58	-87.4(9)
C35-N4-C38-C39	-94.5(9)	C50-C55-C59-C60	-122.8(15)
C35-N4-C38-C43	84.2(11)	C50-C55-C59-C61	116.3(15)
C35-N5-C36-C37	-0.8(10)	C50-C55-C59A-C60A	-130(4)
C35-N5-C50-C51	94.3(9)	C50-C55-C59A-C61A	97(6)
C35-N5-C50-C55	-87.8(9)	C51-C50-C55-C54	-3.0(12)
N5-C36-C37-N4	0.2(10)	C51-C50-C55-C59	-178.5(12)
N5-C50-C51-C52	179.8(7)	C51-C50-C55-C59A	175(3)
N5-C50-C51-C56	-3.6(12)	C51-C52-C53-C54	-1.1(14)
N5-C50-C55-C54	179.2(7)	C52-C51-C56-C57	-34.5(11)
N5-C50-C55-C59	3.7(14)	C52-C51-C56-C58	89.0(10)
N5-C50-C55-C59A	-3(3)	C52-C53-C54-C55	0.1(14)
C36-N5-C50-C51	-90.5(10)	C53-C54-C55-C50	1.8(12)
C36-N5-C50-C55	87.4(10)	C53-C54-C55-C59	177.3(12)
C37-N4-C35-Au2	174.0(6)	C53-C54-C55-C59A	-177(2)
C37-N4-C35-N5	-0.9(9)	C54-C55-C59-C60	62(2)

C37-N4-C38-C39	85.2(11)	C54-C55-C59-C61	-59.0(19)
C37-N4-C38-C43	-96.1(10)	C54-C55-C59A-C60A	48(5)
C38-N4-C35-Au2	-6.2(11)	C54-C55-C59A-C61A	-85(6)
C38-N4-C35-N5	178.8(7)	C55-C50-C51-C52	2.0(12)
C38-N4-C37-C36	-179.2(8)	C55-C50-C51-C56	178.6(8)
C38-C39-C40-C41	-0.1(14)	C56-C51-C52-C53	-176.6(8)
C38-C39-C44-C45	104(2)	C63-C64-C65-C66	172.2(12)
C38-C39-C44-C46	-133(2)	C63-C64-N6-C68	-175.2(12)
C38-C39-C44A-C45A	125(2)	C64-C65-C66-C67	2(2)
C38-C39-C44A-C46A	-106(3)	C65-C64-N6-C68	0(2)
C38-C43-C47-C48	114.4(11)	C65-C66-C67-C68	1(3)
C38-C43-C47-C49	-119.8(10)	C66-C67-C68-N6	-4(3)
C39-C38-C43-C42	0.9(14)	C67-C68-N6-C64	3(3)
C39-C38-C43-C47	-179.2(9)	N6-C64-C65-C66	-3(2)
C39-C40-C41-C42	-0.3(15)	C63A-C64A-C65A-C66A	-176(4)
C40-C39-C44-C45	-68(2)	C63A-C64A-N6A-C68A	-179(3)
C40-C39-C44-C46	54(3)	C64A-C65A-C66A-C67A	-7(7)
C40-C39-C44A-C45A	-62(3)	C65A-C64A-N6A-C68A	-5(6)
C40-C39-C44A-C46A	67(3)	C65A-C66A-C67A-C68A	-1(8)
C40-C41-C42-C43	0.9(15)	C66A-C67A-C68A-N6A	7(8)
C41-C42-C43-C38	-1.2(14)	C67A-C68A-N6A-C64A	-3(6)
C41-C42-C43-C47	178.9(9)	N6A-C64A-C65A-C66A	10(7)
C42-C43-C47-C48	-65.7(13)		

The crystal structure of **4a**

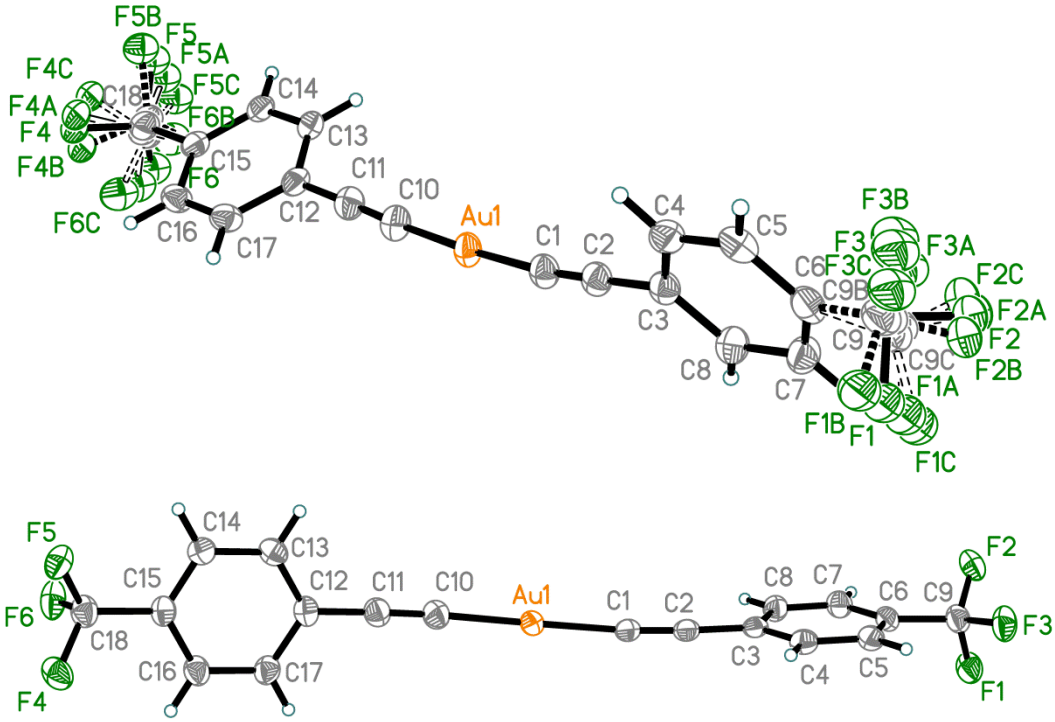

Figure S68. The structure of the complex anion in compound **4a** (with disorder – top, and without disorder – bottom). Thermal ellipsoids are shown at a 50% probability level. Hydrogen atoms are drawn as fixed-size spheres. Both CF_3 groups are disordered over four positions with disorder ratios of 0.430(3) : 0.306(3) : 0.207(3) : 0.057(3) for atoms C9, F1..F3 / C9A, F1A..F3A / C9B, F1B..F3B / C9C, F1C..F3C and 0.307(3) : 0.453(3) : 0.116(3) : 0.124(3) for atoms F4..F6 / F4A..F6A / F4B..F6B / F4C..F6C.

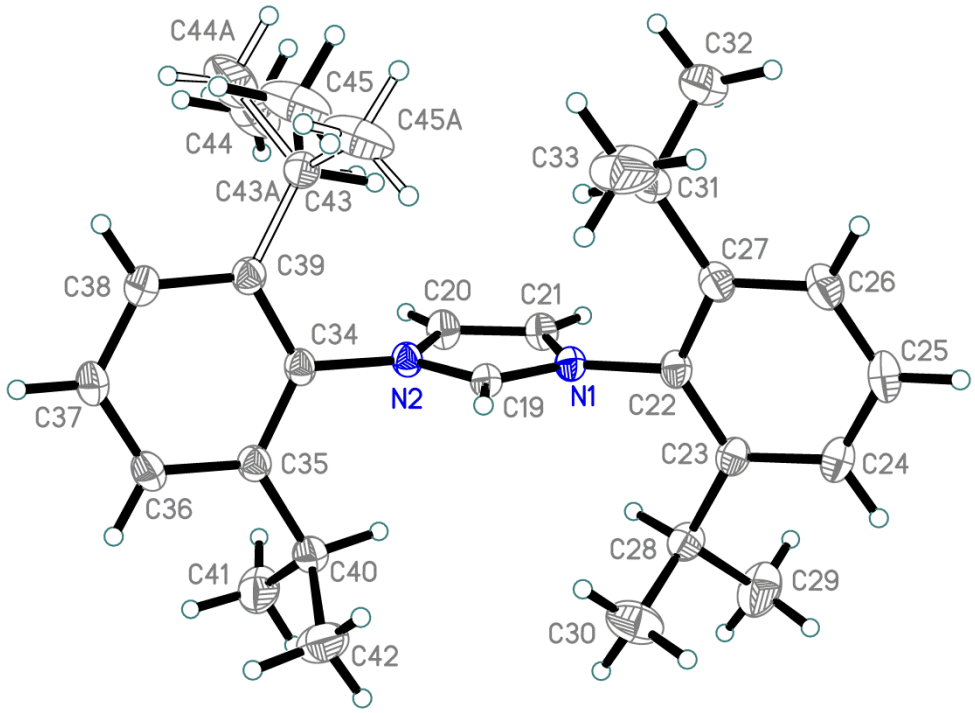

Figure S69. The structure of the cation in compound **4a**. Thermal ellipsoids are shown at a 50% probability level. Hydrogen atoms are drawn as fixed-size spheres. The minor component of disorder of an *iso*-propyl group is drawn with open solid lines. The disorder ratio for atoms C43..C45 / C43A..C45A) is 0.880(5) : 0.120(5).

Table S22. Selected bond lengths (Å) for **4a**.

Au1-C1	1.980(2)	C12-C13	1.399(3)	C20-C21	1.352(3)
Au1-C10	1.977(2)	C12-C17	1.405(3)	C22-C23	1.400(3)
C1-C2	1.213(3)	C13-C14	1.386(3)	C22-C27	1.401(3)
C2-C3	1.436(3)	C14-C15	1.386(3)	C23-C24	1.397(3)
C3-C4	1.397(3)	C15-C16	1.389(3)	C23-C28	1.521(3)
C3-C8	1.399(3)	C15-C18A	1.498(3)	C24-C25	1.388(3)
C4-C5	1.383(3)	C15-C18	1.498(3)	C25-C26	1.381(3)
C5-C6	1.381(3)	C15-C18C	1.498(3)	C26-C27	1.392(3)
C6-C7	1.390(3)	C15-C18B	1.499(3)	C27-C31	1.518(3)
C6-C9B	1.499(3)	C16-C17	1.384(3)	C28-C29	1.522(3)
C6-C9C	1.499(3)	C18-F6	1.350(2)	C28-C30	1.532(3)
C6-C9	1.499(3)	C18-F5	1.350(2)	C31-C33	1.530(3)
C6-C9A	1.499(3)	C18-F4	1.351(2)	C31-C32	1.530(3)
C7-C8	1.386(3)	C18A-F5A	1.349(2)	C34-C35	1.395(3)
C9-F3	1.349(2)	C18A-F6A	1.350(2)	C34-C39	1.398(3)
C9-F2	1.350(2)	C18A-F4A	1.352(2)	C35-C36	1.399(3)
C9-F1	1.351(2)	C18B-F6B	1.350(2)	C35-C40	1.518(3)
C9A-F3A	1.350(2)	C18B-F5B	1.351(2)	C36-C37	1.382(3)
C9A-F2A	1.350(2)	C18B-F4B	1.351(2)	C37-C38	1.384(3)
C9A-F1A	1.351(2)	C18C-F5C	1.350(2)	C38-C39	1.398(3)
C9B-F3B	1.349(2)	C18C-F6C	1.350(2)	C39-C43	1.520(3)
C9B-F2B	1.350(2)	C18C-F4C	1.351(2)	C39-C43A	1.520(4)
C9B-F1B	1.350(2)	N1-C19	1.334(2)	C40-C41	1.527(3)
C9C-F3C	1.350(2)	N1-C21	1.384(2)	C40-C42	1.531(3)
C9C-F2C	1.350(2)	N1-C22	1.450(2)	C43-C44	1.523(3)
C9C-F1C	1.350(2)	C19-N2	1.332(2)	C43-C45	1.523(3)
C10-C11	1.216(3)	N2-C20	1.384(2)	C43A-C45A	1.523(4)
C11-C12	1.431(3)	N2-C34	1.451(2)	C43A-C44A	1.523(4)

Table S23. Selected bond angles (°) for **4a**.

C10-Au1-C1	176.58(9)	F5A-C18A-F4A	107.3(6)
C2-C1-Au1	174.84(19)	F6A-C18A-F4A	106.7(5)
C1-C2-C3	177.3(2)	F5A-C18A-C15	112.3(3)
C4-C3-C8	118.90(19)	F6A-C18A-C15	112.0(4)
C4-C3-C2	121.22(19)	F4A-C18A-C15	112.4(7)
C8-C3-C2	119.86(19)	F6B-C18B-F5B	104.3(9)
C5-C4-C3	120.8(2)	F6B-C18B-F4B	103.9(10)

C6-C5-C4	119.8(2)	F5B-C18B-F4B	108.1(9)
C5-C6-C7	120.34(19)	F6B-C18B-C15	113.0(8)
C5-C6-C9B	114.0(6)	F5B-C18B-C15	114.8(10)
C7-C6-C9B	125.3(6)	F4B-C18B-C15	111.9(10)
C5-C6-C9C	129.2(11)	F5C-C18C-F6C	110.0(11)
C7-C6-C9C	110.2(11)	F5C-C18C-F4C	107.0(10)
C5-C6-C9	117.8(3)	F6C-C18C-F4C	103.3(10)
C7-C6-C9	121.8(3)	F5C-C18C-C15	116.2(11)
C5-C6-C9A	129.6(5)	F6C-C18C-C15	113.0(12)
C7-C6-C9A	110.0(4)	F4C-C18C-C15	106.3(10)
C8-C7-C6	120.0(2)	C19-N1-C21	108.94(15)
C7-C8-C3	120.1(2)	C19-N1-C22	125.12(15)
F3-C9-F2	106.1(7)	C21-N1-C22	125.59(15)
F3-C9-F1	106.3(5)	N2-C19-N1	108.26(15)
F2-C9-F1	106.1(5)	C19-N2-C20	108.84(15)
F3-C9-C6	116.3(8)	C19-N2-C34	123.93(15)
F2-C9-C6	111.1(5)	C20-N2-C34	127.21(15)
F1-C9-C6	110.3(4)	C21-C20-N2	107.12(16)
F3A-C9A-F2A	106.9(9)	C20-C21-N1	106.84(16)
F3A-C9A-F1A	105.7(8)	C23-C22-C27	124.14(17)
F2A-C9A-F1A	105.9(8)	C23-C22-N1	118.81(16)
F3A-C9A-C6	107.6(11)	C27-C22-N1	117.04(17)
F2A-C9A-C6	116.0(9)	C24-C23-C22	116.45(18)
F1A-C9A-C6	114.1(7)	C24-C23-C28	121.58(18)
F3B-C9B-F2B	107.0(11)	C22-C23-C28	121.95(17)
F3B-C9B-F1B	108.5(11)	C25-C24-C23	121.01(19)
F2B-C9B-F1B	107.2(9)	C26-C25-C24	120.57(19)
F3B-C9B-C6	113.4(16)	C25-C26-C27	121.29(19)
F2B-C9B-C6	110.0(10)	C26-C27-C22	116.52(19)
F1B-C9B-C6	110.4(11)	C26-C27-C31	120.67(18)
F3C-C9C-F2C	107.6(15)	C22-C27-C31	122.80(17)
F3C-C9C-F1C	106.9(14)	C23-C28-C29	112.62(18)
F2C-C9C-F1C	105.9(14)	C23-C28-C30	110.94(17)
F3C-C9C-C6	109(2)	C29-C28-C30	110.7(2)
F2C-C9C-C6	103(3)	C27-C31-C33	110.2(2)
F1C-C9C-C6	124(3)	C27-C31-C32	112.00(18)
C11-C10-Au1	173.6(2)	C33-C31-C32	111.32(19)
C10-C11-C12	178.5(3)	C35-C34-C39	124.69(17)
C13-C12-C17	118.39(19)	C35-C34-N2	117.69(16)
C13-C12-C11	121.7(2)	C39-C34-N2	117.62(16)

C17-C12-C11	119.9(2)	C34-C35-C36	116.49(18)
C14-C13-C12	120.8(2)	C34-C35-C40	122.89(16)
C15-C14-C13	119.76(19)	C36-C35-C40	120.61(17)
C14-C15-C16	120.50(18)	C37-C36-C35	120.70(18)
C14-C15-C18A	123.0(2)	C36-C37-C38	120.97(18)
C16-C15-C18A	116.5(2)	C37-C38-C39	121.08(18)
C14-C15-C18	120.0(4)	C38-C39-C34	116.04(17)
C16-C15-C18	119.5(4)	C38-C39-C43	121.3(2)
C14-C15-C18C	121.4(5)	C34-C39-C43	122.6(2)
C16-C15-C18C	117.7(6)	C38-C39-C43A	120.3(11)
C14-C15-C18B	115.0(5)	C34-C39-C43A	123.6(10)
C16-C15-C18B	124.5(5)	C35-C40-C41	110.34(17)
C17-C16-C15	119.7(2)	C35-C40-C42	111.15(17)
C16-C17-C12	120.7(2)	C41-C40-C42	111.9(2)
F6-C18-F5	107.9(6)	C39-C43-C44	110.3(2)
F6-C18-F4	106.6(8)	C39-C43-C45	112.3(2)
F5-C18-F4	103.3(7)	C44-C43-C45	110.6(3)
F6-C18-C15	111.9(7)	C39-C43A-C45A	114.9(14)
F5-C18-C15	113.2(5)	C39-C43A-C44A	114.2(15)
F4-C18-C15	113.3(11)	C45A-C43A-C44A	108.4(15)
F5A-C18A-F6A	105.7(4)		

Table S24. Torsion angles (°) for **4a**.

C8-C3-C4-C5	-1.1(3)	C14-C15-C18C-F5C	10.0(14)
C2-C3-C4-C5	-179.42(19)	C16-C15-C18C-F5C	-162.8(9)
C3-C4-C5-C6	1.0(3)	C14-C15-C18C-F6C	138.5(9)
C4-C5-C6-C7	-0.2(3)	C16-C15-C18C-F6C	-34.3(12)
C4-C5-C6-C9B	-173.2(6)	C14-C15-C18C-F4C	-108.9(9)
C4-C5-C6-C9C	-173.5(17)	C16-C15-C18C-F4C	78.3(10)
C4-C5-C6-C9	-177.1(3)	C21-N1-C19-N2	0.7(2)
C4-C5-C6-C9A	178.4(5)	C22-N1-C19-N2	174.15(16)
C5-C6-C7-C8	-0.4(3)	N1-C19-N2-C20	-0.4(2)
C9B-C6-C7-C8	171.8(6)	N1-C19-N2-C34	-178.89(16)
C9C-C6-C7-C8	174.1(14)	C19-N2-C20-C21	-0.1(2)
C9-C6-C7-C8	176.4(3)	C34-N2-C20-C21	178.39(18)
C9A-C6-C7-C8	-179.2(4)	N2-C20-C21-N1	0.5(2)
C6-C7-C8-C3	0.2(3)	C19-N1-C21-C20	-0.7(2)
C4-C3-C8-C7	0.5(3)	C22-N1-C21-C20	-174.15(17)
C2-C3-C8-C7	178.8(2)	C19-N1-C22-C23	101.5(2)

C5-C6-C9-F3	-13.5(8)	C21-N1-C22-C23	-86.0(2)
C7-C6-C9-F3	169.7(7)	C19-N1-C22-C27	-79.3(2)
C5-C6-C9-F2	-135.1(6)	C21-N1-C22-C27	93.1(2)
C7-C6-C9-F2	48.1(7)	C27-C22-C23-C24	1.5(3)
C5-C6-C9-F1	107.6(5)	N1-C22-C23-C24	-179.40(16)
C7-C6-C9-F1	-69.3(6)	C27-C22-C23-C28	-179.70(18)
C5-C6-C9A-F3A	-3.1(11)	N1-C22-C23-C28	-0.6(3)
C7-C6-C9A-F3A	175.6(8)	C22-C23-C24-C25	-0.6(3)
C5-C6-C9A-F2A	-122.7(10)	C28-C23-C24-C25	-179.39(19)
C7-C6-C9A-F2A	56.0(10)	C23-C24-C25-C26	-0.6(3)
C5-C6-C9A-F1A	113.7(7)	C24-C25-C26-C27	1.1(3)
C7-C6-C9A-F1A	-67.5(8)	C25-C26-C27-C22	-0.2(3)
C5-C6-C9B-F3B	-30.5(12)	C25-C26-C27-C31	178.95(19)
C7-C6-C9B-F3B	156.9(12)	C23-C22-C27-C26	-1.1(3)
C5-C6-C9B-F2B	-150.3(8)	N1-C22-C27-C26	179.80(17)
C7-C6-C9B-F2B	37.1(12)	C23-C22-C27-C31	179.71(18)
C5-C6-C9B-F1B	91.6(10)	N1-C22-C27-C31	0.6(3)
C7-C6-C9B-F1B	-81.1(11)	C24-C23-C28-C29	-33.1(3)
C5-C6-C9C-F3C	1(3)	C22-C23-C28-C29	148.2(2)
C7-C6-C9C-F3C	-172.7(17)	C24-C23-C28-C30	91.7(2)
C5-C6-C9C-F2C	-113(2)	C22-C23-C28-C30	-87.0(2)
C7-C6-C9C-F2C	73.4(17)	C26-C27-C31-C33	-70.6(3)
C5-C6-C9C-F1C	128(2)	C22-C27-C31-C33	108.5(2)
C7-C6-C9C-F1C	-46(2)	C26-C27-C31-C32	53.9(3)
C17-C12-C13-C14	-1.6(3)	C22-C27-C31-C32	-127.0(2)
C11-C12-C13-C14	178.86(19)	C19-N2-C34-C35	-82.7(2)
C12-C13-C14-C15	1.0(3)	C20-N2-C34-C35	99.1(2)
C13-C14-C15-C16	0.3(3)	C19-N2-C34-C39	96.6(2)
C13-C14-C15-C18A	-178.1(3)	C20-N2-C34-C39	-81.6(2)
C13-C14-C15-C18	179.6(4)	C39-C34-C35-C36	-2.2(3)
C13-C14-C15-C18C	-172.3(7)	N2-C34-C35-C36	177.04(16)
C13-C14-C15-C18B	177.5(5)	C39-C34-C35-C40	176.49(18)
C14-C15-C16-C17	-0.9(3)	N2-C34-C35-C40	-4.3(3)
C18A-C15-C16-C17	177.5(3)	C34-C35-C36-C37	0.7(3)
C18-C15-C16-C17	179.7(4)	C40-C35-C36-C37	-178.01(18)
C18C-C15-C16-C17	171.9(7)	C35-C36-C37-C38	0.5(3)
C18B-C15-C16-C17	-177.9(6)	C36-C37-C38-C39	-0.4(3)
C15-C16-C17-C12	0.3(3)	C37-C38-C39-C34	-0.9(3)
C13-C12-C17-C16	1.0(3)	C37-C38-C39-C43	176.14(19)
C11-C12-C17-C16	-179.5(2)	C37-C38-C39-C43A	-178.7(9)

C14-C15-C18-F6	96.5(6)	C35-C34-C39-C38	2.3(3)
C16-C15-C18-F6	-84.2(8)	N2-C34-C39-C38	-176.95(16)
C14-C15-C18-F5	-25.7(9)	C35-C34-C39-C43	-174.72(19)
C16-C15-C18-F5	153.6(6)	N2-C34-C39-C43	6.0(3)
C14-C15-C18-F4	-143.0(7)	C35-C34-C39-C43A	180.0(10)
C16-C15-C18-F4	36.3(8)	N2-C34-C39-C43A	0.7(10)
C14-C15-C18A-F5A	-5.3(6)	C34-C35-C40-C41	-119.9(2)
C16-C15-C18A-F5A	176.2(4)	C36-C35-C40-C41	58.7(2)
C14-C15-C18A-F6A	113.5(4)	C34-C35-C40-C42	115.4(2)
C16-C15-C18A-F6A	-65.0(5)	C36-C35-C40-C42	-66.0(3)
C14-C15-C18A-F4A	-126.4(4)	C38-C39-C43-C44	-66.3(3)
C16-C15-C18A-F4A	55.2(5)	C34-C39-C43-C44	110.5(3)
C14-C15-C18B-F6B	72.9(11)	C38-C39-C43-C45	57.5(4)
C16-C15-C18B-F6B	-110.0(10)	C34-C39-C43-C45	-125.6(3)
C14-C15-C18B-F5B	-46.5(11)	C38-C39-C43A-C45A	91(2)
C16-C15-C18B-F5B	130.6(9)	C34-C39-C43A-C45A	-87(2)
C14-C15-C18B-F4B	-170.2(8)	C38-C39-C43A-C44A	-35(2)
C16-C15-C18B-F4B	6.9(11)	C34-C39-C43A-C44A	147.1(14)